MASTERARBEIT | MASTER'S THESIS

Titel | Title

Non-canonical STAT1 activation in natural killer cells

verfasst von | submitted by

Natalie Schindler BSc

angestrebter akademischer Grad | in partial fulfilment of the requirements for the degree of

Master of Science (MSc)

Wien | Vienna, 2025

Studienkennzahl lt. Studienblatt | Degree programme code as it appears on the student record sheet:	UA 066 863
Studienrichtung lt. Studienblatt | Degree programme as it appears on the student record sheet:	Masterstudium Biologische Chemie
Betreut von | Supervisor:	Univ.-Prof. i.R. Dr. Thomas Decker

ACKNOWLEDGEMENTS

First of all, I would like to thank my amazing PI and supervisor Dr. Eva König for giving me the opportunity to join her wonderful lab and to work on this fascinating project! Over the past year you have taught me so much, from planning experiments to arranging and delivering the perfect presentation and, most importantly, how to believe in myself as a researcher. I am incredibly thankful for this time and to have had you as a mentor!

Next, I want to truly thank Faith O. David for being the best PhD supervisor I could have wished for and for guiding me throughout this year. Working with you was always a lot of fun! You taught me everything I know and due to your patience, honesty, and helpfulness I had a wonderful experience and I will never forget this time. Thank you so much! A big thank you also goes to all the Putz lab members Michelle Buri, Andreas Borojević, Lisa Marie Wittmann, Katalin Kiss and Hayeon Baik for making the last year so unforgettable, fun, and supportive!

Further, I would like to thank Prof. Thomas Decker for reading and grading my Master's thesis and being part of my thesis committee. I truly appreciate you taking the time to support my work!

Thank you to Max Schwab for being my Master's thesis buddy and for making everyday in the lab enjoyable. I really valued our daily writing sessions, coffee breaks and insightful discussions! Thanks to Christoph Trenk for always providing silly jokes, helpful comments and home-baked bread with Nutella. Many thanks to Maša Bereš, Monika Homolya, Jaqueline Horvath, Michael Machtinger, Marija Trkulja, Sarah Trouvilliez for being such great colleagues, always offering a helping hand and making the time in the lab fun and supportive. Finally, I want to extend my gratitude to Prof. Emilio Casanova and Dr. Herwig Moll for welcoming me into their lab and making this Master's thesis possible.

Next, I want to say a big thank you to all my friends outside of the lab for being there for me in times of need and always encouraging me. I would never be where I am today without you: Lena Bachler, Jessica Brunner, Elif Kahraman, Manuel Lutz, Manuel Pires, Nina Poitschek, Annie Stepec, Paul Thrakl, and Sophie Wannenmacher.

Finally, I want my mum and my dad for always believing in me, for showing so much interest in my research, and for supporting me with food, love and strength.

Lastly, my greatest appreciation goes to my partner Gregor. You were my rock through all the ups and downs, you read and corrected this entire thesis, sat through all of my trial presentations, lifted me up when I had a bad day and celebrated with me when I got good results. Thanks my love.

1 ABSTRACT

Natural killer (NK) cells are innate lymphoid cells which play a vital part in immunosurveillance by detecting and eliminating transformed, stressed, or infected cells without prior sensitization. The rapid and potent cytotoxic activity of NK cells against tumor cells, while sparing healthy tissue, underlines their therapeutic potential in cancer immunotherapies. Hence, improving NK cell functionality is a key focus in current research. Signal transducer and activator of transcription 1 (STAT1) is a component of the Janus kinase (JAK)/STAT signaling pathway and serves as an essential transcription factor involved in various cellular processes, especially NK cell-mediated cytotoxicity and tumor surveillance. Our lab previously demonstrated that serine 727 (S727) phosphorylation of STAT1 restrains NK cell cytotoxicity. Additional preliminary data revealed co-localization of STAT1 with the serine-threonine kinases (STK) 38 and STK38-like (STK38L) at the immunological synapse upon mouse NK-tumor cell contact, suggesting STK38(L) as potential mediators of the STAT1-S727 phosphorylation.

The aim of this study was to investigate this non-canonical STAT1-S727 phosphorylation in NK cells upon tumor cell contact by performing co-culture assays with NK and tumor cells and analyzing STAT1-pS727 levels via Western blotting. Further, in vitro kinase activity assays using recombinant proteins, along with cellular assays in HEK293T cells, were used to assess whether STK38(L) are capable of directly mediating this phosphorylation. Finally, confocal microscopy, proximity ligation assays, and immunofluorescence stainings were employed to elucidate the spatial proximity of STAT1 and STK38(L) at the immunological synapse.

This study revealed robust STAT1-S727 phosphorylation in primary human NK cells, NK-92 cells, primary mouse NK cells, and murine CD8+ T cells upon co-culture with tumor cells. Notably, phosphorylation at STAT1 tyrosine 701 (Y701) was absent under these conditions, indicating JAK/STAT-independent signaling. The ablation of STK38 in NK-92 cells led to reduced STAT1-pS727 levels, along with reduced total STAT1 protein and mRNA levels, suggesting cross-reactions between both signaling pathways. Additionally, the kinase activity assays confirmed the ability of STK38(L) to phosphorylate STAT1 at S727. Collectively, these findings strongly suggest a role for STK38(L) in non-canonical STAT1 signaling, potentially as part of a negative feedback loop, resulting in the reduction of NK cell cytotoxicity. While the localization and spatial proximity of STAT1 and STK38 remain to be conclusively determined due to non-specific antibodies, this study identifies STAT1-pS727, together with STK38(L), as promising targets to enhance NK cell cytotoxicity and potential future immunotherapies.

2 ZUSAMMENFASSUNG

Natürliche Killerzellen (NK-Zellen) sind Lymphozyten des angeborenen Immunsystems, die mutierte, gestresste oder infizierte Zellen ohne vorherige Sensibilisierung erkennen und eliminieren. Ihre rapide und effiziente Zytotoxizität gegenüber Tumorzellen bei gleichzeitiger Schonung gesunden Gewebes unterstreicht ihr therapeutisches Potenzial in der Krebsimmuntherapie. Daher ist die Verbesserung ihrer Funktionalität ein zentraler Schwerpunkt der aktuellen Forschung. Der Signaltransduktor und Transkriptionsaktivator 1 (STAT1) ist Teil des Januskinase (JAK)/STAT Signalwegs und fungiert als entscheidender Transkriptionsfaktor, der an verschiedenen zellulären Prozessen beteiligt ist, insbesondere an der NK-Zell-vermittelten Zytotoxizität und Tumorüberwachung. Unsere Arbeitsgruppe konnte zuvor zeigen, dass die Phosphorylierung von STAT1 an Serin 727 (S727) die Zytotoxizität von NK-Zellen hemmt. Weitere vorläufige Daten zeigten eine Ko-Lokalisierung von STAT1 mit den Serin-Threonin Kinasen STK38 und STK38-like (STK38L) an der immunologischen Synapse bei Kontakt von Maus NK- und Tumorzellen, was STK38(L) zu potenziellen Vermittlern der STAT1-S727 Phosphorylierung macht.

Ziel dieser Masterarbeit war es, die nicht-kanonische STAT1-S727 Phosphorylierung in NK-Zellen nach Tumorzellkontakt zu untersuchen. Dazu wurden Ko-Kultur-Assays mit NK- und Tumorzellen etabliert, und anschließend die S727 Phosphorylierung mittels Western Blot analysiert. Zudem wurden *in vitro* Kinaseaktivitätsassays mit rekombinanten Proteinen sowie zelluläre Assays in HEK293T Zellen durchgeführt, um zu prüfen, ob STK38(L) in der Lage sind, diese Phosphorylierung direkt zu vermitteln. Schließlich wurden konfokale Mikroskopie, Proximity Ligation Assays und Immunfluoreszenzfärbungen verwendet, um die räumliche Nähe von STAT1 und STK38(L) an der immunologischen Synapse zu untersuchen.

Diese Arbeit zeigt eine ausgeprägte STAT1-S727 Phosphorylierung in primären humanen NK-Zellen, NK-92 Zellen, primären Maus NK-Zellen und murinen $CD8^+$ T-Zellen nach Ko-Kultur mit Tumorzellen. Da unter diesen Bedingungen die Phosphorylierung von STAT1 an Tyrosin 701 (Y701) nicht nachweisbar war, deutet dies auf einen JAK/STAT-unabhängigen Signalweg hin. Der Verlust von STK38 in NK-92 Zellen verringerte sowohl STAT1-pS727 sowie die gesamten STAT1-Protein- und mRNA-Mengen, was auf mögliche Wechselwirkungen zwischen den Signalwegen hindeutet. Kinaseaktivitätsassays zeigten zudem die Fähigkeit von STK38(L), STAT1 an S727 zu phosphorylieren. Insgesamt deuten diese Ergebnisse darauf hin, dass STK38(L) eine Rolle im nicht-kanonischen STAT1 Signalweg spielt, möglicherweise als Teil eines negativen Rückkopplungsmechanismus, der die Zytotoxizität von NK-Zellen verringert. Auch wenn die Lokalisierung und räumliche Nähe von STAT1 und STK38 aufgrund unspezifischer Antikörper noch nicht abschließend geklärt ist, identifiziert diese Studie STAT1-pS727 und STK38(L) als vielversprechende Zielstrukturen zur Steigerung der NK-Zell Zytotoxizität und für potenzielle zukünftige Immuntherapien.

3 TABLE OF CONTENTS

4 LIST OF ABBREVIATIONS

ADCC	Antibody dependent cellular cytotoxicity
BF	Bright field
CCL5	C-C motif chemokine ligand 5
CD	Cluster of differentiation
CDK	Cyclin-dependent kinase
cNK	Conventional NK cells
CRISPR	Clustered regularly interspaced short palindromic repeats
cSMAC	Central supramolecular activation cluster
CTFR	CellTrace Far Red
CTLA-4	Cytotoxic T-lymphocyte–associated antigen 4
CTV	CellTrace Violet
DAMPs	Damage-associated molecular patterns
DAPI	4',6-diamidino-2-phenylindole
DISC	Death inducing signaling complex
E. coli	Escherichia coli
E:T	Effector to target ratio
eGFP	Enhanced green fluorescent protein
EOMES	Eomesodermin
FasL	Fas ligand
FBS	Fetal bovine serum
FDA	Food and Drug Administration
FITC	Fluorescein Isothiocyanate
GAF	Gamma interferon activated factor
GAS	Gamma interferon-activated site
GFP	Green fluorescent protein
GPC(R)	G-protein coupled (receptor)
GST	Glutathione S-transferase
HLA	Human leukocyte antigen
hNK	Human NK cells
HSC-70	Heat shock cognate 70 protein
HSCs	Hematopoietic stem cells
IF	Immunofluorescence staining
IFN	Interferon

IFNAR	IFNα receptor
IL	Interleukin
ILCs	Innate lymphoid cells
IRF9	Interferon regulatory factor 9
IS	Immunologic synapse
ISGF3	IFN-stimulated gene factor 3
ISGs	Interferon-stimulated genes
ISRE	Interferon-stimulated response elements
ITAM	Immunoreceptor tyrosine-based activation motif
ITIM	Immunoreceptor tyrosine-based inhibitory motif
JAK	Janus kinase
KIR	Killer immunoglobulin-like receptor
LATS	Large tumor suppressor kinase
LB	Lysogenic Broth
MAP4K	Mitogen-activated protein kinase
MFI	Mean fluorescent intensity
MHC-I	Major histocompatibility complex I
MIP	Macrophage Inflammatory Proteins
miR146a	Micro-RNA 146a
mNK	Mouse NK cells
MOB	Monopolar spindle-one-binder protein
MST	Mammalian Ste20-like kinase
MyD88	Myeloid differentiation primary response 88
NCAM	Neuronal cell adhesion molecule-1
NDR	Nuclear Dbf2-related
NF-κB	Nuclear factor kappa B
NK	Natural killer
NKP	Pre-NK cell precursors
NTR	N-terminal regulatory domain
OVA	Ovalbumin
p53MAPK	p38 mitogen-activated protein kinase
PAGE	Polyacrylamide gel electrophoresis
PBS	Phosphate-buffered saline
PD-1	Programmed cell death protein 1
PD-L1	Programmed cell death-ligand 1

PIAS	Protein inhibitor of activated STAT
PKA	cAMP-dependent protein kinase 1
PKC	Protein kinase C
PKG	cGMP-dependent protein kinase
PLA	Proximity ligation assay
PMA	Phorbol-12-myristat-13-acetat
PP2A	Protein phosphatase type 2A
pS727	Phospho-serine 727
pSMAC	Peripheral supramolecular activation cluster
PTPs	Protein tyrosine phosphatases
rh	Recombinant human
rm	Recombinant mouse
RT	Room temperature
S727	Serine 727
S727A	Serine 727 alanine point mutation
SAV	Salvador homolog 1
SDS	Sodium dodecyl sulfate
SH2	Src homology 2
SOCS	Suppressors of cytokine signaling
STAT	Signal transducer and activator of transcription
STK38	Serine-threonine kinase 38
STK38(L)	Serine-threonine kinase 38-like
TAZ	Transcriptional co-activator with PDZ-binding motif
T-bet	T-box expressed in T cells
TEAD	TEA domain transcription factor
TIGIT	T cell immunoglobulin and ITIM domain
TIM-3	T-cell immunoglobulin and mucin-domain containing
TLR	Toll-like-receptor
TNF	Tumor necrosis factor
TRAF6	TNF Receptor Associated Factor 6
TRAIL	TNF- related apoptosis-inducing ligand
TYK	Tyrosine kinase
WB	Western blot
Y701	Tyrosine 701
YAP	Yes-associated protein

5 INTRODUCTION

5.1 Natural killer cells

Natural killer (NK) cells are innate lymphocytes which play a crucial role in our body's defense against cancer and infections by recognizing and eliminating stressed, damaged, and virally infected cells. Immunotherapy was revolutionized over the past decade, but many cancers are still able to evade existing treatments cellular immunotherapy (e.g. chimeric antigen receptor T-cell- or NK cell therapy[1]), or immune checkpoint inhibition (with e.g. anti-CTLA-4, anti PD-1 or anti-PD-L1[2]). With their unique properties, NK cells present an exciting therapeutic option next to existing therapies in the fight against cancer[3].

NK cells were first described by the group of Eva Klein at Karolinska Institutet, Sweden, in 1975[4,5], and were defined as small lymphocytes displaying cytolytic activity against certain leukemia cells[5]. Herbermann *et al.* further report a different type of cytotoxicity on the newly found cell type, compared to T-cells or macrophages, namely the ability of NK cells to kill tumor cells without the need of antibody dependent cellular cytotoxicity (ADCC)[6]. Now, more than 50 years after the discovery of NK cells, they are defined as cells belonging to the group 1 innate lymphoid cells (ILCs), comprising around 5-10% of all peripheral blood lymphocytes[7], which are capable of mediating cellular cytotoxicity and produce cytokines without the need of V(D)J antigen receptor rearrangement or prior sensitization like T cells[8]. Following stimulation from infected or diseased cells *via* activating or inhibiting receptors or activating cytokines (such as interleukin (IL)-2, -12, -15, -18, interferon (IFN) type I), NK cells are quickly able to mediate cellular cytotoxicity via formation of an immunological synapse. Through this synapse they deliver lytic granules, containing the pore forming protein perforin and granzymes, into the target cell leading to cell lysis. NK cell cytotoxicity and effector function is further dictated by the production of cytokines, especially interferon γ (IFNγ) and tumor necrosis factor α (TNFα)[8]. These mechanisms make NK cells truly important to maintain human health, which is why they are considered to stand in the first line of defense against pathogens[9], autoimmune disease[10,11], and cancer[10,12]

5.1.1 NK cell development and NK cell subsets

All human blood cells are derived from multipotent, hematopoietic stem cells (HSCs)[13], which differentiate into progenitor cells, that can be distinguished by differential expression of cell- and lineage type specific surface markers[14]. This process is called human hematopoietic differentiation hierarchy[15] and consists of two main lineages: myeloid and lymphoid progenitor

cells. HSCs differentiate into the common lymphoid progenitor by upregulating cluster of differentiation (CD) 34, CD45RA, and other cell surface markers[15]. Common lymphoid progenitor cells then give rise to pro-B, pre-T, and ILCs[16]. ILCs miss specific lineage markers present on T cells (CD3, CD5, T cell receptor), and B cells (CD19, CD20, B cell receptor)[17]. Depending on the NK cell type, such as immature or specialized tissue resident NK cell, the maturation process may vary, which is why in this context solely the development of conventional NK (cNK) cells is described[18]. cNK cells are known to develop mainly in the bone marrow[19], but can also further mature in other tissues, such as secondary lymphoid tissue namely tonsils, spleen, or lymph nodes[17]. From the common lymphoid progenitor cell, cells differentiate into pre-NK cell precursors (NKP) through expression of CD122 (IL-2Rβ)[8], which is further promoted *via* binding of cytokines, interleukin (IL)-12 and IL-15[20]. Finally, through upregulation of the neuronal cell adhesion molecule-1 (NCAM, also called CD56) on immature NK cells, cells reach the mature NK cell stadium[21]. During the maturation process NK cells acquire cell type specific cytotoxic functions, namely synthesis of lytic molecules (perforin and granzymes), and inflammatory cytokines (e.g. IFNγ)[21]. NK cell development and survival depends on interaction with specific cytokines, especially IL-2 and IL-15, but also on expression of certain transcription factors, such as eomesodermin (EOMES), T-box expressed in T cells (T-bet)[22] or signal transducer and activator of transcription 5 (STAT5)[23].

After describing cNK cell development, the question arises on how to define NK cell lineage? NK cells are generally immunophenotypically identified via flow cytometry by excluding typical lineage markers of T and B lymphocytes, and gating on $CD45^+$ lymphocytes. The most common expression markers are CD56 (NCAM), and/or CD16 (FcγRIIIA), killer immunoglobulin-like receptors (KIRs), and/or activating receptors like NKG2D, NKp30, NKp46 or NKp80[17], but NKp46 is considered the only NK cell specific marker.

Human peripheral blood NK cells can be further distinguished into subsets, which differ in phenotype and cellular function. Two major NK cell subsets have been described: $CD56^{bright}$ and $CD56^{dim}$, referring to the abundance of the CD56 surface marker on the cell. In healthy individuals, $CD56^{dim}$ NK cells represent the majority of the two subsets, making up >90% of peripheral blood NK cells[24]. $CD56^{dim}$ subsets are generally considered to be more cytotoxic against target cells compared to $CD56^{bright}$ NK cells[25]. $CD56^{dim}$ express CD16[26], which is a low affinity IgG Fc receptor responsible for mediating ADCC[27]. $CD56^{dim}$ NK cells are further able to synthesize granzymes and perforin, as well as show baseline expression of activating NK cell receptors[25]. $CD56^{bright}$ on the other hand are known as the less mature subset[28], and only account for around 5% of NK cells[25]. $CD56^{bright}$ NK cells produce inflammatory cytokines[25], and are considered to play a part in immunoregulatory mechanisms[29].

5.1.2 NK cell education

NK cells are able to lyse stressed, infected or deformed cells without the need of prior sensitization to antigens, or antigen specific receptors such as TCR or BCRs. In order to identify target cells, they follow the "missing self" and "induced self" recognition by relying on germline-encoded activating and inhibiting receptors[12]. The traditional explanation of NK cell activation is characterized as "missing self" and was first described in 1981 by Klas Kärre[30]. This hypothesis states that major histocompatibility complex I (MHC-I) downregulation makes target cells susceptible to NK cell induced killing, because they no longer display the necessary ligand to engage NK cell inhibitory receptors. These corresponding receptors were later identified as KIRs and CD94/NKG2A. These receptors are specific for MHC-I and non-classical MHC-I molecule HLA (human leukocyte antigen)-E, respectively, and prevent NK cells from killing normal and healthy cells[31]. Malignant or infected cells frequently downregulate the expression of MHC-I to evade cytotoxic T cells, making them ideal targets for NK cell surveillance by "missing-self" recognition[16].

"Induced self" recognition describes ligands, which are rarely present on healthy cells, but upregulated on stressed or infected ones, that can bind to activating receptors present on NK cells. As NK cell activation is strictly regulated, cytolytic activation occurs solely if activating signals prevail over inhibitory ones[16]. Today this model has been further expanded by including NK cell education, or "licensing", to recognize self MHC-I. Studies with F_1 hybrid mice demonstrated, that NK cell mediated rejection of transplanted bone marrow occurred after receiving a graft from either parent, but not from F_1 siblings[32]. This was the foundation for understanding that functional differences in NK cells are a consequence of an education process, through which NK cells interact with MHC-I. Licensing is a process in which inhibitory NK cell receptors specific for MHC-I interact with their corresponding MHC-I ligand during NK cell development. This is a very crucial step during NK cell maturation, as licensed NK cells are capable of expressing inhibitory receptors, are able to bind self MHC-I and thus, are functional[33]. Unlicensed NK cells however are incapable of expressing inhibitory receptors and produce large amounts of SHP-1[34], which leads them to be hyporesponsive towards target cells in regard to cytotoxicity and production of cytokines[31]. Finally, cytokines such as IL-12, IL-15, IL-18, and type I interferons (IFNα and IFNβ)[35] have also shown to have a strong impact on NK cell maturation and can also re-license uneducated NK cells to enhance their functionality[18].

5.1.3 NK cell activation

NK cells do not posses a single receptor recognizing antigens, but they express various germline encoded activating and inhibitory cell surface receptors. The balance of activating and inhibitory signals from these receptors then decides, whether the NK cell will become activated or inhibited towards a target cell[36]. Additionally, NK cells express different cytokine receptors, which induce intracellular signaling cascades upon cytokine binding. Depending on the NK cell subset and activating cytokine, this signaling cascade can lead to enhanced cytotoxicity, cytokine production, enhanced ADCC, or proliferation[37].

5.1.3.1 NK cell activating and inhibitory receptors

NK cells possess receptors, which are able to recognize molecules upregulated on infected or stressed cells. Adaptor molecules transmit signals from NK cell activation receptors through an immunoreceptor tyrosine-based activation motif (ITAM) or an activating tyrosine-based signaling motif (YINM), located within their cytoplasmic domains. This mechanism then triggers downstream signaling which leads to NK cell activation[16]. Activating NK cell signals are mediated by co-stimulatory receptors (2B4), cytokine-binding receptors, natural cytotoxicity receptors (NKp30, -44, -46), activating receptors (NKG2D, CD16 or FCγRIIIA, DNAM-1), death receptors (FasL, TRAIL), and receptors binding non-self antigen (TLRs, KIRs)[8,38]. In general, NK cells need multiple activating signals, except for the CD16 receptor, where a single ligation is sufficient to trigger a response. CD16 is a particularly important activating receptor responsible for ADCC, where CD16a binds the Fc region of IgGs linked to target cells[8].

In addition to activating receptors, NK cells express a multitude of inhibitory receptors, which are crucial for restraining NK cells from killing self-MHC-I expressing cells, as well as preventing autoimmune reactions[8]. NK inhibitory receptors contain an immunoreceptor tyrosine-based inhibitory motif (ITIM) within their cytoplasmic domain, which is phosphorylated upon ligand binding. This leads to mobilization of protein tyrosine phosphatases SHP-1 and SHP-2, which dephosphorylate tyrosine residues and thus inhibit cytotoxic activity and NK cell activation[22]. Malignant or infected cells frequently downregulate expression of MHC-I to evade cytotoxic T cells, making them ideal targets for NK cell surveillance by “missing-self” recognition[16]. Inhibitory receptors can be distinguished into three broad classes: MHC-I specific or non-related. Receptors that specifically bind to MHC-I are various KIRs (KIR2DL, -3DL), and NKG2A. KIRs interact mainly with HLA type molecules (A, B, or C), whereas NKG2A, in a dimeric structure with CD94, binds the highly conserved HLA-E[38]. Checkpoint protein receptors (PD-1, TIM-3, TIGIT) and siglecs (siglec-3, -7, and -9) on the other hand belong to the MHC-I non-related inhibitory receptors[10].

5.1.3.2 NK cell cytokine receptors

NK cells express a broad range of cytokine receptors responding to activation *via* IL-2, -10, -12, -15, and -18, as well as type 1 IFNs (IFNα and IFNβ). Cytokines are released by various sources including T cells, dendritic cells, the bone marrow, or even tumor cells. Synergies between various cytokines can enhance the expression of receptors for one cytokine in response to the binding of a different one. Further, it was shown that combined activation through different cytokine receptors leads to a stronger cytotoxic NK cell response[37]. For example, individual activation of IL-12, -15, or -18 results in low IFNγ production, however, production is largely increased upon combined stimulation[39]. While most of the cytokines activate NK cells, anti-inflammatory cytokines, like TGF-β, were shown to exert an inhibitory function on NK cell killing[40]. IL-2 and IL-15 induce a similar signaling cascade involving JAK/STAT and PI3K pathways, together with Ras/Raf/MAPK signaling. This leads to enhanced cytokine production, as well as NK cell cytotoxicity, and stronger proliferation[41]. IL-12 activates NK cells and enhances cytotoxic functions by activating JAK/STAT signaling, resulting in IFN*γ* and TNF*α* production. Data suggests, that IL-12 most likely acts combinatory together with IL-2 and IL-18[37]. IL-18 belongs to the pro-inflammatory IL-1 family and induces signaling through MyD88 and TRAF6, resulting in MAP kinase and NF-kB activation. IL-18 works co-stimulatory with IL-12 and IL-15, leading to strong cytokine production[42]. Finally, binding of IL-21 to NK cell receptors was shown to induce phosphorylation of various STATs, ultimately leading to enhanced cytotoxicity and ADCC[43].

5.1.4 NK cell effector functions

The purpose of NK cells is to eliminate "unhealthy" cells, such as stressed, malignant, or virus-infected cells, or cells undergoing cellular senescence[44]. NK cell cytotoxic activity can be described by three main effector functions, namely immunologic synapse (IS) formation for targeted release of cytolytic granules, binding of activating or death receptors to the target cell, and NK cell cytokine secretion[8,45].

5.1.4.1 Immune synapse formation

A big hallmark of NK cell functionality is their ability to kill through activating and inhibitory receptors, as described above. The NK cell is activated, when signals originating from activating ligands outweigh inhibitory signals, resulting in IS formation and ultimately cytotoxic response via the release of lytic granules, which is referred to as degranulation process[46]. Degranulation is strictly regulated to four phases[47]: In the first step, the target cell is recognized by the NK cell, which leads to re-organization of actin filaments in the cytoskeleton, as well as clustering of cell adhesion molecules, which ultimately leads to formation of an IS[48]. The IS consists of two domains: The peripheral supramolecular activation cluster (pSMAC), which circles the point of contact

between the two cells. Inside the pSMAC the central SMAC (cSMAC) is located, facilitating the exocytosis of secretory granules[49]. Next, the cellular microtubule organizing center together with the lysosome, responsible for granule secretion, are centered towards the IS. In the third step, the secretory lysosomes move closer to the NK cell membrane and finally fuse with the target cell plasma membrane before releasing the cytotoxic granules into the IS to kill the target cell[47]. In detail, the cytolytic granules consist of two main molecules: perforin and granzyme. While perforin is responsible for generating pores in the target cell membrane, granzymes (mainly granzyme B) enter through these pores and induce caspase-dependent apoptosis by cleaving caspases and other proteins through their protease activity[10]. Concisely, the formation of the IS serves two main purposes, namely to shield surrounding cells and to protect the NK cell itself by targeted release of lytic granules[45].

5.1.4.2 Ligand-based cytotoxicity

Besides cytolytic granules, NK cells can also kill through activation of death receptors on the target cell membrane triggering extrinsic apoptosis. There exist two different death ligands, belonging to the TNF superfamily, namely TNF- related apoptosis-inducing ligands (TRAIL) and FasL (CD95L)[10]. FasL is stored in distinct granules, separate from perforin and granzymes, inside the NK cell and is expressed on the cell surface upon NK cell degranulation. FasL can then stimulate Fas (CD95), which activates the assembly of the death inducing signaling complex (DISC), ultimately resulting in apoptosis[50]. TRAIL binding to its cognate ligands TRAIL receptor 1 and -2 also leads to DISC formation and target cell apoptosis. Studies with $Ifng^{-/-}$ mice have shown that TRAIL expression is likely IFNγ dependent[51]. Further, TRAIL is not expressed on freshly isolated human NK cells, but can be induced via cytokine stimulation with IL-2, IL-15, or IL-12[45].

Compared to death receptor-mediated apoptosis, which can take 1–2 hours, NK cell killing via cytolytic granules induces target cell death within minutes of IS formation[52]. To induce target cell killing, a higher amount of FasL is required on the NK cell surface, whereas only 2-4 cytolytic granules were shown to induce target cell death[53]. Additionally, apoptosis induced by death ligands involves multiple signaling steps, whereas granzyme B directly cleaves caspases upon entering target cell cytosol, rapidly leading to apoptosis[45].

Another important receptor-based killing mechanism is ADCC-mediated cytotoxicity, where the CD16a receptor present on NK cells binds the Fc region of IgG antibody coated target cells. This leads to activation of NK cell killing through increasing intracellular Ca^{2+} levels and further activation of downstream signaling cascades[27]. Subsequent degranulation leads to secretion of

perforin, which ultimately results in lysis of the target cell[29]. There are ongoing studies to use monoclonal antibodies as immunomodulatory drugs to activate NK cells via ADCC to improve their cytotoxic effect against tumors[54], some of which (Trastuzumab[55], Rituximab[56], Cetuximab[57]) are already applied in clinical practice for that purpose.

5.1.4.3 Cytokine secretion

The third effector function of NK cells is their potent release of pro-inflammatory cytokines, particularly IFNγ and TNFα, and chemokines, following stimulation of cytokine- or activating receptors[37]. NK cell mediated cytokine release has many benefits including the communication with other immune cells causing activation of innate as well as adaptive immune cells by recruiting them to the site of infection, upregulation of MHC-I aiding T-cell recognition, and facilitating Th1 differentiation[8]. IFNγ is the most prominent cytokine, produced by activated NK cells and is responsible for a plethora of mechanisms against infected or malignant cells, as well as effector functions on other immune cells. IFNγ particularly exerts anti-tumor effects and was shown to regulate the expression of death receptors FasL and TRAIL on NK cells[58]. Compared to lytic granule release, cytokines typically experience non-directed secretion. However, binding of the activating receptor NKG2D promotes directed IFNγ release partly through the IS[59].

Besides cytokine production, active NK cells are also able to produce a variety of chemokines including MIP-1α, MIP-1β, IL-8, and CCL5, which recruit other immune cells to the site of action[16]. The production of cytokines and/or chemokines is induced *via* signaling of activating receptors, as well as activation of cytokine receptors binding IL-2, -12, -15, or -18[8]. While signaling through CD16, 2B4, or NKG2D receptors was sufficient for chemokine production, additional receptors need to be co-stimulated in order to release TNFα and IFNγ. Studies also showed, that co-culturing human NK cells with K562 tumor cells leads to ample secretion of TNFα, IFNγ, MIP-1α, MIP-1β, as well as CCL5 after 1 hour up until 12 hours after stimulation[60].

5.2 STAT1 signaling in NK cells

The signal transducer and activator of transcription 1 (STAT1) protein is one of seven members of the STAT family. In NK cells, it is a crucial transcription factor mediating various cellular processes, such as maturation, proliferation, as well as NK cell mediated cytotoxicity. STAT1 is activated by a plethora of specific cytokines, namely type I-III IFNs, IL-2, -12, -21, -27 and -35[61–63]. Further, STAT1 promotes MHC-I upregulation and is responsible for protection from pathogens and tumor surveillance, by regulating IFNγ production, which is known to be a major component of disease monitoring[61,62,64].

In mice, a complete knockout of STAT1 results in increased susceptibility to infections and tumor development[65]. This may result from decreased expression of MHC-I molecules, possibly leading to less responsive, unlicensed NK cells[63]. STAT1 deficiency was also observed to induce compromised NK cell maturation as well as cytotoxic functions, specifically the impaired rejection of injected tumor cells by NK cells[62,65,66]. The defect in NK cell maturation was speculated to result from impaired IL-15-presentation by macrophages[67], monocytes, and dendritic cells, which is dependent on IFN-induced STAT1 signaling[61]. In a separate study, the two splice variants of STAT1, STAT1-α and STAT1-β, have been individually knocked out to reveal distinct roles in NK cell maturation and differentiation. While STAT1β is capable of inducing target gene transcription, the effects are delayed with a reduced transcriptional amplitude, compared to STAT1α. Despite these functional differences, the isoform-specific roles of STAT1 in the context of tumorigenesis and immune regulatory mechanisms have not been completely characterized yet[61].

In patients, gain- or loss-of-function mutations in STAT1 can lead to compromised NK cell functions, but the underlying mechanism is not yet fully understood. However, NK cell cytotoxicity was partially rescued after introducing a STAT1-Y701F mutant, inhibiting Y701 phosphorylation[62]. In general, NK cell cytotoxicity is influenced by phosphorylation of STAT1, through which it acts as a transcription factor and NK cells acquire effector function and secrete immunogenic cytokines. In gain-of-function STAT1 mutations, total STAT1 protein and/or its phosphorylation levels are abnormally elevated[68]. Studies suggest that this may be the reason for altered NK cell responses to specific cytokines, resulting in impaired proliferation, IFNγ production, and cellular cytotoxicity[69,70]. STAT1 has the ability to form heterodimers with other members of the STAT1 family. Mutations may lead to in- or decreased formation of these heterodimers, which alters their transcriptional activity and can therefore have an effect on NK cell functionality[71]. In general, gain-of-function STAT1 mutations lead to chronic mucocutaneous candidiasis, increased risk of developing several types of cancer, as well as autoinflammatory and -immunity reactions, whereas loss-of-function mutations result in immunodeficiency, and increasing susceptibility to bacterial and viral infections[72,73].

5.2.1 The canonical STAT1 signaling pathway

The activation of STAT1 is strictly regulated, for the most part through IFNs. In total, three types of IFNs are known, namely type I (mainly IFNα and IFNβ), type II (IFNγ), and type III (IFNλ)[74]. In the canonical STAT1 signaling pathway, all three types of IFNs are able to activate STAT1 as a transcription factor through receptor-mediated JAK signaling[75] (**Figure 1**). Stimulation through type I or type III IFNs leads to phosphorylation of STAT1 and STAT2 by JAK1 and tyrosine kinase 2 (TYK2), followed by STAT1-STAT2 heterodimer formation [75,76]. STAT1-STAT2 heterodimers form

a complex with interferon regulatory factor 9 (IRF9), namely IFN-stimulated gene factor 3 (ISGF3), which is able to bind interferon-stimulated response elements (ISRE) and mediate gene expression[74]. Type II IFN interacts with JAK1 and JAK2 associated cytokine receptors, which exclusively forms STAT1 homodimers, following STAT1 phosphorylation. These homodimers, also known as gamma interferon activated factor (GAF), translocate to the nucleus, where they bind to the gamma interferon-activated site (GAS) of interferon-stimulated genes (ISGs), resulting in gene expression[74] As type I IFN-mediated stimulation is used in this thesis, activation of STAT1 though IFNα and IFNβ will be described in more detail below [75].

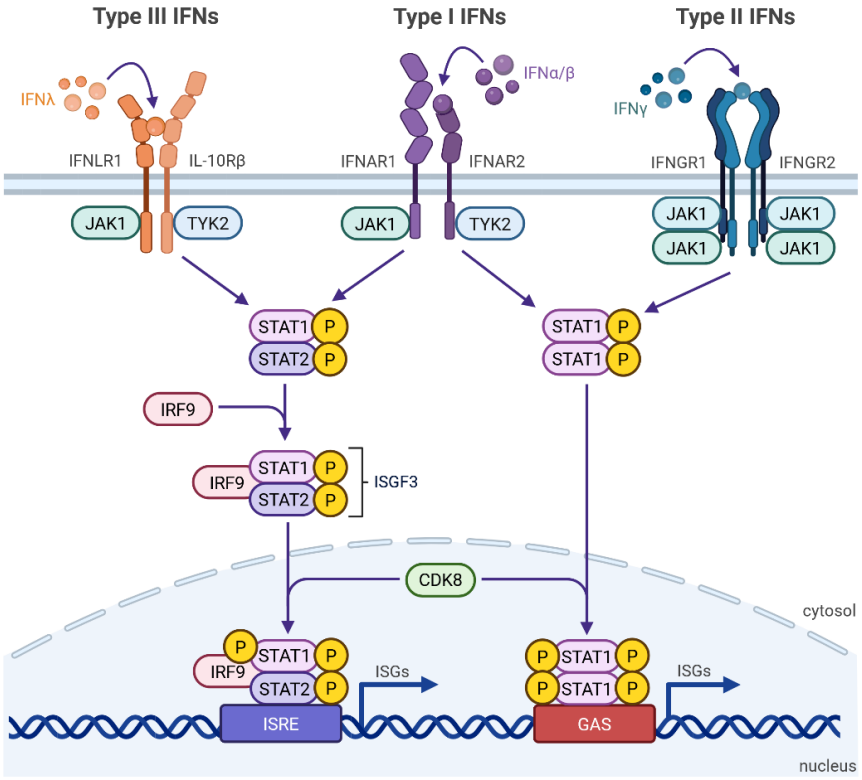

Figure 1. Type I interferon JAK/STAT signaling pathway. *Upon binding of type I and III IFNs to the IFN-α-receptor (IFNAR1 and IFNAR2) and the IFNLR1/IL-10Rβ, respectively, JAK1 and TYK2 are activated. This initiates the phosphorylation of STAT proteins and heterodimerization of STAT1-STAT2, recruiting IRF9, which results in the formation of the ISGF3 complex. These complexes translocate to the nucleus, where STAT1 is further phosphorylated on S727 by CDK8. The heterodimers then bind to IFN-stimulated response element (ISRE) sequences, which induces transcription of IFN-stimulated genes (ISG). Type II IFNs bind the IFNG1/IFNGR2 complex, promoting STAT1-Y701 phosphorylation by JAK1 and JAK2. The phosphorylated STAT1 forms homodimers, which enter the nucleus to be phosphorylated by CDK8 on S727, and bind gamma-activated sequences (GAS), inducing pro-inflammatory gene expression. JAK, Janus kinase; TYK, tyrosine kinase; IRF, interferon regulatory factor; ISGF3, IFN-stimulated gene factor 3; CDK8, cyclin-dependent kinase 8; Created with Biorender.com. Adapted from[77].*

Type I IFNs, IFNα and IFNβ, are both able to engage with the IFNα receptor (IFNAR), which consists of two subunits, IFNAR1 and IFNAR2. Dimerization of this receptor activates auto-phosphorylation of receptor-associated JAK1 and phosphorylation of TYK2. This leads to the recruitment of STAT1 and STAT2 proteins through conserved Src homology 2 (SH2) phospho-

tyrosine-binding domains[78]. JAK1 and TYK2 phosphorylate STAT1 on tyrosine 701, as well as STAT2 on Y690[79,80]. Tyrosine phosphorylation of STAT1 and STAT2 leads to dimerization and the formation of STAT1-STAT1 homo- and STAT1-STAT2 heterodimers. The heterodimers assemble with IRF9, which form the ISGF3 trimolecular complex, and translocate to the nucleus[76,78]. In the nucleus, S727 on STAT1 and STAT3, situated on the conserved PMSP motif, is further phosphorylated by cyclin-dependent kinase 8 (CDK8) to achieve full transcriptional activation[81]. ISGF3 binds to ISRE DNA sequences in promotor regions, leading to the transcription of many ISGs. STAT1 homodimers conversely, directly bind to GAS motifs[75]. ISRE and GAS elements drive the induction of ISGs associated with antiviral and pro-inflammatory responses, respectively. In general, activated STAT1 regulates the transcription of many ISGs, including *STAT1* itself, as well as various microRNAs that subsequently modulate protein expression at the translational level[61].

5.2.2 Targeting the STAT1 pathway to enhance NK cell functionality

Even though there are many different strategies, drugs, and immunotherapeutic approaches to enhance NK cell cytotoxicity, none of these therapies include the JAK/STAT pathway[82,83]. It was shown that in mNK cells, CDK8 mediates the constitutive phosphorylation of STAT1-S727 in the absence of cytokine stimulation or concomitant STAT1-Y701 phosphorylation. The inhibition of the STAT1-S727 phosphorylation by either introducing a S727A point mutation or by inhibiting CDK8 significantly enhanced NK cell cytotoxicity against tumor cells, as shown *in vitro* and *in vivo*[65,84]. Even though selective CDK8/19 inhibitors proved to enhance hNK cell cytotoxicity as well as tumor surveillance[85], unfortunately, they turned out to be unsuitable for in patient use due to their high systemic toxicity and were thus prohibited by the Food and Drug Administration (FDA)[86,87]. In supplementary studies, it is important to note that STAT1-S727 phosphorylation was still detected in spite of inhibition of CDK8[85], as well as in CDK8-deficient mNK cells[84]. CDK19 is a close relative to CDK8, and is known to share functional redundancy. It was thus suggested that CDK19 may be able to mediate STAT1-S727 phosphorylation in the absence of CDK8. Indeed, CDK8/CDK19 double-KO HEK cells showed significantly reduced basal STAT1-S727 phosphorylation. However, depending on the cytokine or cytotoxic drug that was used to stimulate STAT1, pS727 levels were still detectable to variable degrees in the absence of CDK8 and CDK19[87]. This led to the hypothesis that there may exist an additional kinase, responsible for the phosphorylation of STAT1-S727, representing a novel target to potentially boost NK cell functionality. Co-immunoprecipitation assays exploring the STAT1 interactome in mNK cells showed the physical interaction of STAT1 with STK38 and STK38L, particularly in tumor cell-stimulated conditions[62]. Hence, these kinases might phosphorylate STAT1-S727 and may represent possible targets to enhance NK cell cytotoxicity.

5.3 Serine-threonine kinase (STK) 38 and STK38-like

5.3.1 STK38(L): Cellular functions, activation and Hippo pathway signaling

The serine-threonine kinase (STK) 38 and STK38-like (STK38L), also known as NDR1 and NDR2, respectively, belong to the nuclear Dbf2-related (NDR) kinase family[88]. Both kinases are members of the AGC kinase group, characterized by a catalytic domain sequence resembling those of cAMP-dependent protein kinase 1 (PKA), cGMP-dependent protein kinase (PKG) or protein kinase C (PKC)[89,90]. STK38 and STK38L proteins are highly similar genes, which share approximately 87% amino acid identity, and are highly conserved from yeast to humans. Despite their close similarity, they exert distinct functions[91]. STK38 is involved in the regulation of various cellular processes, such as centrosome duplication, cell cycle progression, DNA damage signaling, or apoptosis. Further, the protein kinase is important for embryonic growth, development of the brain, and exerts a dual role in cancer, which will be further described later[88,92]. STK38L proteins mediate quality control of mitochondria and are suggested to be involved in autophagy[93].

Mouse models show that loss of STK38 leads to predisposition of T cell lymphoma development as well as reduced cytokine secretion efficiency. Interestingly, upon knockout of either STK38 or STK38L, the loss of function is compensated by the remaining kinase. Mice with the complete loss of both proteins, however, are not viable and die at an early embryonic stage[94]. Initially, STK38 was believed to be present only in the nucleus, but studies showed that it is also localized in the cytoplasm. STK38L on the other hand, has only been found in the cytosol, close to the cell surface[89].

STK38 and STK38L proteins are composed of three main domains: the N-terminal regulatory domain (NTR), a kinase-specific catalytic domain, and the C-terminal kinase domain. In general, the kinases have three distinct phosphorylation sites, which are required for full activation[91]. The NTR consists of many hydrophobic amino acids and is crucial for binding to monopolar spindle-one-binder protein (MOB) 1 and MOB2, as well as S100B proteins, leading to phosphorylation of Thr74/75[95,96]. The kinase domain of STK38(L) possesses an autophosphorylation site at Ser281/282 in the T-loop, which is important for kinase activity. The final phosphorylation site is located in the hydrophobic motif at the C-terminus of STK38(L), where mammalian Ste20-like kinases (MST1, MST2 and MST3) and mitogen-activated protein kinase (MAP4K) phosphorylate Thr444/442[91,97]. Kinase activity can be regulated by protein phosphatase type 2A (PP2A), by dephosphorylation of Ser281/282 or Thr444/442[89].

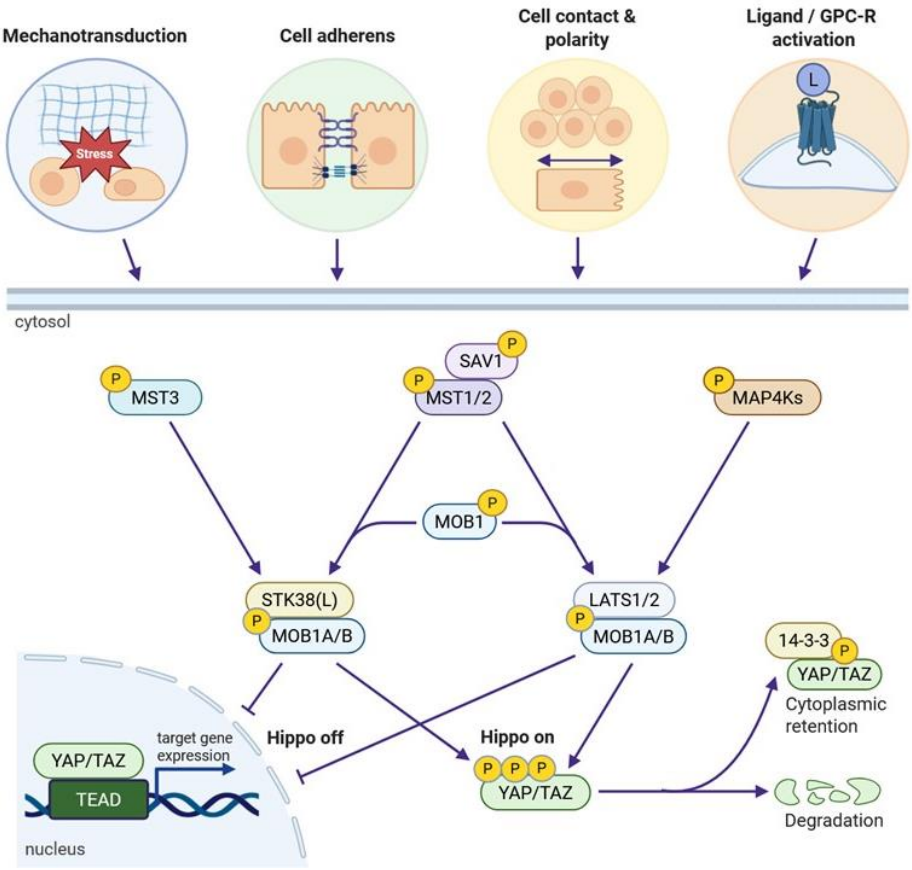

Figure 2. Hippo signaling pathway*. The Hippo pathway can be switched on by various cellular mechanisms, like mechanotransduction (extracellular matrix stiffness, cellular stress), cell adherens (e.g. tight junctions), cell contact and polarity, and ligand G-protein coupled (GPC) receptor interactions. The Hippo kinases MST1/2, activated by SAV1, MST3 and MAP4Ks phosphorylate STK38(L) and LATS1/2 proteins, which are further activated by MOB1. This leads to the inhibitory phosphorylation of YAP/TAZ, resulting either in cytoplasmic retention via interaction with 14-3-3 or proteasomal degradation. When Hippo signaling is turned off, activated YAP/TAZ translocate into the nucleus to recruit TEAD1-4 transcription factors to regulate cell proliferation, survival, and stemness. MST, mammalian Ste20-like kinases; SAV, Salvador homolog 1; MAP4Ks, mitogen-activated protein kinase; STK, serine-threonine kinase; LATS, large tumor suppressor kinase; MOB, monopolar spindle-one-binder protein; YAP, Yes-associated protein; TAZ, transcriptional co-activator with PDZ-binding motif; TEAD, TEA domain transcription factor; Created with Biorender.com. Adapted from[97,98].*

STK38 and STK38L are part of the Hippo pathway, which further comprises MST1, MST2 and MST3, the AGC serine-threonine kinases LATS1 and LATS2, and MAP4K[97]. The Hippo pathway (**Figure 2**) regulates cell differentiation, proliferation, and apoptosis, and was named after enlarged organs, resembling a hippopotamus, caused by mutations in the Hippo kinases[99]. Many different cellular mechanisms can lead to Hippo pathway activation, including mechanotransduction, change of cellular shape or polarity, stiffness of extracellular matrix, cell adhesion and high cell density, or activation *via* ligand binding[97]. Once the pathway is activated, MST1/2/3 and MAP4K kinases phosphorylate STK38, STK38L, and LATS1/2 proteins, which leads to their activation. The scaffolding proteins MOB1 and SAV1 further activate the Hippo kinases, which in turn phosphorylate and thereby inhibit the transcriptional co-activators Yes-associated

protein 1 (YAP1) and transcriptional co-activator with PDZ-binding motif (TAZ)[100]. Ultimately, phosphorylated YAP/TAZ become sequestrated in the cytosol and are degraded by the proteasome resulting in reduced cell proliferation and apoptosis. Conversely, when the Hippo pathway is inactive, YAP/TAZ are not phosphorylated and accumulate in the nucleus, where they associate with transcription factors and activate the transcription of target genes involved in cell growth and proliferation, organ development and homeostasis[99,101].

5.3.2 The role of STK38(L) in disease and cancer

STK38(L) seems to play a dual role in cancer and tumorigenesis, acting as an oncogene as well as a tumor suppressor[92,97]. Studies revealed upregulated mRNA levels of *STK38* in various cancerous tissues, including the breast, ovaries, and lung, as well as elevated protein expression in melanoma[97]. Overexpression of STK38 can lead to chromosomal instability due to excessive centrosome duplication[102], aberrant expression of the proto-oncogene MYC[103], as well as dysregulation of nuclear protein export[97].

STK38 also plays a crucial role in immunology. A study showed that STK38 downregulates Toll-like receptor 9-mediated signaling, thereby reducing the production of inflammatory cytokines to protect the host during bacterial infection[104]. STK38 was also shown to mediate IL-17-dependent signaling, which causes tissue inflammation in autoimmune responses. Hence, STK38 expression levels are elevated in patients with ulcerative colitis[88]. STK38 may also be involved in HIV-1 infection, as it has been shown that the HIV-1 protease can target STK38(L)[94]. Interestingly, STK38 expression appears to be positively associated with increased infiltration of NK cells in most cancer types, while negatively correlating with infiltration levels of $CD4^+$ T cells. Furthermore, STK38 promotes the recruitment of cancer-associated fibroblasts, which are strongly linked to pro-tumorigenic activity[92]. These results underline the potential of hyperactive STK38(L) to contribute to malignancies.

In contrast, STK38 was shown to suppress glioblastoma proliferation and inhibit metastasis formation in prostate cancer by inhibiting epithelial-to-mesenchymal transition[92]. Additionally, STK38 directly binds to the intergenic region of microRNA146a, a known negative regulator of STAT1, thereby partially inhibiting its transcription. This enhances STAT1 translation, which is crucial for type I IFN-dependent antiviral signaling, suggesting an important role of STK38 in mediating viral responses[105]. These data, however, do not confirm a direct interaction between STAT1 and STK38(L) proteins. This, along with the role of STK38(L) in non-canonical STAT1 signaling in NK cells has not been studied yet and will be addressed in this thesis.

6 PRELIMINARY DATA AND HYPOTHESIS

As previously described, in the canonical cytokine-induced STAT1 signaling pathway, STAT1 is activated via JAK-mediated phosphorylation of Y701 and further phosphorylated on S727 by CDK8[65]. This activation is crucial for NK cell proliferation, maturation, as well as activation[63]. Previous research also demonstrated, that CDK8 is the kinase responsible for the basal phosphorylation of STAT1-S727[81]. Our lab and others showed in mNK cells, that deletion of CDK8[84], mutation of STAT1-S727A[65], and pharmacologic inhibition of CDK8[85] led to increased NK cell cytotoxicity towards tumor cells (**Figure 3.A**). Unfortunately, CDK8 inhibitors exhibited pronounced toxicity in pre-clinical studies and thus did not meet the safety requirements for use in humans[85]. Interestingly, a Western Blot conducted with CDK8 KO mNK cells showed intact STAT1-S727 phosphorylation on basal levels and upon stimulation with cytokines (**Figure 3.B**).

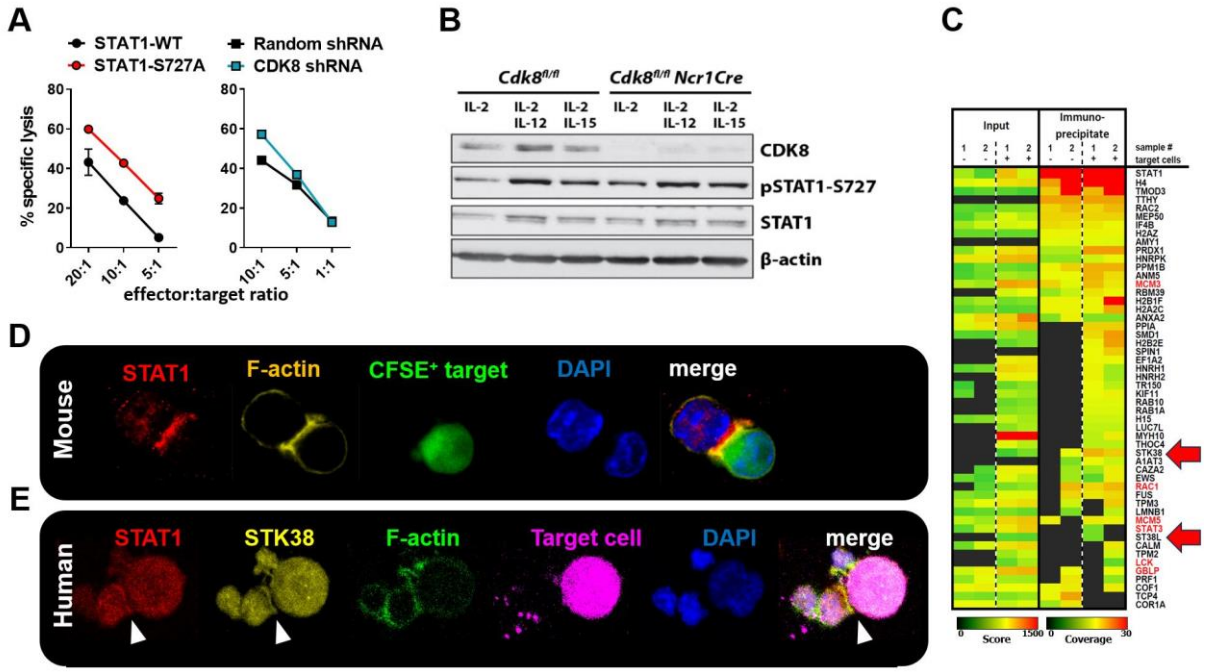

Figure 3. Preliminary data. *(A) Cytotoxicity assay with mNK cells isolated from STAT1-S727A mice (left) show increased cytotoxicity against YAC-1 tumor cells at different effector-to-target (E:T) ratios. (right) A shRNA-mediated knock-down of CDK8 in a murine NK cell line led to enhanced killing of YAC-1 target cells[65]. (B) CDK8 KO mouse NK cells show basal STAT1-S727 phosphorylation, and after stimulation with IL-2 and IL-12 or IL-2 and IL-15 for 2 hours in a Western Blot[84]. (C) Data shows the STAT1α interactome in untreated mNK cells and after co-culture with Jurkat tumor cells for 30 minutes. The FLAG-tagged STAT1 protein was immunoprecipitated, and was found in physical contact with STK38 and STK38L in NK cells stimulated with target cells[62]. (D) Confocal imaging of mNK cells, co-cultured with STAT1 KO B-ALL target cells (green, CFSE labeled) for 30 minutes, that were stained for STAT1 (red), F-actin (yellow), and DAPI (blue)[62]. (E) hNK cells were co-cultured with K562 tumor cells (pink, CTFR labeled) for 30 minutes, after which the cells were stained for STAT1 (red), STK38 (yellow), F-actin (green), and DAPI (blue) (unpublished data).*

This finding led to the hypothesis, that there is an additional upstream kinase, which is responsible for STAT1-pS727 phosphorylation and ultimately restraining NK cell cytotoxicity against tumor cells. An interactome study in mNK cells was performed to determine potential STAT1 binding partners. As prior experiments suggested that STAT1-S727 phosphorylation impacts NK cell cytotoxicity, in this assay NK cells were either left untreated or stimulated with tumor cells. Besides well-known interaction partners (highlighted in red in **Figure 1.C**), this study revealed many membrane-associated proteins as novel STAT1 binding partners. These results suggested a so far unrecognized function of STAT1 in the immunological synapse of NK cells[62]. Amongst others, upon tumor cell contact, STAT1 was shown to interact with STK38 and STK38L, which are serine-threonine kinases known to be involved in DNA damaging signaling, cell cycle progression[106], and are part of the Hippo pathway[107]. First, STAT1 localization was determined in mNK cells *via* immunofluorescence staining and confocal imaging (**Figure 3.D**). The results clearly showed an accumulation of STAT1 between the NK and tumor cell, in the immunological synapse. Preliminary unpublished data of immunofluorescence stainings revealed a co-localization of STK38 and STAT1 in the immunological synapse between hNK and K562 tumor cells (**Figure 3.E**). These data led to the question on how this non-canonical STAT1 phosphorylation occurs and whether STK38(L) are the kinases responsible for this phosphorylation.

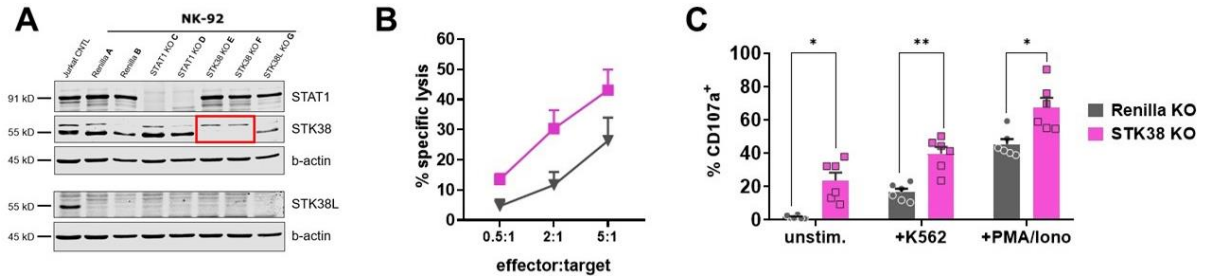

Figure 4. Preliminary data of former Master's student Susanne Stofner. *(A) NK-92 cells were transduced with lentiCRISPR v2 plasmids (Addgene, Plasmid #52961) containing Renilla, used as off-target control, or STK38 gRNA. The efficient knockout of STK38 in the NK-92 cell line was verified by Western Blot. (B) Cytotoxicity assay with NK-92 STK38 KO cells against K562 tumor cells showed increased cytotoxicity at different effector-to-target (E:T) ratios, compared to Renilla KO control. (C) NK-92 Renilla KO and STK38 KO cells were either left untreated, co-cultured with K562 cells or activated with PMA/ionomycin for 4 hours in the presence of an anti-CD107a antibody. After incubation, NK-92 cell degranulation was quantified as percentage CD107a⁺ cells via flow cytometry. Shown in (B) and (C) are means±SD of three independent experiments with n=2 cell lines per genotype.*

Former Master's student of the lab, Susanne Stofer, conducted experiments to elucidate the role of STK38(L) in NK cells. She created STK38 KO and Renilla KO NK-92 cell lines (**Figure 4.A**) and performed cytotoxicity and degranulation assays, discovering that STK38 KO NK-92 cells showed higher cytotoxicity against tumor cells compared to control (**Figure 4.B**). Further, she revealed that STK38 KO cells displayed enhanced potential to degranulate in unstimulated conditions, but also after co-culture with K562 tumor cells or after stimulation with PMA/ionomycin (**Figure 4.C**).

In conclusion, we hypothesize that, besides the canonical JAK/STAT pathway, a non-canonical STAT1 signaling pathway exists in NK cells, which is initiated during target cell killing. Upon target cell binding, STAT1-S727 is phosphorylated by STK38(L) in the immunological synapse of NK cells. This ultimately limits NK cell-mediated cytotoxicity (**Figure 5**). While colleagues are currently investigating the functional role of STK38(L) in NK cells *in vitro* as well as in tumor surveillance *in vivo*, this work focusses on the molecular details of non-canonical STAT1-S727 phosphorylation in NK cells under basal conditions and upon tumor cell killing.

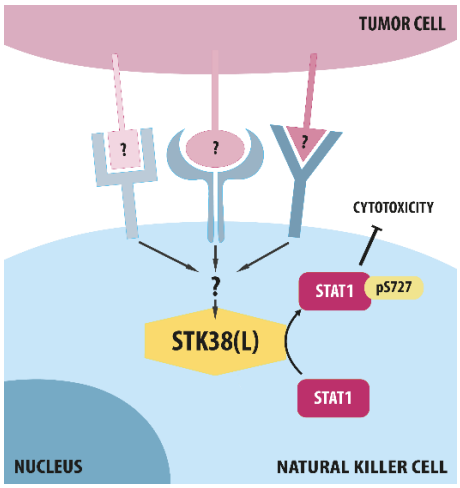

Figure 5. Hypothesis: *Upon tumor cell contact, STK38(L) phosphorylates STAT1-S727, resulting in lower NK cell cytotoxicity.*

7 AIMS

This Master thesis addresses the following three aims. The primary objective is to investigate the non-canonical phosphorylation of STAT1-S727 in NK cells upon contact with tumor cells. This is achieved by conducting stimulation- and co-culture assays with NK and tumor cells, and by analyzing STAT1-pS727 levels *via* Western blotting. The second goal is to verify, whether STK38 and/or STK38L are able to phosphorylate STAT1 on S727. This is an important step in elucidating the role of STK38(L) in non-canonical STAT1 signaling. Hence *in vitro* kinase activity assays are developed using recombinant proteins. Further, the kinases are overexpressed in HEK293T cells, and STAT1-pS727 levels are analyzed *via* Western blot. The final aim of this thesis is to determine, if STAT1 and STK38 co-localize in the immunological synapse following NK and tumor cell contact. A proximity ligation assay as well as immunofluorescence staining and confocal imaging should reveal the spatial proximity of the two proteins in NK cells, possibly enabling functional interaction. These three questions aim to provide substantial insights to further support the hypothesis that STK38(L) mediates phosphorylation of STAT1-S727 in the immunological synapse of NK cells upon tumor cell contact.

8 MATERIALS & METHODS

8.1 Lists of antibodies, materials, buffers & devices

Table 1. List of antibodies used for Western Blot (WB), Immunofluorescence (IF), and Proximity Ligation Assay (PLA).

Antibody	Manufacturer	Catalogue number	dilution for (WB/IF/PLA)
Anti-mouse IgG (H+L), F(ab')2 Fragment (Alexa Fluor® 594 Conjugate)	Cell Signaling Technology	8890	IF (1:1000)
Anti-mouse IgG, HRP-linked Antibody	Cell Signaling Technology	7076	WB (1:3000)
Anti-rabbit IgG (H+L), F(ab')2 Fragment (Alexa Fluor® 488 Conjugate)	Cell Signaling Technology	4412	IF (1:1000)
Anti-rabbit IgG, HRP-linked	Cell Signaling Technology	7074	WB (1:3000)
Anti-STK38L (165-464) (for mouse)	St John's Laboratory	STJ117601	WB (1:500)
Anti-β-Actin (13E5)	Cell Signaling Technology	4970	WB (1:1000)
Anti-CDK8 (P455)	Cell Signaling Technology	4106	WB (1:1000)
CellTrace™ Far Red Cell Proliferation Kit	Thermo Fisher Scientific	C34572	IF (1:20000) PLA (1:20000)
DAPI solution, 1mg/mL	Thermo Fisher Scientific	62248	IF (1:1000) PLA (1:1000)
DyLight 554 Phalloidin	Cell Signaling Technology	13054	IF (1:50) PLA (1:50)
Anti-HSPA8/HSC70 (B-6)	Santa Cruz Biotechnology	sc-7298	WB (1:2000)
Anti-STK38 (3A5)	Sigma-Aldrich	SAB1408832	IF (1:250 & 1:500)
Anti-NDR1 (YJ-7)	Santa Cruz Biotechnology	SC-100404	WB (1:250) IF & PLA (1:100)
Anti-Phospho-STAT1 (Ser727)	Cell Signaling Technology	9177	WB (1:1000) PLA (1:100)
Anti-Stat1 (pY701)	BD Biosciences	612132	WB (1:1000) PLA (1:100)
Anti-Stat1 (D1K9Y)	Cell Signaling Technology	14994	WB (1:1000) IF & PLA (1:200)
Anti-STAT1 (2F16)	Proteintech	82016-1-RR	WB (1:20000)
Anti-STK38 (M01), clone 2G8-1F3	Abnova	H00011329-M01	IF (1:200 & 1:100)
Anti-STK38L (OTI4D8)	Origene	TA505176	WB (1:500)
Anti-Vinculin	Cell Signaling Technology	5650	WB (1:1000)

Table 2. List of Antibodies used for Flow Cytometry.

Antibody	Manufacturer	Catalogue number	dilution for FACS
CellTrace™ Violet (CTV)	Invitrogen	C34557	1 µM
Fixable viability dye eFluor 780	Invitrogen	65-0865-18	1:1000
Fixable viability dye eFluor 450	Invitrogen	65-0863-14	1:2000
mCD3-APC	Miltenyi Biotec	130-122-943	1:200
mCD8a-FITC	BioLegend	100705	1:200
mCD45.2-PerCP	Miltenyi Biotec	130-124-087	1:400
mCD45-PE	BioLegend	103105	1:200
mNK1.1-PE-Vio770	Miltenyi Biotec	130-120-509	1:200
mNKp46-FITC	Miltenyi Biotec	130-112-200	1:100

Table 3. List of Materials and Reagents used during the course of the Master's thesis in the laboratory.

Item	Manufacturer	Catalogue number
µ-Slide Angiogenesis	Ibidi	81506
2-Mercaptoethanol	Sigma-Aldrich	M6250
2-Propanol, for molecular biology, ≥99.5%	Merck	I9516-1L
4x Laemmli Sample Buffer	BioRad	1610747
70µm cell strainer	Fisher Scientific	22444
AccuCheck Counting Beads	Invitrogen	PCB100
Acrylamid/Bis-Solution 30 (29:1) (ROTIPHORESE®)	Roth	A124.1
Ammonium persulfate (APS)	Sigma-Aldrich	A6761
ATP stock solution	Sino Biological	A50-09
BD Pharmingen™ Purified Rat Anti-Mouse CD16/CD32 (Mouse BD Fc Block™)	BD Biosciences	553141
Bovine Serum Albumin (BSA)	Sigma-Aldrich	A7906-500G
Cell stimulation cocktail 500X (PMA, Ionomycin)	Thermo Fisher Scientific	00-4970-93
Columns LS	Miltenyi Biotec	130042401
Corning® Matrigel® hESC-Qualified Matrix	Corning	354277
DMEM Medium with high glucose, Glutamax and phenol red	Gibco	41965062
Dimethyl sulfoxide (DMSO)	Sigma-Aldrich	D2438
Duolink® In Situ Detection Reagents Red	Sigma-Aldrich	DUO92008
Duolink® In Situ PLA® Probe Anti-Mouse MINUS	Sigma-Aldrich	DUO92004
Duolink® In Situ PLA® Probe Anti-Rabbit PLUS	Sigma-Aldrich	DUO92002
Duolink® In Situ Wasch Buffer	Sigma-Aldrich	DUO082049-4L
EndoFree Plasmid Maxi Kit	Qiagen	12362

Fetal Bovine Serum Advanced (FBS)	Capricorn Scientific GmbH	FBS11A
Fixation buffer	BioLegend	420801
Folic acid	Sigma-Aldrich	F87585G
Horse Serum, New Zealand origin, 500 ml	Gibco	16050122
Human Serum, from human male AB plasma, USA origin, sterile-filtered	Sigma-Aldrich	H4522-100ML
Intracellular Staining Permeabilization Wash Buffer (10X)	BioLegend	421002
Kinase Assay Buffer I	Sino Biological	K01-09
Kinase Dilution Buffer III	Sino Biological	K23-09
L-Glutamine (200 mM, 100x)	Gibco	25030024
MACS DX5 positive selection kit	Miltenyi Biotec	130-052-501
MACS® MultiStand	Miltenyi Biotec	130-042-303
MEM Non-Essential Amino Acids Solution (100X)	Thermo Fisher Scientific	11140050
Millicell EZ SLIDE 8-well glass, sterile	Merck	PEZGS0816
Minimum Essential Medium Eagle	Sigma-Aldrich	M4526-500ML
myo-Inositol	Sigma-Aldrich	I750850G
N,N,N′,N′-Tetramethylethylendiamin (TEMED)	Sigma-Aldrich	T9281-25ML
Naive CD8a+ T Cell Isolation Kit, mouse	Miltenyi Biotec	130-096-543
Nitric Acid 65%	Merck	100456
NK MACS® Basal Medium & NK MACS® Supplement (100×), human	Miltenyi Biotec	130-114-429
Normal Goat Serum	Cell Signaling Technology	5425S
PageRuler Plus Protein Ladder	Thermo Fisher Scientific	26619
Paraformaldehyde	Sigma-Aldrich	158127
Penicillin-Streptomycin (10,000 U/mL, 100x)	Gibco	15140122
Pierce™ ECL Plus Western Blotting Substrate	Thermo Fisher Scientific	32132X3
Poly-L-Lysine	Sigma-Aldrich	P4832
Power Blotter 1-Step Transfer Buffer (5x)	Invitrogen	PB7300
Power Blotter, Pre-cut Membrane and Filters, Nitrocellulose	Invitrogen	PB7320
Prolong Diamond Antifade Mountant	Thermo Fisher Scientific	P36961
Prolong Gold antifade mounting medium without Dapi	Invitrogen	P36934
PureFection™ Transfection Reagent	System Biosciences	LV750A-1
QuadroMACS™ Separator	Miltenyi Biotec	130-090-976
recombinant human IFNα	Miltenyi Biotec	130-131-352

recombinant human IFNβ	Miltenyi Biotec	130-107-889
recombinant human IL-2 (rhIL-2) protein	Miltenyi Biotec	130-097-743
recombinant human STAT1 protein	Sino Biological	S52-50G (Lot: F495-1)
recombinant human STK38/NDR protein	Sino Biological	S49-14G (Lot: E3138-8)
recombinant human STK38/NDR protein, active	Sino Biological	S49-10G (Lot: E4152-1)
recombinant human STK38L protein, active	Sino Biological	S50-10G (Lot: W3028-6)
recombinant mouse IFNβ1a	Biolegend	581302
recombinant mouse IL-15	Thermo Fisher Scientific	21015
recombinant mouse IL-7	Thermo Fisher Scientific	21717
RPMI 1640 Medium	Gibco	11875093
Sodium Chloride	Sigma-Aldrich	S3014-1KG
Sodium Pyruvate (100 mM)	Thermo Fisher Scientific	11360070
SuperSignal™ West Femto Maximum Sensitivity Substrate	Thermo Fisher Scientific	34095
Triton® X 100	Roth	3051.4
Trypsin-EDTA (0.05%), phenol red	Gibco	25300054
Tween® 20	Sigma-Aldrich	P9416-50ML

Table 4. List of buffers made and used during the course of the Master's thesis in the laboratory.

Buffer name	Components	Concentrations
MACS buffer	BSA EDTA (292.1 g/mol) diluted in PBS	0.5% 2 mM
TBS (10x)	Tris Base (121.1 g/mol) Tris-HCl (158.6 g/mol) NaCl (58.4 g/mol) ddH_2O adjust to pH 7.6	24 g 5.6 g 88 g fill up to 1000 ml
TGS (10x)	Tris Base (121.1 g/mol) Glycine (75.1 g/mol) SDS (288.4 g/mol)	0.25 mol/l 1.92 mol/l 1 w%
pY-TBS-T (10x)	Tris-HCl (158.6 g/mol) 1M NaCl (58.4 g/mol) EDTA 500mM, pH 8.0 TWEEN 20 ddH_2O	100ml 43.8 g 20 ml 10 ml fill up to 1000 ml
TBS-T (10x)	Tris Base (121.1 g/mol) Tris-HCl (158.6 g/mol) NaCl (58.4 g/mol) TWEEN 20 ddH_2O adjust to pH 7.4	24 g 5.6 g 88 g 10 ml fill up to 1000 ml
Stripping Buffer (10x)	Glycine (75.07 g/mol) SDS (288.4 g/mol)	15 g 0.1%

	TWEEN 20 ddH_2O adjust to pH 2.2	10 ml fill up to 1000 ml
4x SDS sample buffer	SDS (288.4 g/mol) Glycerol (92.1 g/mol) 2-Mercaptoethanol Orange G ddH_2O	20% 20% 10% trace amount
Lysogenic Broth (LB)	NaCl (58.4 g/mol) Tryptone Yeast extract ddH_2O to be autoclaved	10 g 10 g 5 g fill up to 1000 ml

Table 5. List of all devices used during the course of the Master's thesis in the laboratory.

Device	Manufacturer
LUNA-II™ Automated Cell Counter	Logos Biosystems
Power Blotter System	Invitrogen
ChemiDoc™ Imaging System	BIO-RAD
CytoFLEX S Flow Cytometer	Beckman Coulter
Infinite® 200 Pro Nanoquant plate reader	Tecan
AX / AX R with NSPARC Confocal Microscope System	Nikon
Confocal Microscope	Leica SP8

8.2 Cultivation of cells

Primary hNK cells were previously isolated from leukocyte reduction chambers (AKH, Blutgruppenserologie und Transfusionsmedizin 4i) by former lab members and were thawn and cultivated in NK MACS medium supplemented with 5% human serum, 1% NK MACS supplement, and 500 U/ml recombinant human IL-2 (rhIL-2) at a cell density of 0.3 million cells/ml.

The immortalized NK-92 cell line, originally derived from a non-Hodgkin's lymphoma patient, was cultured in Minimum Essential Medium Eagle (Alpha Modification, with sodium bicarbonate and Earl's salts, without L-glutamine, ribonucleosides and deoxyribonucleosides) supplemented with 12.5% fetal bovine serum (FBS), 12.5% horse serum, 2 mM L-glutamine, 0.2 mM myo-inositol, 1% penicillin/streptavidin, 0.02 mM folic acid, and 100 U/ml rhIL-2. Cells were kept at 0.3 million cells/ml. NK-92 STK38 KO, STAT1 KO, and Renilla KO cell lines were generated by former master student Susanne Stofner.

The HEK293T cell line (human embryonic kidney cells, containing SV40 T-antigen for enhanced transfection rates, and replication of transfected plasmids) was cultured in DMEM medium

supplemented with 10% FBS. For cell detachment, cells were trypsinized with 0.5% trypsin-EDTA for 3 minutes at 37°C, 5% CO_2. Cells were maintained at total maximal confluency of 90%.

Primary mouse NK (mNK) cells were isolated from spleens using the positive selection MACS DX5 positive selection kit, as described later in methods "mNK cell isolation". Cells were cultivated in cRPMI supplemented with 2500U/ml rhIL-2 and were split every 2-3 days at a ratio of 1:3.

Primary mouse $CD8^+$ T cells were isolated from spleen and mesenteric lymph nodes of C57BL/6-Tg(TcraTcrb)1100Mjb/J mice[108] using the negative selection Naive $CD8a^+$ T Cell Isolation Kit, as described later in methods "$CD8^+$ T cell isolation". Cells were cultivated in RPMI supplemented with 10% FBS, 5% penicillin/streptavidin, 1% 2-Mercaptoethanol, 1% Non-Essential Amino Acids Solution (100X), 1% Sodium Pyruvate (100 mM), 10 ng/ml rmIL-7 and 10 ng/ml rmIL-15.

The following leukemic cell lines of mouse and human origin were cultured in RPMI 1640 medium supplemented with 10% FBS, 1% penicillin/streptavidin and 50 µM 2-mercaptoethanol (cRPMI): K562 cells are human lymphoblast cells, isolated from bone marrow of a chronic myelogenous leukemia patient. K562 cells were maintained at a cell density of 0.5 million cells/ml. K562 STAT1 KO cell lines were generated by PhD student Faith Oluwakemi David using CRISPR/Cas9.

STAT1 KO v-abl^+ cells are mouse B cell acute lymphoblastic leukemia cells, originally generated by retroviral infection of bone marrow cells isolated from BALB/c mice with the v-abl oncogene, containing a knock-out of STAT1[65]. Cells were maintained at a cell density of 0.3 million cells/ml.

BCR/ABL^{p185+} cells are mouse B cell acute lymphoblastic leukemia cells, generated by Michelle Buri[109] by retroviral infection of bone marrow isolated from C57BL/6J mice with a MSCV-BCR/ABL^{p185} vector. BCR/ABL^{p185+} cells were maintained at a cell density of 0.3 million cells/ml.

The KPO STAT1 KO cell line was isolated from lung tumors, generated through inhalation of C57BL/6 K-ras^{G12D}: $p53^{\Delta/\Delta}$: $STAT1^{\Delta/\Delta}$: eGFP-OVA mice with Ad5mSPC-Cre recombinase. The cell line was generated and generously provided by Christoph Trenk from the Casanova Lab. Cells were cultured in cRPMI and 0.5% trypsin-EDTA was used for trypsinization for 10 minutes at 37°C, 5% CO_2. Cells were maintained at a maximal confluency of 95% and were split 1:10 if needed.

All cells were split every two to three days and were kept at 37°C, 5% CO_2. Cell lines were kept in culture for a maximum of 4 months, before thawing younger cells. Primary human NK cells were maintained in culture for a maximum of 5 weeks. Cell counting and cell viability analyses were performed using the LUNA-II™ Automated Cell Counter (Logos Biosystems).

8.2.1 Freezing and thawing of cells

For cryopreservation cells were counted and washed twice in cRPMI for 5 minutes at 400xg. Per cryovial, 5-10 million cells were dissolved in 0.5 ml freeze down medium, which consisted of 70% cRPMI, 20% FBS and 10% DMSO. The cryovials were placed in freezing containers at -80°C, and were transferred into liquid N_2 after a few days for long time storage.

To thaw, cryovials were placed in warm water and instantly washed with 20 ml pre-warmed cRPMI for 5 minutes at 400xg. Subsequently, cells were plated at approximately 1 million cells/ml in cell specific culture medium. The next day, cells were washed again in 20 ml cRPMI and plated at their normal cell density.

8.3 Mouse NK cell isolation

Spleens were isolated from healthy mice aged between 12 and 18 weeks. Two spleens were smashed at once through a 70µm cell strainer with a 5 ml syringe plunger and were washed twice in 5 ml PBS. The splenocytes were centrifuged at 400xg for 5 minutes, and were filtered again to remove any excess fat tissue. For mNK cell isolation the CD49b (DX5) MicroBeads positive selection kit was used, where cells are magnetically labeled with a MicroBeads-coupled anti-CD49b antibody, which is a marker for tissue-resident and circulating mNK cells. Cells were labeled according to manufacturer's instructions, loaded onto a LS MACS column, placed into the QuadroMACS™ Separator magnet, where $CD49b^+$ cells were retained in the column and unlabeled cells ran through. After complete elution of unlabeled cells and some washing steps, the column was removed from the magnet and the remaining $CD49b^+$ mNK cells were eluted into a separate tube. mNK cells were centrifuged to remove MACS buffer, and were finally plated in a concentration of two spleens per 24-well in cRPMI + 2500 U/ml rhIL-2. Cells were split 1:3 on day 2 after isolation and used on day 4 for further downstream analysis. A purity check was performed via flow cytometry, after staining the whole spleen and isolated NK cells using the following antibodies: mNKp46-FITC (1:100), mCD45.2-PerCP (1:400), mNK1.1-PE-Vio770 (1:200), mCD3-APC (1:200), and fixable viability dye eFluor780 (1:1000). Samples were stained for 10 minutes at 4°C, before washing with 1 ml PBS and centrifugation at 400xg for 5 minutes. 100 µl AccuCheck Counting Bead solution (1:9 counting beads in MACS buffer) was added per sample and cells were recorded on a CytoFLEX S Flow Cytometer and analyzed in FlowJo (version 10).

8.4 Mouse CD8+ T cell isolation

Mouse CD8+ T cells were isolated from the spleen and mesenteric lymph nodes from one OT-1 transgenic mouse. Single cells were generated by smashing spleen and lymph nodes through a 70 µm cell strainer with a 5 ml syringe plunger in CD8+ T cell medium without cytokines, and subsequently centrifuged at 300xg for 5 minutes. Cells were re-suspended in CD8+ T cell medium without cytokines and the cell number was determined. Afterwards, CD8+ cells were isolated using the negative selection Naive CD8a+ T Cell Isolation Kit (mouse), where non-target cells are magnetically labeled with biotin-conjugated monoclonal antibodies against CD4, CD11b, CD11c, CD19, CD45R, CD49b, CD105, Ter-119, MHC II, and TCRγ/δ. These antibodies are then mixed with a secondary anti-biotin antibody, bound to MicroBeads. Cells were labeled according to manufacturer's instructions and loaded onto a LS MACS column that was placed into the magnet, where unwanted, MicroBeads labeled cells were retained while unlabeled CD8+ T cells were collected as flow through. Cells were centrifuged to remove MACS buffer, and plated in a 10 cm dish in CD8+ T cell medium + 10 ng/ml rmIL-7 + 10 ng/ml rmIL-15. Cells were left to rest and were used on the fourth day after isolation.

A purity check was performed by flow cytometry. After washing with MACS buffer (500xg, 6 minutes, 4°C), Fcγ block was applied using anti-mouse CD16/CD32 monoclonal antibodies (1:100) for 30 minutes at 4°C. Subsequently, cells were washed with MACS buffer, stained with anti-mCD8a-FITC, anti-CD45-PE and a fixable viability dye eFluor780 (1:2000) for 30 minutes at 4°C, washed twice with MACS buffer, and resuspended in 250 µl MACS buffer. Stained cell suspensions were recorded on a CytoFLEX S Flow Cytometer and analyzed in FlowJo.

8.4.1 Cell lysis for protein isolation

Prior to cell lysis, cells were counted, and 1 million cells were harvested into a 1.5 ml Eppendorf tube. Cells were centrifuged at 400xg for 5 minutes, the supernatant was discarded and subsequently the pellet was washed twice with cold PBS. After the last washing step, the supernatant was completely removed and the pellet was snap frozen in liquid nitrogen. The pellet was then either stored at -20°C or cell lysis was performed immediately according to the following protocol.

The snap frozen pellet was thawed slowly on ice, mixed with 150µl SDS lysis buffer (1:4, 4x SDS sample buffer in 400mM Tris-HCl, pH 6.8), and denatured at 95°C for 20 minutes. The mixture was centrifuged at 13.000 rpm for 10 minutes, and the supernatant was transferred into a new Eppendorf tube, ready to use for Western Blot. Protein lysates were stored at -20°C.

8.5 Functional assays to assess STAT1 activation

8.5.1 Stimulation of NK cells

NK cells (NK-92, hNK, mNK) were counted, brought to a concentration of 1 million cells/ml in NK cell specific medium, and 1 or 2 ml were transferred into a 24 well plate. Tumor cells (K562 STAT1 KO or v-abl STAT1 KO) were also counted and brought to a concentration of 4 million cells/ml. Tumor cells were added into the dedicated wells to the NK cell suspension to obtain a 2:1 tumor-to-NK cell ratio. As a control, cells were stimulated with cell stimulation cocktail 500x (NK-92 1:500, hNK 1:2000, or mNK 1:500), rhIFNα (NK-92 100 ng/ml), rhIFNβ (NK-92 1000 U/ml, hNK 1000 U/ml), or rmIFN-β1a (mNK 250U/ml). The plate was centrifuged at 100xg for 1 minute, allowing NK and tumor cells to interact. Cells were incubated at 37°C for 30 minutes and harvested as described before in "*cell lysis and protein pellet preparation"*.

For the time curve experiments, tumor cells (K562 STAT1 KO) and NK cells (NK-92, hNK) were co-cultured in a 2:1 ratio, and all cells were harvested after incubation for 10, 20, 30 minutes, 1, 4, or 24 hours. Cell lysates were prepared as described before, and all protein lysates were analyzed via Western Blot.

8.5.2 Stimulation of mouse $CD8^+$ T cells

One day prior to the co-culture assay, KPO STAT1 KO cells were counted and 0.2 million cells were seeded in a 24 well plate, which resulted in approximately 90% confluency on the next day. On the day of co-culture, the medium was aspirated from KPO cells, and 1 million $CD8^+$ OT-1 T cells (1 ml) were added to the designated wells, placed on top of KPO cells. As a control, $CD8^+$ OT-1 T cells were stimulated with 500 U/ml murine IFN-β1a or with cell stimulation cocktail (1x), and were centrifuged at 100xg for 1 minute before incubating at 37°C for 30 minutes. After stimulation, cells were harvested as described in "*cell lysis and protein pellet preparation"*, and analyzed via Western Blot.

8.6 SDS-PAGE and Western Blot

SDS gels were prepared according to recipes in Table 6 in 1.5mm thick glass plates, containing 10 or 15 slots. For SDS-PAGE, 5-15µl of protein lysates, containing the protein extract of approximately 5000 – 15.000 cells, were loaded onto the gel and SDS-PAGE was performed in TGS buffer for 20 minutes at 60 V and for 90-110 minutes at 100-110 V. After separation, the proteins were transferred onto a nitrocellulose membrane via semi-dry transfer (25 V, 1.3 A, 12.5 minutes)

in Power Blotter 1-Step Transfer Buffer with the Power Blotter System. The membrane was blocked with 5% BSA for 1 hour at room temperature (RT), washed once with pY-TBS-T, and probed with primary antibodies against STAT1-pS727, STAT1-pY701, STK38, CDK8, HSC-70, β-actin, STK38L, and Vinculin (Table 1) at 4°C overnight. Before incubation with anti-STAT1 antibody the membrane was blocked with 5% skim milk. The next day, the primary antibody was removed, and the membrane was washed 3 times for 5 minutes with pY-TBS-T before incubating with secondary antibody, conjugated to horseradish peroxidase for chemiluminescent detection, for 1 hour at RT. After three washing steps for 5 minutes each with pY-TBS-T, protein bands were developed using Pierce™ ECL Plus Western Blotting Substrate or SuperSignal™ West Femto Maximum Sensitivity Substrate according to the manufacturer's recommendation. Chemiluminescence was detected using the ChemiDoc™ Imaging System. If STAT1-pY701 or STAT1-pS727 was detected on a membrane, the membrane was stripped before proceeding with STAT1 primary antibody incubation. For membrane stripping, the membrane was incubated with 20 ml stripping buffer at 37°C for 20-30 minutes, and was then placed on the shaker for an additional 15 minutes, before washing once with pY-TBS-T and blocking with 5% skim milk for 1 hour at RT. Next, the membrane was incubated with the secondary antibody again to verify, whether stripping had worked. After the detection process, the membrane was washed once with pY-TBS-T, and was finally incubated with the next primary antibody overnight. All primary antibodies used for Western Blot (Table 1) were incubated overnight, except for HSC-70, which was incubated on a shaker for 1 hour at 4°C. All primary and secondary antibodies, as well as blocking solutions were diluted in pY-TBS-T. Image Studio Lite Ver 5.2.5 was used for membrane visualization, editing, and quantification.

Table 6. Recipe for 2 mini gels for SDS-PAGE: 7% separation gel and 5% stacking gel.

Separation Gel 7%		Stacking Gel 5%	
H_2O	9.9 ml	H_2O	4.15 ml
1.5 M Tris-HCl pH 8.8	5 ml	1.0 M Tris-HCl pH 8.8	0.75 ml
10% SDS	0.2 ml	10% SDS	0.06 ml
Acrylamide	4.7 ml	Acrylamide	1.0 ml
10% APS	0.2 ml	10% APS	0.06 ml
TEMED	0.02 ml	TEMED	0.006 ml

8.7 Maxi Prep

Expression vectors (see Table 7) containing a FLAG-tagged hSTK38 and green fluorescent protein (GFP) (1) or GFP only (2) were obtained from VectorBuilder as Escherichia (E.) coli glycerol stocks (15% glycerol). For amplification, 300 µl pre-warmed liquid Lysogeny Broth (LB)

was inoculated with 1 µl thawed glycerol stock, and was incubated on a shaker at 200 rpm at 37°C for 30 minutes. Next, E. coli were plated on LB agar plates (10^{-3} dilution) containing 100 µg/ml ampicillin, to select for bacteria containing the desired plasmid harboring ampicillin resistance, and were incubated at 37°C overnight. The next day, three individual colonies from each plate were picked, pre-expanded in 2 ml liquid LB for 8 hours shaking at 200 rpm at 37°C, and finally grown overnight in 200 ml liquid LB (37°C, 200 rpm). The following day, plasmids were isolated from E. coli and purified using EndoFree Plasmid Maxikit following the manufacturer's protocol including minor changes. All centrifugation steps were carried out at 4000 rpm for 20 minutes, instead of 4700 rpm for 15 minutes due to centrifuge limitations. Concentration of the purified DNA was measured using the Infinite® 200 Pro Nanoquant plate reader.

Table 7. Details of hSTK38-containing (1) or empty control vectors (2) in One Shot™ Stbl3™ chemically competent E. coli.

Nr.	Vector name (size)	overexpression
1	pRP[Exp]-Puro-CAG>FLAG/hSTK38[NM_001305102.2]/P2A/EGFP (7776 bp)	hSTK38
2	pRP[Exp]-Puro-CAG>EGFP (6291 bp)	empty control

8.8 HEK293T cell transfection

The HEK293T cell line is frequently used for transfection due to the expression of an SV40 T-antigen, which promotes high transfection efficiency. Cells were used at 80% confluency in a 10 cm dish on the day of transfection. The PureFection reagent consists of nanoparticles, which are automatically assembled in the presence of DNA, and easily internalized by target cells. The transfection was performed using PureFection™ Transfection Reagent and following manufacturer's protocol using 15 µg per DNA plasmid (Table 7). After 30 hours, the transfection efficiency was assessed via flow cytometry gating on $eGFP^+$ cells compared to an untransduced sample.

8.9 Kinase activity assay

For the kinase activity assay full-length recombinant human proteins expressed by baculovirus in Sf9 insect cells containing an N-terminal GST tag were used. Kinases (NDR1, NDR1 active, and NDR2 active) were co-incubated with STAT1 and ATP to observe whether the kinases are able to mediate the phosphorylation on STAT1-S727. As negative control STAT1 + ATP only was used. Proteins were stored at –80°C, and kinase assay buffers and ATP stock solution were stored at -20°C. All reagents were kept on ice during assay preparation.

4 µl of 0.1 µg/µl of each NDR kinase (NDR1, NDR1 active, and NDR2 active) were diluted in 16 µl kinase dilution buffer III, resulting in 400 ng of each protein. As negative control, no NDR protein was added, instead 20 µl kinase dilution buffer III was placed into an Eppendorf tube to obtain an equal volume. Next, a 500 µM ATP solution was prepared by diluting the 10 mM ATP stock solution 1:20. For the STAT1 + ATP master mix, 2 µl of 0.2 µg/µl STAT1 and 3.3 µl of 500 µM ATP were added to 7.7 µl kinase assay buffer I, which added up to 13 µl per condition. Finally, 13 µl STAT1 + ATP master mix were added to the 20 µl kinase solution or control tubes, which added up to a final concentration of 400 ng STAT1 and 50 µM ATP. During assay development, different STAT1-to-kinase ratios were tested, but the here described 1:1 ratio showed the best results. All tubes were briefly centrifuged and immediately incubated at 37°C for 30 minutes. After incubation, 11 µl 4x Laemmli buffer was added per condition to lyse the proteins followed by denaturation at 95°C for 5 minutes. Subsequently, 5-7 µl of the protein lysates were analyzed with Western Blot using a 7% separating gel and a 5% stacking gel.

8.10 Immunofluorescence staining

Glass plates were pre-treated overnight with concentrated HNO_3, to remove all traces of grease. After acid removal, plates were washed twice with ddH_2O and fully dried. To enhance cell adhesion to the glass surface, plates were coated with 150 µl poly-L-lysine per well for 5 minutes, subsequently washed three times with ddH_2O, and dried overnight at 4°C. The following day, tumor cells (K562, p185 or v-abl$^+$) were counted, and the desired number of cells was washed in warm PBS. Cells were stained with 0.05 µM (1:20.000) Cell Trace Far Red for 20 minutes at 37°C. Afterwards, 20 ml cRPMI was added to stop the reaction, and the cells were incubated for an additional 5 minutes in the dark, before being centrifuged at 400xg for 5 minutes. Tumor cells were re-counted and brought to a concentration of 0.5 million cells per 100 µl. Per well, a total of 0.5 million cells in 100µl medium were plated, which means 0.5 million cells from one cell line for control wells and single stains, or for co-culture of NK and tumor cells 0.25 million cells of each cell type. NK cells (hNK or NK-92) were counted and the respective cell number was added into the designated wells. After plating, glass plates were centrifuged at 100xg for 2 minutes to facilitate the interaction between NK and tumor cells. Cells were incubated for 15 minutes at 37°C and then immediately put on ice. After careful washing with PBS once, 3% paraformaldehyde was added for cell fixation and incubated for 15 minutes at RT. Cells were washed once with PBS and neutralized with 50 mM NH_4Cl for 30 minutes at RT, before being centrifuged at 300xg for 2 minutes. Next, 0.1% Triton-100 in PBS was added for 10 minutes at RT to achieve cell permeabilization. Cells were washed twice with TBS for 30 minutes at 4°C, and were then blocked in 2.5% goat serum in TBS for 100 minutes at RT. Primary antibodies (Table 1) diluted in 1% goat

serum in TBS-T were added without further washing, and plates were placed on the shaker for the first 20 minutes of incubation, and left overnight without shaking in the dark at 4°C.

The following day, cells were washed three times with TBS-T for 10 minutes at 4°C, and secondary antibodies (Table 1) diluted in 5% goat serum in TBS-T were incubated for 90 minutes at 4°C in the dark. Meanwhile, DAPI was diluted in TBS and filtered once through 0.2 µm filter to remove dye aggregates. Phalloidin dilution was prepared in DAPI working solution. After the incubation with the secondary antibody, cells were washed twice with TBS-T, and TBS for 10 minutes each, before incubating with DAPI + Phalloidin for 15 minutes. Eventually, any remaining solution was aspired and glass plates were taken apart. For the last wash, plates were dipped twice into TBS and once into ddH_2O and were left to dry for 30 minutes to one hour. The glass plates were embedded in mounting medium and a cover slip was put on top. The finished plates were stored at 4°C in the dark and were imaged after maximum 5 days using an AX / AX R with NSPARC Confocal Microscope System by Nikon.

8.11 Proximity Ligation Assay

For the Proximity Ligation Assay (PLA) the Duolink® PLA Fluorescence Protocol from Sigma-Aldrich was used. Prior to beginning, wash buffers A and B were diluted according to manufacturer's recommendations. For enhanced cell adhesion, µ-Slides Angiogenesis were coated with poly-L-lysine for hNK and tumor cells (K562) as described in "Immunofluorescence staining", and with Matrigel for NK-92 cells. Matrigel, which had been kept at 4°C to prevent solidification at RT, was pipetted into each well. After 1 minute of incubation at RT, the Matrigel was removed and the slides were dried overnight at 37°C. The following day, K562 cells were counted and labeled with 0.05 µM Cell Trace Far Red as previously described. NK cells (hNK and NK-92) and K562 were brought to a concentration of 2 million cells/ml. In total, 0.1 million cells were plated per well in a final volume of 50 µl. NK and tumor cells were co-cultured in a E:T ratio of 1:1. As control, cells were stimulated with PMA (1:500 for NK-92, 1:2000 for hNK) or 1000 U/ml rhIFNβ. Before incubation, slides were centrifuged at 100xg for 2 minutes. For unstimulated controls and co-cultures, primary hNK cells were incubated for 5 minutes, while NK-92 cells were incubated for 15 minutes. Cells stimulated with PMA or IFNβ were incubated for 20 minutes at 37°C. All cells were subsequently washed once with PBS. Cell fixation, neutralization, and permeabilization were carried out as previously described in "Immunofluorescence staining". For blocking, 15 µl of Duolink® Blocking Solution was added to each sample, and slides were incubated in a humidity chamber sealed with parafilm for 1 hour at 37°C. Blocking solution was aspired from the wells and primary antibodies (anti-STK38, -STAT1, -pS-STAT1, -pY-STAT1, see Table 1) were incubated diluted in Duolink® Antibody Diluent in a humidity chamber at 4°C overnight.

The next day, probe incubation, ligation, and amplification were carried out according to manufacturer's recommendations, with minor changes regarding reaction volumes per well. For probe incubation, the final reaction volume was 15 µl, resulting in 3 µl of Duolink® Anti-Rabbit PLUS, 3 µl Duolink® Anti-Rabbit MINUS, and 9 µl Duolink® Antibody Diluent. For the ligation procedure, 3 µl 5x Duolink® Ligation buffer were diluted in 11.625 µl MilliQ water and 0.375 µl Ligase was added. For amplification, 3 µl 5x Duolink® Amplification buffer were diluted in 14.81 µl MilliQ water and mixed with 0.1875 µl Polymerase. The amplification solution was aspired from the slides, and cells were washed twice for 10 minutes with wash buffer B at RT. Cells were incubated for 15 minutes at RT in a 1:1000 DAPI and 1:50 phalloidin solution in PBS. Afterward, slides were washed once with and 0.01x wash buffer B for 10 minutes and for 1 minute, respectively. Excess buffer was aspired from all wells and slides were mounted with Prolong Gold mounting medium without DAPI. Slides were imaged the next day on a SP8 Confocal Microscope (Leica), and were finally stored at 4°C in the dark.

8.12 Cytotoxicity Assay

K562 tumor cells were counted and washed once with PBS. Cells were stained with 1 µM CellTrace™ Violet (CTV) in PBS for 20 minutes at 37°C, during which the tube was inverted two to three times. The staining reaction was stopped by adding 10 ml cRPMI and incubating an additional 5 minutes in the dark at RT. Cells were centrifuged at 300xg for 5 minutes and resuspended in NK-92 medium without rhIL-2 at a concentration of 1 million cells per ml. NK-92 cells were counted and serial dilutions for the following effector target ratios: 5:1, 2:1, and 0.5:1 and a final volume per well of 50 µl were prepared. 50 µl tumor cells, which equaled 50.000 tumor cells per well, and 50 µl of the designated dilution of NK-92 cells were added into a 96-U well plate and centrifuged at 100xg for 2 minutes. Cells were incubated for 4 hours at 37°C. After incubation, cells were washed with PBS, centrifuged at 400xg for 10 minutes at 4°C, and incubated in 50 µl Fixable viability dye eFluor 780 1:1000 in PBS for 20 minutes at 4°C. Cells were washed again with PBS and subsequently fixed with 200 µl Fixation Buffer for 20 minutes at RT in the dark. The plate was centrifuged at 400xg for 10 minutes at 4°C, cells were resuspended in 150 µl MACS buffer and were analyzed using flow cytometry gating on single CTV+ tumor cells and determining the proportion of dead cells (Fixable viability dye+). The specific lysis of tumor cells (%) was calculated using the following formula:

$$\%\ specific\ lysis = \frac{(dead\ tumor\ cells\ after\ co-culture - spontaneous\ lysis)}{(100 - spontaneous\ lysis)} * 100$$

8.13 Statistics

All statistical analyses were performed using GraphPad Prism 8.0.1 program. To pool multiple independently conducted kinase assay experiments, a paired t-test was used to compare the control and experimental groups. In general, the significance level α was set to 0.05, which considered every value below 0.05 as significant and was marked with one (*) star. Further, p values lower than 0.01 or 0.001 were marked with two (**), three (***), and four (****) stars, respectively.

9 RESULTS

9.1 STK38 deficiency boosts NK cell-mediated cytotoxicity

The previous finding that STK38 KO NK-92 cells show increased cytotoxicity compared to Renilla KO control cells is of utter importance for further experiments, and was thus re-evaluated in this thesis. A cytotoxicity assay was performed in which Renilla KO and STK38 KO NK-92 cells were co-incubated with CTV$^+$ stained K562 tumor cells for 4 hours at different effector to target ratios. After co-culture, cells were stained with fixable viability dye to visualize dead cells, and were analyzed by flow cytometry. **Figure 6.A** shows that the specific lysis of tumor cells was considerably higher when co-cultured with STK38 KO NK-92 cells compared to Renilla KO control. These data are the basis for the hypothesis discussed above and are crucial for further evaluation of the role of STK38(L) in the novel, non-canonical STAT1 signaling pathway.

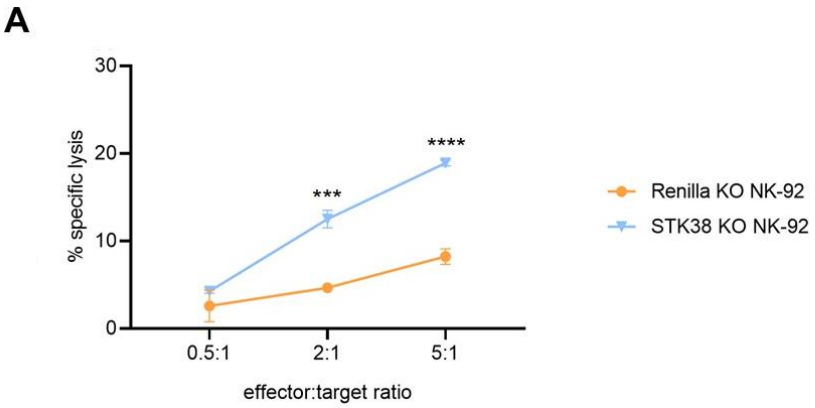

Figure 6. STK38 KO NK-92 cells show enhanced cytotoxicity against K562 cells. *A 4-hour cytotoxicity assay was performed using Renilla KO or STK38 KO NK-92 cells co-incubated with CTV-stained K562 target cells at different effector:target ratios. (A) Data shows the percentage of specific lysis of K562 tumor cells after co-incubation with Renilla KO or STK38 KO NK-92 cells. Shown are means±SD of one experiment, which was performed in technical triplicates. (B) The actual effector:target cell ratio of NK-92 Renilla KO and STK38 KO to K562 cells was plotted as mean of technical triplicates. E:T: effector (NK-92) to target (K562) cell ratio. (unpaired T test p values: 2:1 ratio *** 0.0002, 5:1 ratio **** <0.0001).*

9.2 Non-canonical phosphorylation of STAT1-S727 in NK cells

Previous data showed that STAT1-S727 phosphorylation represents an inhibitory signal, limiting NK cell cytotoxicity. Given the physical interaction between STAT1 and STK38(L) in mNK cells during co-culture with tumor cells, we hypothesized that STAT1 may be phosphorylated on S727 in response to target cell contact. To explore this non-canonical STAT1 activation, co-culture and activation assays were performed with human NK cells, the human NK-92 cell line, mouse NK cells, as well as murine CD8$^+$ T cells.

9.2.1 Co-culture of NK cells with tumor cells induces STAT1-pS727

Human NK cells were co-cultured with K562 tumor cells or activated with rhIFNβ or phorbol 12-myristate 13-acetate (PMA) and ionomycin for 30 minutes. STAT1-S727 phosphorylation was assessed by Western blotting. To ensure detection of STAT1 exclusively from NK cells, K562 tumor cells were genetically modified to lack STAT1 by generating a STAT1 KO cell line using CRISPR/Cas9. PMA/ionomycin served as positive control to induce maximal cellular activation, as

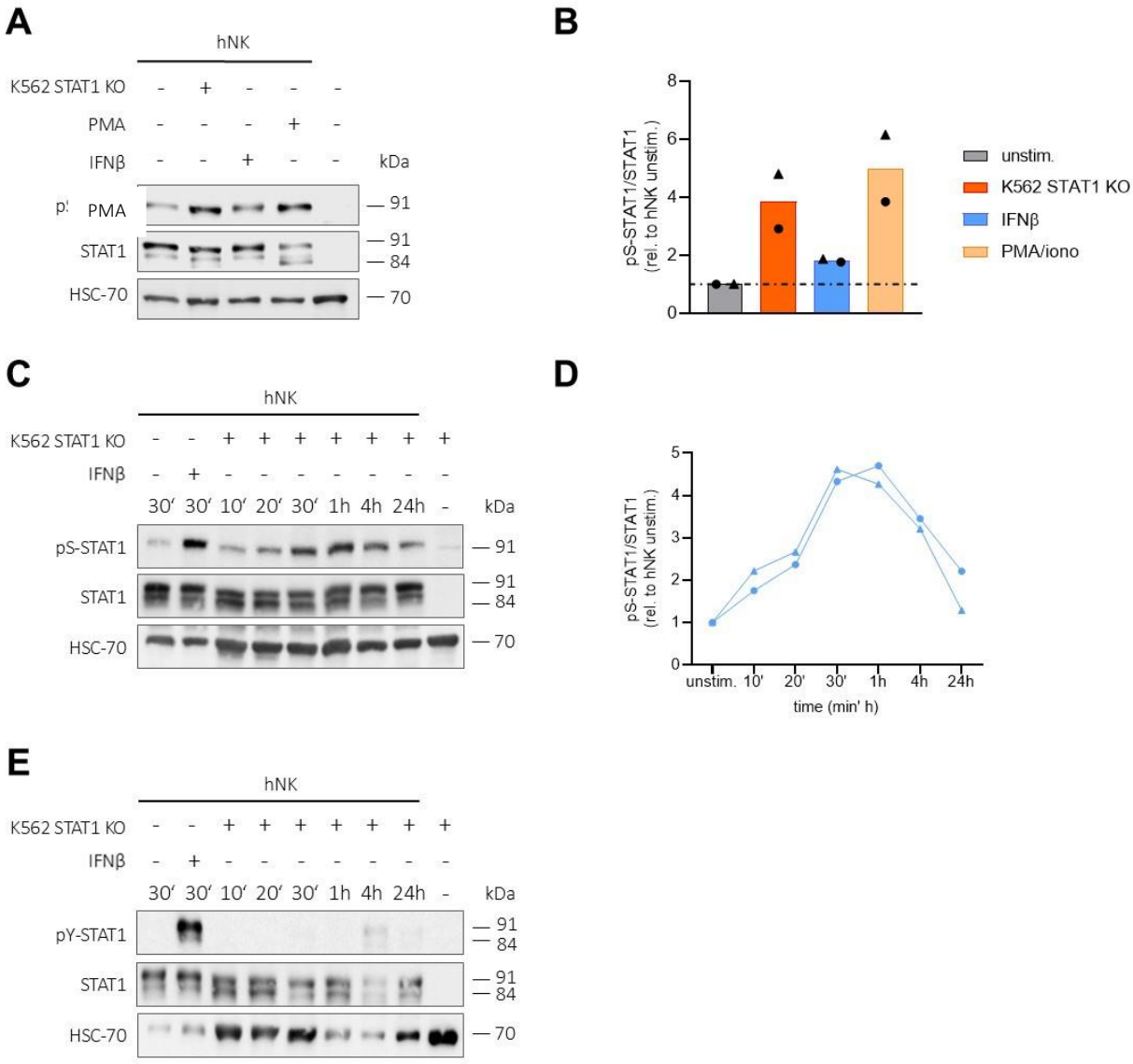

Figure 7. Stimulation of human NK cells with tumor cells leads to a peak in STAT1-pS727 levels after 1 hour. *(A) Primary hNK cells were co-cultured with STAT1 KO K562 tumor cells or activated with PMA or rhIFNβ for 30 minutes. STAT1-pS727 levels were assessed by Western blotting. (B, D) Western Blot results were quantified using Image Studio 5.5 program. Data shows STAT1-S727 levels normalized to total STAT1 protein in hNK cells, relative to unstimulated controls, from two independent experiments. (B) Summary data are presented as mean values. (C, E) Primary human NK cells were co-cultured with STAT1 KO K562 cells for different time points ranging from 10 minutes to 24 hours and (C) STAT1-pS727 or (E) STAT1-pY701 were analyzed by Western blotting. PMA stimulation was used as positive control for STAT1-pS727, while rhIFNβ treatment was used as positive control for STAT1-pY701. kDa: kilo Dalton, unstim.: unstimulated*

it stimulates Ca^{2+}/calmodulin-dependent signaling pathways mimicking NK cell receptor engagement, which induces Ca^{2+} influx and subsequent cell stimulation[110,111]. rhIFNβ was used as a primary inducer and activator of canonical STAT1 signaling. After stimulation, cells were lysed and STAT1-pS727 levels were analyzed *via* Western blot (**Figure 7**.**A**). Notably, STAT1-pS727 only appears as a single band at 91 kDa, as only the STAT1α isoform harbors this phosphorylation site, while STAT1β lacks 38 amino acids, including the STAT1-S727 residue[112]. In contrast, STAT1-pY701 occurs on both STAT1 isoforms, STAT1α and STAT1β at 91 kDa and 84 kDa, respectively. Unstimulated hNK cells served as negative control. As shown in **Figure 7**.**B,** co-culture with tumor cells strongly induced STAT1-pS727 compared to unstimulated- or rhIFNβ-stimulated hNK cells. PMA/ionomycin stimulation induced the strongest phosphorylation, as expected, due to its potent and broad activation of Ca^{2+}-dependent kinases. To evaluate the peak of phosphorylation, time-course experiments were conducted, in which hNK cells were co-cultured with STAT1 KO K562 cells for up to 24 hours. As displayed, (**Figure 7**.**C-D**) STAT1-S727 phosphorylation reached its maximum after 30 minutes to 1 hour of co-culture, before declining again to almost baseline phosphorylation levels after 24 hours. Interestingly, analysis of the same cell lysates for STAT1-Y701 phosphorylation mostly showed induction in the positive control PMA/ionomycin condition, and only a very faint band in co-cultured NK cells after four hours (**Figure 7**.**E**). This indicates, that STAT1 activation in response to tumor cell contact occurs independently of the canonical JAK/STAT signaling, suggesting a potential non-canonical signaling mechanism.

To further elucidate the STAT1-S727 phosphorylation in NK cells after tumor cell contact, time-course experiments the malignant NK cell line NK-92 were conducted. **Figure 8.A** presents a Western blot of the parental NK-92 cell line after co-culture with STAT1 KO K562 tumor cells or stimulation with PMA/ionomycin as positive control. STAT1-pS727 levels, normalized to total STAT1 protein, peaked at 24 hours (**Figure 8.B**), differing from the earlier peak observed in time course experiments with primary hNK cells. This phenomenon could originate from two possible factors. First, based on our lab's experience, NK-92 cells exhibit slower killing, which may explain the delayed activation of STAT1-S727 phosphorylation during co-culture. In contrast, other studies have reported, that NK-92 cells form twice as many cell contacts, which lead to a more rapid target cell death with shorter contact durations, compared to primary hNK cells. If the STAT1-S727 phosphorylation is indeed induced by receptor-mediated interactions with tumor cells, these cellular engagement dynamics could also account for the slower increase of pS727 levels in NK-92 cells. Further experiments need to be performed to confirm the before mentioned hypotheses. **Figure 8.C** displays STAT1-pY701 levels in NK-92 cells after co-culture with tumor cells for up to 24 hours. Similar to primary hNK cells, STAT1-Y701 phosphorylation was observed only after rhIFNβ stimulation confirming that tumor cell contact does not activate the canonical JAK/STAT pathway in this context.

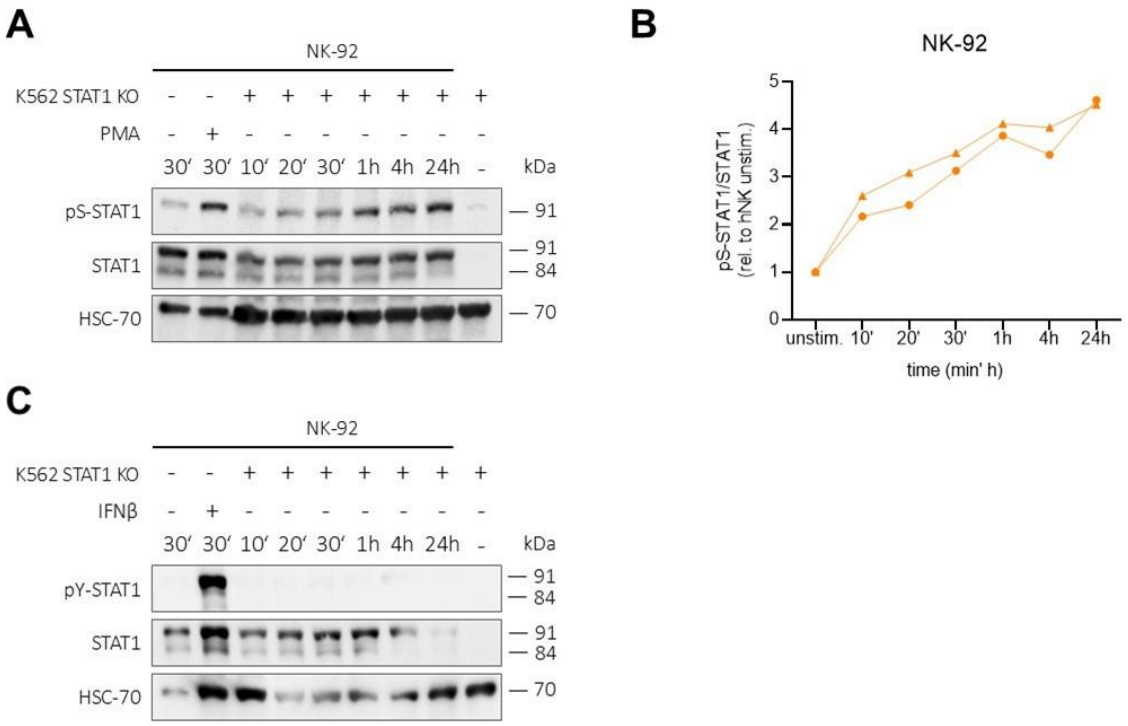

Figure 8. Co-culture of NK-92 cells with STAT1 KO K562 tumor cells induces STAT1-S727 phosphorylation. *(A, C) NK-92 cells were co-cultured with STAT1 KO K562 cells for various time points ranging from 10 minutes to 24 hours. (A) STAT1-pS727 and (C) STAT1-pY701 levels were analyzed by Western blotting. (B) Western blot data from two independent experiments was quantified, showing STAT1-pS727 levels normalized to total STAT1 protein in NK-92 cells. KO: knock-out*

9.2.2 STK38 influences STAT1-S727 phosphorylation

To investigate whether the serine-threonine kinases STK38 and STK38L, identified in the STAT1 interactome study conducted in NK cells stimulated with tumor cells, impact STAT1-S727 phosphorylation, STK38 KO and Renilla KO (control) NK-92 cell lines, as well as hNK cells harboring a CRISPR-mediated knock-down of STK38 were used for co-incubation and activation assays (**Figure 9**).

STK38 KO and Renilla KO NK-92 cell lines (generated by Susanne Stofner, a former Master's student of the lab) were co-incubated with STAT1 KO K562 tumor cells or activated with PMA/ionomycin or rhIFNβ for 30 minutes. Western Blot analysis was performed to quantify STAT1-pS727 levels (**Figure 9.A-B**). Normalizing STAT1-pS727 to total STAT1 levels in unstimulated Renilla KO NK-92 control cells showed that STK38 deficiency generally reduced STAT1-pS727 levels in NK-92 cells, especially in samples stimulated with tumor cells. Notably, the basal phosphorylation levels were also reduced in the unstimulated condition, suggesting a possible cross-talk of STK38(L) to CDK8 signaling, as CDK8 was identified as the kinase responsible for basal STAT1-S727 phosphorylation.

To reproduce those findings in primary NK cells, similar experiments were conducted using hNK cells isolated from healthy donors harboring a CRISPR/Cas9 mediated knock-down of STK38 (cells were generated and kindly provided by Faith O. David, a PhD student in the lab). As negative control, hNK cells were electroporated with a FITC dextran (150 kDa) matching the size of the CRISPR/Cas9 complex. In the upper section of the Western blot (**Figure 9.C**), STAT1-Y701 phosphorylation was assessed and is displayed in **Figure 9.D**. Interestingly, hNK cells with STK38

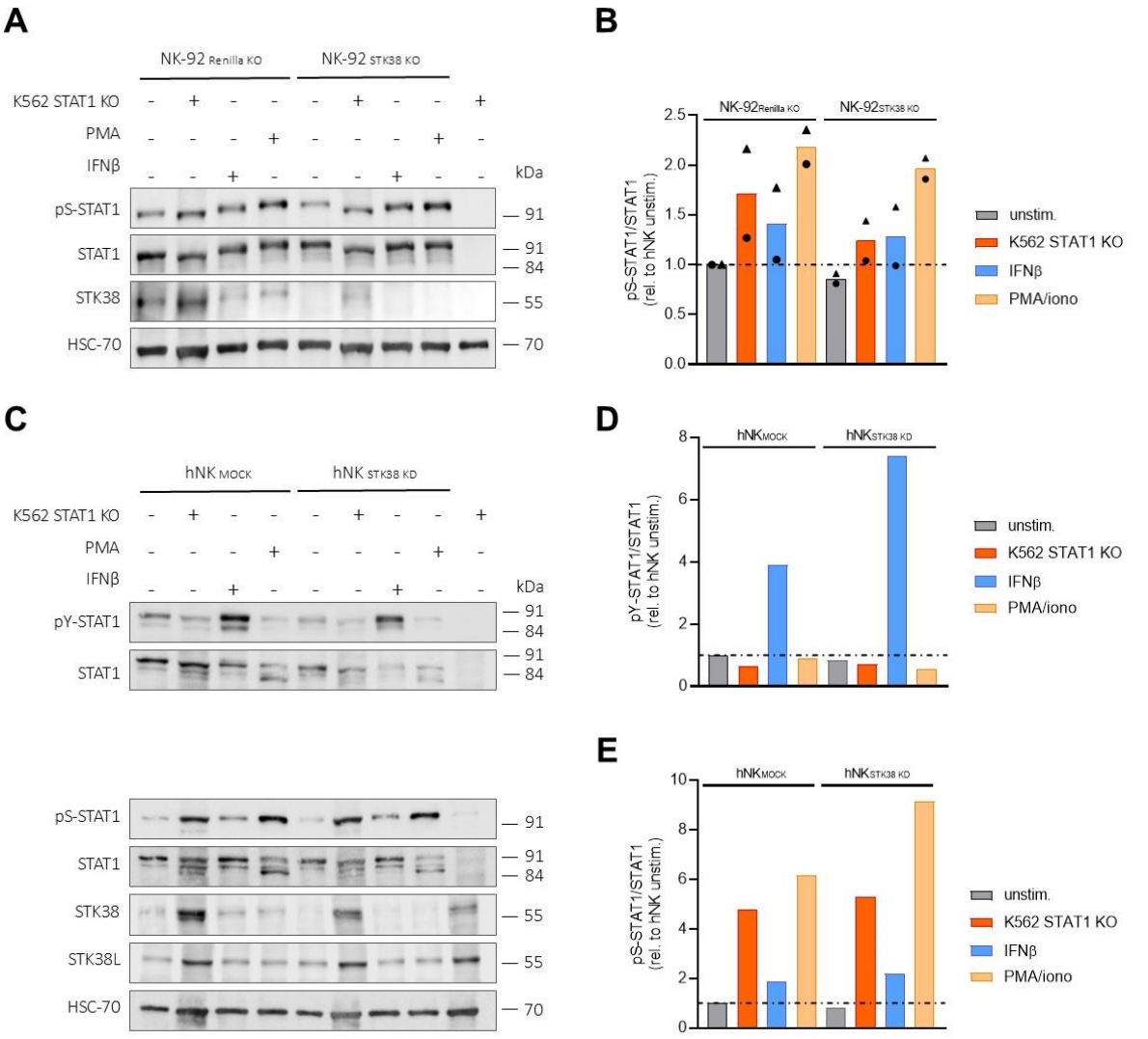

Figure 9. STK38 ablation in NK-92 cells reduces STAT1-S727 phosphorylation after co-culture, while STK38 knock-down in primary hNK cells does not have an effect on STAT1-S727 phosphorylation. *(A) STK38 KO and Renilla KO NK-92 were co-cultured with STAT1 KO K562 tumor cells or activated with PMA or rhIFNβ for 30 minutes and STAT1-S727 phosphorylation levels were compared by Western blotting. (B) Quantification of two independent Western blot experiments shows the level of STAT1-pS727 in Renilla KO and STK38 KO NK-92 cell lines, normalized to total STAT1 levels, relative to unstimulated Renilla KO NK-92 cells. (C) Primary hNK cells harboring a CRISPR/Cas9-mediated STK38 knock-down or mock electroporated control cells, were co-cultured with STAT1 KO K562 cells or stimulated with PMA or rhIFNβ for 30 minutes. STAT1-pY701 (upper section) and STAT1-pS727 (lower section) protein levels were assessed via Western blot. (D-E) Data shows quantified protein levels of (D) STAT1-pY701 or (E) STAT1-pS727, normalized to total STAT1 and relative to unstimulated mock electroporated hNK cells. MOCK: electroporation control with Fluorescein isothiocyanate dextran 150 kDa, KD: knock-down*

knock-down showed a stronger induction of STAT1-Y701 phosphorylation compared to control cells in response to rhIFNβ (**Figure 9.D**). Similarly, also PMA-induced STAT1-S727 phosphorylation levels were higher upon knock-down of STK38 in hNK cells (**Figure 9.E**). In this preliminary data set (n=1), we could however not detect any obvious differences in the phosphorylation of STAT1-S727 in hNK cells stimulated with tumor cells.

Taken together, the preliminary observations in hNK and NK-92 cells are incongruent, which could be explained by the fact that the primary hNK cells only carried an incomplete STK38 knock-down, and residual protein levels could have influenced STAT1 phosphorylation. Further, while NK-92 cells completely lack STK38L expression (**Figure 2.A**), hNK cells express significant levels of STK38L, which could potentially compensate for the reduced STK38 levels by promoting STAT1-S727 phosphorylation. It is noteworthy, however, that **Figure 9.C-E** only represent preliminary data from a single experiment containing considerable variability due to the complexity and number of individual steps and methods. Therefore, to be able to draw final conclusions, this experiment needs to be repeated.

9.2.3 Non-canonical STAT1 signaling in mouse NK and CD8⁺ T cells

To further explore non-canonical STAT1 signaling beyond human NK cells, the experimental setup was extended to include immune cells isolated from mice. Murine NK cells were isolated from spleens of NDR1 WT or KO mice and activated either through co-culture with STAT1 KO v-abl⁺ B-ALL tumor cells or stimulated with rmIFNβ or PMA/ionomycin for 30 minutes (**Figure 10.A**)**.** It became immediately apparent that mNK cells isolated from NDR1 KO mice exhibited lower levels of total STAT1 protein, hence also presented reduced levels of STAT1-pS727. This finding will be further discussed later in this work (chapter 6.2.4). In **Figure 10.B**, STAT1-pS727 protein levels, relative to total STAT1 and normalized to unstimulated mNK cells, of NDR1 KO versus WT mNK cells were compared. NDR1 KO mNK cells showed drastically reduced absolute levels of STAT1-pS727, however, this reduction was less pronounced when normalized to total STAT1. Nevertheless, NDR1 KO mNK cells consistently displayed lower relative STAT1-S727 phosphorylation under all experimental conditions, including standard culture, stimulation with rmIFNβ, PMA/ionomycin, or co-culture with STAT1 KO v-abl⁺ B-ALL tumor cells.

To elevate the study of the non-canonical STAT1 phosphorylation upon tumor cell contact further, mouse CD8⁺ T cells were inspected for comparable signaling behavior. CD8⁺ T cells and NK cells share several functional as well as molecular similarities, particularly with regard to target cell killing. Therefore, analyzing both cell types in parallel could provide valuable insights. CD8⁺ T cells were isolated from the spleen and mesenteric lymph nodes of OT-1 transgenic mice and co-

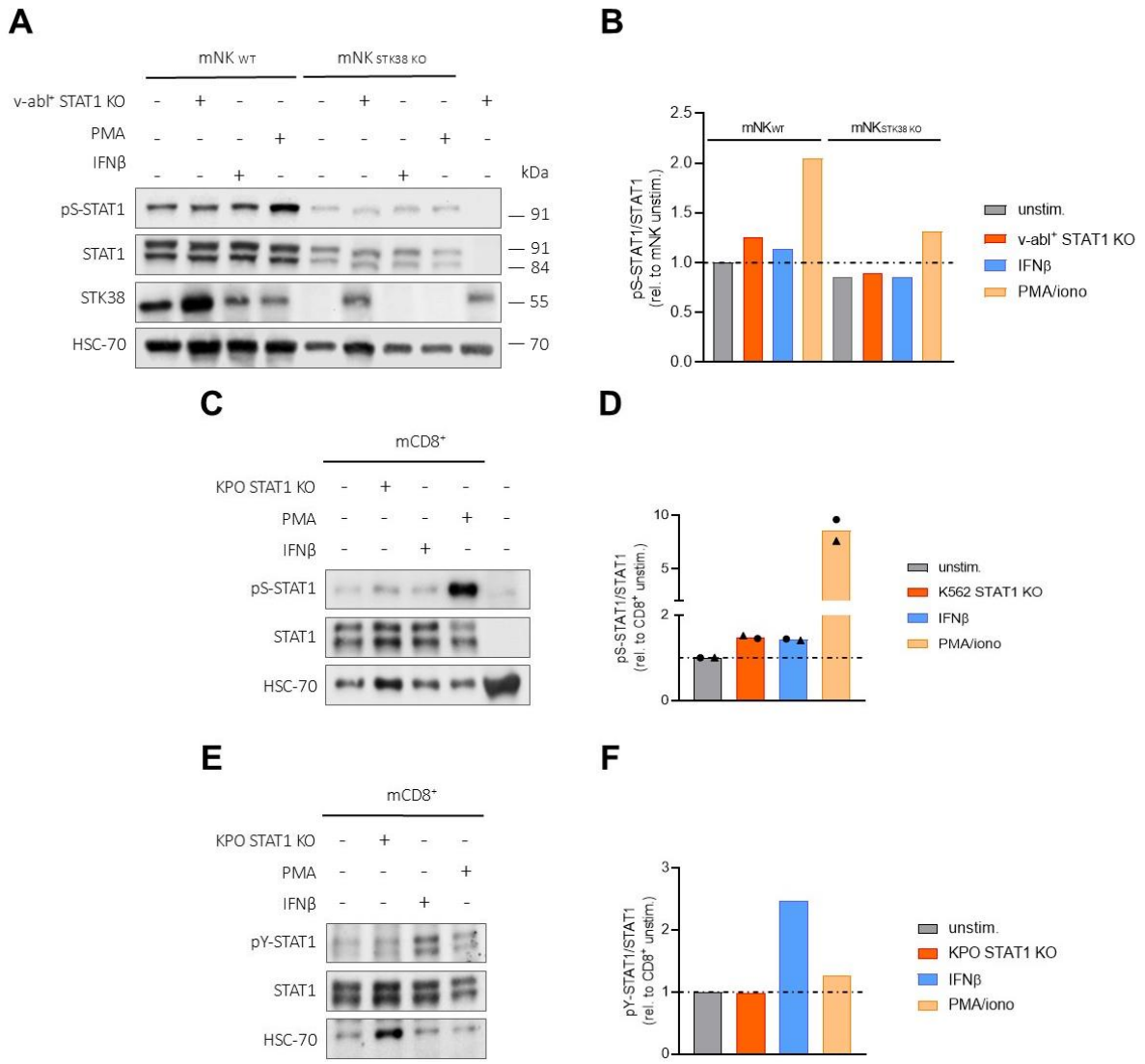

Figure 10. Mouse NK and CD8⁺ T cells show induction of STAT1-pS727 after tumor cell co-culture. *(A) Mouse NK cells, isolated from spleens of NDR1 WT or KO mice, were either co-cultured with STAT1 KO v-abl⁺ B-ALL tumor cells or activated with rmIFNβ or PMA/ionomycin for 30 minutes. Western Blot analysis shows STAT1-pS727 levels which were quantified in (B) and plotted normalized to total STAT1 protein levels and relative to unstimulated WT mNK cells. (C-E) Mouse CD8⁺ T cells, isolated from the spleens and mesenteric lymph nodes of OT-1 transgenic mice, were co-incubated with STAT1 KO KPO lung adenocarcinoma cells or stimulated with rmIFNβ or PMA/ionomycin for 30 minutes. Western Blot analysis was performed to assess (C) STAT1-pS727 and (E) STAT1-pY701 phosphorylation. The data was quantified to display (D) STAT1-pS727 (n=2) and (F) STAT1-pY701 (n=1) relative to total STAT1 protein levels, normalized to unstimulated CD8⁺ T cells.*

cultured with ovalbumin-expressing STAT1 KO KPO lung adenocarcinoma cells, or stimulated with rmIFNβ or PMA/ionomycin for 30 minutes. Western Blot data illustrating STAT1-pS727 and -Y701 levels are depicted in **Figure 10.C** and **Figure 10.E**, respectively. Upon PMA/ionomycin stimulation, a very strong induction of STAT1-pS727 was observed (**Figure 10.D**). Additionally, both co-culture with KPO cells and rmIFNβ stimulation led to a slight increase in STAT1-S727 phosphorylation. This is an interesting outcome, possibly suggesting that this novel non-canonical STAT1 signaling pathway may also be active in CD8⁺ cells. Data representing STAT1-pY701 levels showed a similar

pattern to that observed in mNK cells (**Figure 10.F**), with strong induction occurring only upon rmIFNβ stimulation. PMA/ionomycin stimulated CD8⁺ cells showed slight induction of STAT1-pY701, which is a false signal originating from issues with Western blot membrane development. The small black spots visible on the membrane were mistaken as bands by the analysis software and could not be manually corrected.

9.2.4 STK38 deficiency impacts *STAT1* RNA and protein expression levels

During the performance of the experiments described above, it became apparent that knock-out or knock-down of STK38 led to decreased levels of total STAT1 protein. To address this topic, RNA sequencing data from NK-92 cell line and mouse NK cells were analyzed for abundance of STAT1 RNA present in WT *versus* STK38 KO cells.

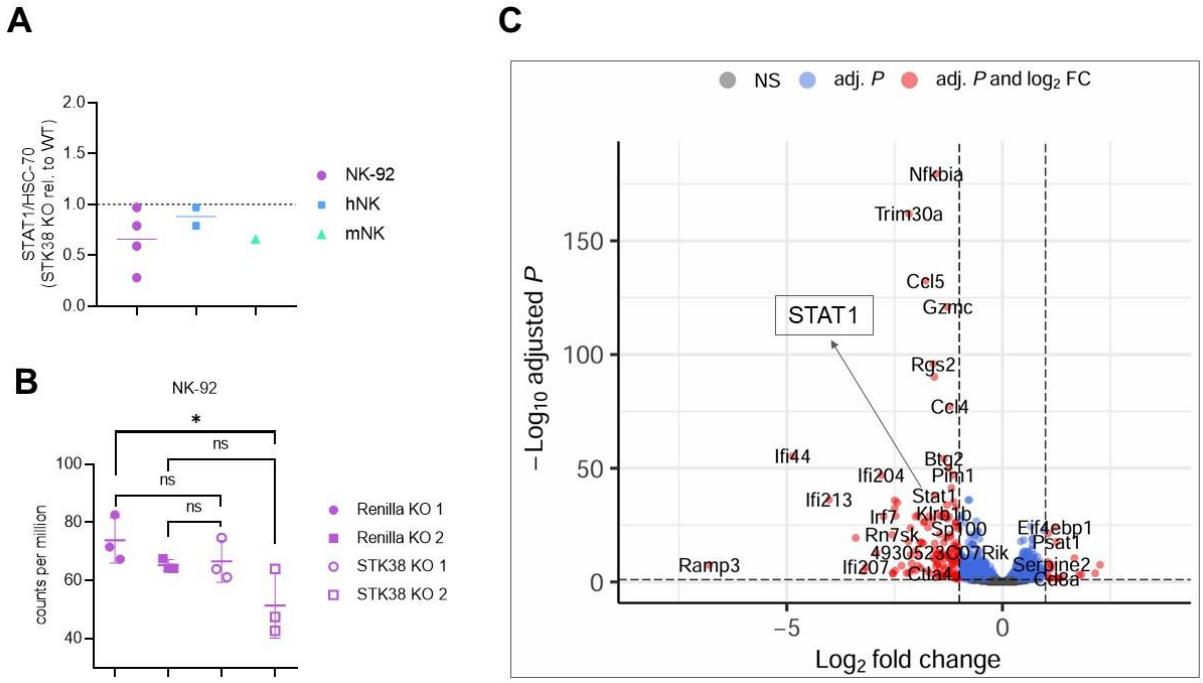

Figure 11. The impact of STK38 on the expression of STAT1 on protein and RNA level. *(A) Relative STAT1 protein levels normalized to HSC-70 of independent Western blots are shown. Depicted here are the relative STAT1 protein levels of STAT1 KO/KD relative to the respective control in NK-92, hNK and mNK cells. (B) RNA sequencing of two independent Renilla KO or STK38 KO NK-92 cell lines (n=3 technical replicates) was performed and data was normalized to counts per million. One-way ANOVA with multiple comparisons testing was performed (Renilla KO 1 vs STK38 KO 2: p-value=0.0312, *). (C) The volcano plot shows the differentially expressed genes detected in IL-2 cultivated mNK cells, four days after isolation from Ndr1-/- mice compared to WT littermates. Significantly up- and downregulated genes are indicated in red, based on a threshold of ±1 log_2 fold change. ns: not significant, adj.: adjusted, FC: fold change*

Figure 11.A depicts total STAT1 protein levels, normalized to the HSC-70 housekeeping protein, in STK38 KO cells relative to WT across multiple Western blot experiments using NK-92, hNK, and mNK cells in unstimulated conditions. Upon knock-out of STK38, a consistent tendency toward

reduced STAT1 total protein levels were observed across different cell types and species. To investigate this observation further, RNA sequencing data from the human NK-92 cell line and mNK cells were analyzed to assess *STAT1* mRNA abundance in STK38 KO *versus* WT cells. **Figure 11.B** presents normalized counts per million for *STAT1* mRNA in Renilla KO and STK38 KO NK-92 cell lines (n=2 per genotype). In one STK38 KO NK-92 cell line, *STAT1* mRNA levels were significantly reduced compared to Renilla KO cells. Additionally, RNA sequencing of mNK cells revealed a significant downregulation of *Stat1* mRNA expression in Stk38 KO mNK cells compared to WT (**Figure 11.C**). In general, Stk38 deficiency induced strong differential gene expression in mNK cells as visualized in a volcano plot depicting $\log_2$ fold change on the x-axis and –log10 adjusted p-value on the y-axis. Taken together, these data indicate a pivotal role for STK38 in regulating non-canonical STAT1 signaling, not only by functioning as a potential kinase responsible for STAT1-S727 phosphorylation, but also by transcriptionally promoting STAT1 expression.

9.3 STK38-mediated phosphorylation of STAT1

STAT1 and STK38(L) were found to physically interact in murine NK cell in the immunological synapse when stimulated with tumor cells[62]. The question, whether STAT1 and STK38(L) proteins are able to directly interact is important to draw further conclusions in investigating this novel pathway, and further upstream kinase signaling responsible for non-canonical STAT1 activation upon target cell contact. To investigate whether STK38 or STK38L are generally able to phosphorylate STAT1-S727, two complementary *in vitro* kinase activity assays were developed using isolated human proteins *in vitro* and upon overexpression of *STK38* in human HEK293T cells.

9.3.1 STK38(L) are able to phosphorylate STAT1 *in vitro*

For the *in vitro* kinase activity assay, full length recombinant human proteins expressed by baculovirus in Sf9 insect cells carrying an N-terminal GST tag were used. STAT1 protein was mixed with STK38, $STK38_{active}$, or $STK38L_{active}$ proteins in the presence of ATP in specific kinase assay buffer, and was incubated at 37°C for 30 minutes. STAT1 and ATP only served as negative control. Following incubation, proteins were lysed and a Western blot was performed to assess STAT1-pS727 levels. It should be noted here that all recombinant proteins showed a higher molecular weight compared to native proteins isolated from cells due to the GST tag (approx. 26 kDa). During assay development, different STAT1 to kinase ratios were tested, as depicted by the different sized plus symbols in **Figure 12.A**, referring to a STAT1 to kinase ratio of 1:1, 5:1, or 20:1. Best results were obtained with the 1:1 ratio,

which was used in further experiments (**Figure 12.B**). Additionally, two different types of STK38 proteins were tested, namely STK38 and $STK38_{active}$. MOB1 protein binds STK38(L), which releases the autoinhibition originating from an inhibitory sequence, resulting in STK38(L) activation[113]. $STK38_{active}$ was thus expected to exhibit a higher kinase activity compared to STK38 alone.

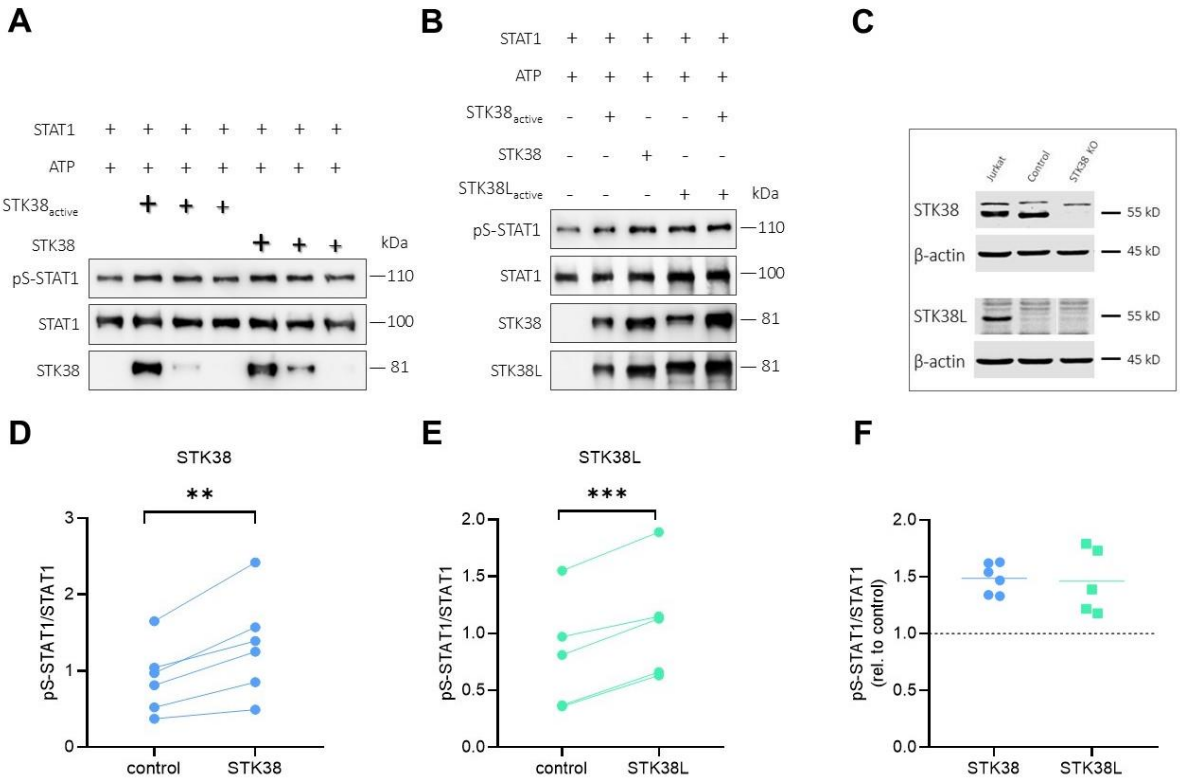

Figure 12. In vitro kinase activity assay demonstrates significant phosphorylation of STAT1-S727 mediated by STK38 and STK38L proteins. *Recombinant STAT1 protein (400 ng) was co-incubated for 30 minutes with (A) $STK38_{active}$, STK38, and (B) $STK38L_{active}$ proteins in the presence of 50 µM ATP and STAT1-pS727 levels were assessed via Western blotting. Total STAT1 and STK38/STKL protein expression was determined as control. Of note, our analysis showed that the individual kinases stained positive for STK38 and STK38L. (C) Western blot analysis confirms the specificity of the STK38 and STK38L antibodies, demonstrating no cross-reactivity. This Western blot was performed by Susanne Stofner, where she compared the expression of STK38 and STK38L in Jurkat (STK38+/STK38L+), Renilla KO NK-92 (STK38+/STK38L-, control), and STK38 KO NK-92 cells (STK38-/STK38L-). (D-E) Summary data shows the quantification of STAT1-pS727 levels normalized to total STAT1 protein when co-incubated with (D) STK38 (n=6 independent experiments) and (E) STK38L (n=5 independent experiments). (F) STAT1-pS727 relative to total STAT1 protein levels from the experimental conditions, normalized to the corresponding control conditions, were plotted as mean. A paired t-test was performed which showed the following P values for (D): 0.0053 (n = 6) and for (E): 0.0005 (n = 5).*

It was interesting to note, that even in the negative control condition, recombinant STAT1 was already phosphorylated to a considerable extent even in the absence of any kinases. However, the addition of STK38 (**Figure 12.A**) or STK38L (**Figure 12.B**) led to further increase in STAT1-pS727 levels. Against our expectations, the results suggested that STK38 alone induced higher levels of STAT1-S727 phosphorylation compared to $STK38_{active}$. Based on these findings, all subsequent

experiments were performed using STK38 alone. Another important observation was the presence of impurities in the recombinant STK38 and STK38L proteins. As highlighted in **Figure 12.B**, the anti-STK38L antibody showed a signal for STK38, and vice versa, when probed on individual membranes. This led us to conclude that all three recombinant kinase preparations likely contained a mixture of both STK38 and STK38L. To rule out antibody cross-reactivity in the Western blot experiments, we performed control tests using NK-92 cells harboring a Renilla KO (control) or STK38 KO. NK-92 cells are known to lack STK38L, while Jurkat cells were used as positive control. The presence of the STK38L band only in Jurkat cells proves the specificity of the anti-STK38L antibody. Similarly, the absence of the STK38 signal in STK38 KO NK-92 cells validated the specificity of the anti-STK38 antibody. We thus concluded that the recombinant proteins were likely a mixture of STK38 and STK38L. The results of the individually performed Western blots showing STK38- and STK38L-mediated STAT1-S727 phosphorylation are summarized in **Figure 12.D** (n=6) and **Figure 12.E** (n=5), respectively. STAT1-pS727 levels, normalized to total STAT1, were quantified for the control condition (STAT1 + ATP only) and for each kinase co-culture condition. The relative increase in STAT1-pS727 levels in the presence of the kinases was approximately 1.5-fold compared to control (**Figure 12.F**).

We therefore concluded that both STK38 and STK38L significantly induced STAT1-S727 phosphorylation. These results represent an important first evidence, that STK38(L) may be involved in the upstream signaling of STAT1. To further validate this finding, HEK293T cells were used as a more physiologically relevant model for *in vitro* kinase activity assays.

9.3.2 STK38 overexpression does not increase STAT1-pS727 in HEK293T cells

To investigate the influence of STK38 on STAT1-S727 phosphorylation in a cellular context, HEK293T cells were transiently transfected to overexpress STK38. We aimed to determine whether STK38 overexpression would lead to increased STAT1-pS727 levels. HEK293T cells were transfected with DNA plasmids encoding FLAG-tagged hSTK38 and eGFP, or eGFP alone (empty control). To assess the transfection efficiency 30 hours after transfection, cells were analyzed via flow cytometry for eGFP expression and compared to untransfected cells. In **Figure 13.A-C**, the gating strategy for (**A**) untransfected, (**B**) empty, or (**C**) STK38 overexpressing cells is shown. In the left panels, debris were excluded and single cells were gated based on forward and side scatter. In the middle panels, doublets were excluded, and in the right panels, $eGFP^+$ cells were gated. The GFP gate was set according to the untransfected sample showing only $eGFP^-$ cells. Transfection efficiency was 57.6% for the hSTK38 plasmid and 73.0% for the empty eGFP plasmid. For the *in vitro* kinase activity assay, transfected HEK293T cells were either left untreated or stimulated with

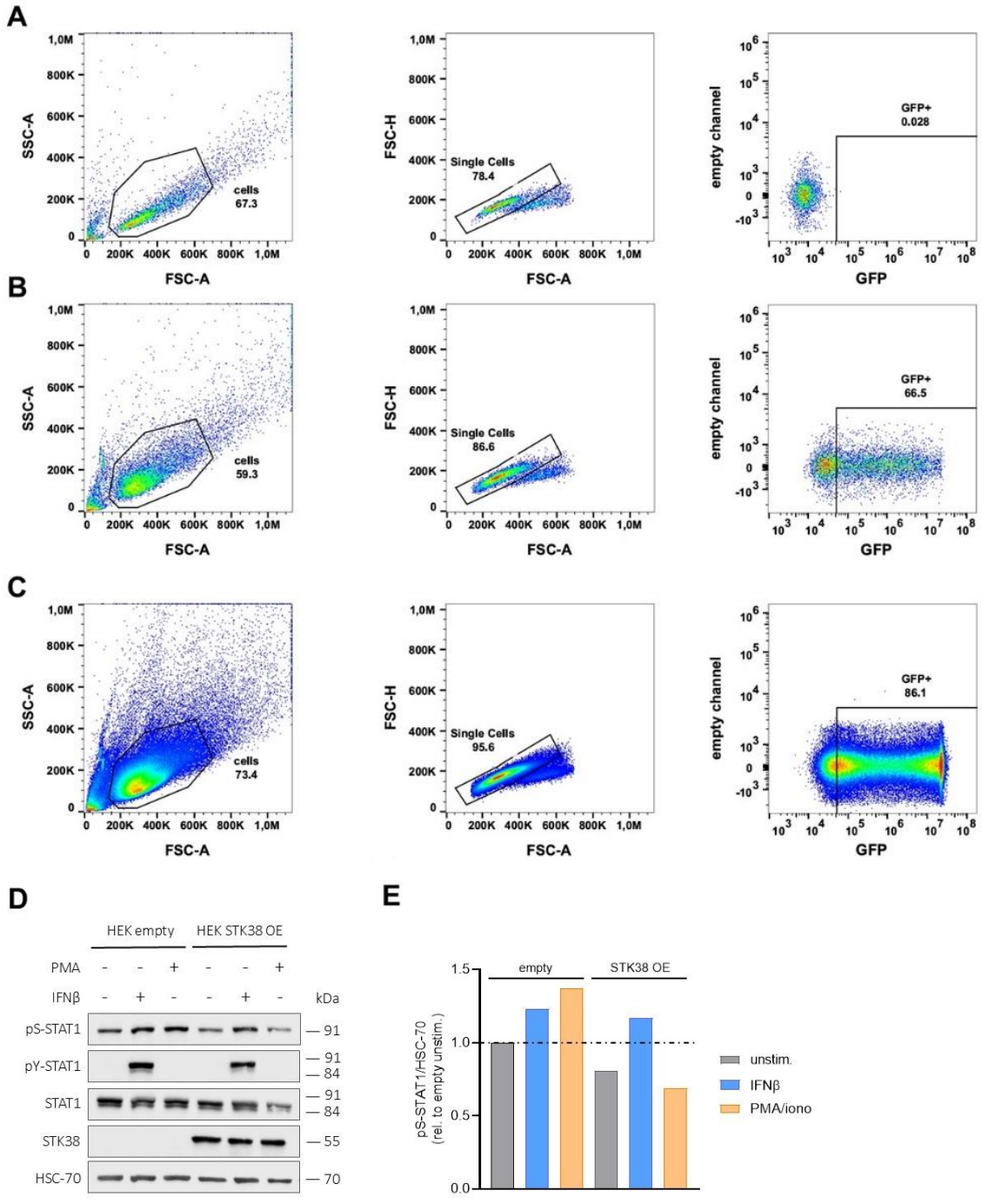

Figure 13. STK38 overexpression in HEK293T cells did not lead to higher expression of STAT1-pS727. *(A-C) 30h after transient transfection of HEK293T cells with a STK38-containing DNA plasmid, cells were analyzed for eGFP expression via flow cytometry. Gating strategy to determine the transfection efficiency in (A) untransfected control cells, and cells containing (B) an empty vector or (C) human STK38: In the first panel on the left, living cells are gated according to forward and side scatter, next, doublets are excluded, after which GFP expression is determined. The GFP-gate is set according to the untransfected control cells. The transduction efficiency varies from 66.5% for the empty control vector to 86.1% for the STK38-containing vector. (D) wegtun! HEK293T cells containing empty or STK38 overexpressing plasmids were either left untreated or activated with PMA or rhIFNβ for 30 minutes and STAT1-pS727 and -pY701 levels were assessed via Western blotting. STAT1, STK38 and HSC-70 were detected as control. (E) Western blot data was quantified and STAT1-pS727 levels were normalized to HSC-70 expression and displayed relative to unstimulated HEK293T cells containing the empty vector. GFP: green fluorescent protein, OE: overexpression*

IFNβ or PMA/ionomycin for 30 minutes. The purpose of this assay was to determine whether STK38 overexpression induces STAT1-S727 phosphorylation. A Western blot was performed to analyze STAT1-pS727 and -pY701 levels and to confirm the expression of STK38 at the protein level (**Figure 13.F**). STK38 overexpressing cells showed a strong band at 55 kDa, whereas no band was detected in empty control cells. This suggests that HEK293T cells do not express detectable levels of endogenous STK38 or that its expression is very low and masked by the strong overexpression. To investigate canonical STAT1 activation, STAT1-pY701 levels were analyzed and detected only in the IFNβ-stimulated positive control. As shown in **Figure 13.G**, STAT1-pS727 levels were normalized to the house-keeping protein HSC-70 and compared to levels in unstimulated HEK293T cells transfected with the empty control vector. In these control cells, we observed a slight induction of STAT1-S727 phosphorylation upon stimulation with IFNβ and PMA/ionomycin. However, in STK38 overexpressing cells, we detected reduced levels of STAT1-pS727 under basal conditions and after PMA/ionomycin stimulation, only showing some degree of activation after stimulation with IFNβ.

These findings did not align with our hypothesis or with previously collected data from NK cells, as STK38 overexpression was supposed to increase STAT1-S727 phosphorylation. One possible explanation for this discrepancy could be misfolding of the overexpressed STK38 protein, which could impair its kinase activity. Another possibility is that STK38 was not sufficiently activated due to the absence of upstream signaling components or input. Our hypothesis proposes that STK38 mediates STAT1-S727 phosphorylation within the immunological synapse upon target cell contact. Since HEK293T cells lack this immunological context, the observed absence of STAT1-pS727 induction may support, rather than contradict, our hypothesis.

9.4 Co-localization of STK38 and STAT1 in the immunological synapse

The final aim of this thesis was to study whether STK38 and STAT1 co-localize in the immunological synapse, which is formed between NK and target cells upon target cell recognition. Previous data from primary mouse NK cells showed the physical interaction of STAT1 and STK38(L) upon tumor cell challenge and suggested that STAT1 locates at the immunological synapse during NK cell-mediated killing[114]. Here, we aimed to translate those findings to the human system, and performed immunofluorescence staining, confocal imaging and a proximity ligation assay (PLA) to investigate the physical (co-)localization of STAT1 and STK38(L) in human NK cells.

9.4.1 Anti-STK38 antibody titration for optimal usage

Antibody titration experiments had to be performed to find the optimal dilution for the immunofluorescence staining. Renilla KO and STK38 KO NK-92 cells were stained for DAPI to visualize the nucleus, and for three different dilutions of an anti-STK38 antibody (Santa Cruz, sc-100404), namely 1:25, 1:50, and 1:100. Immunofluorescence microscopy pictures and bright field images of Renilla KO NK-92 (**Figure 14.A**) and STK38 KO NK-92 cells (**Figure 14.B**) were taken

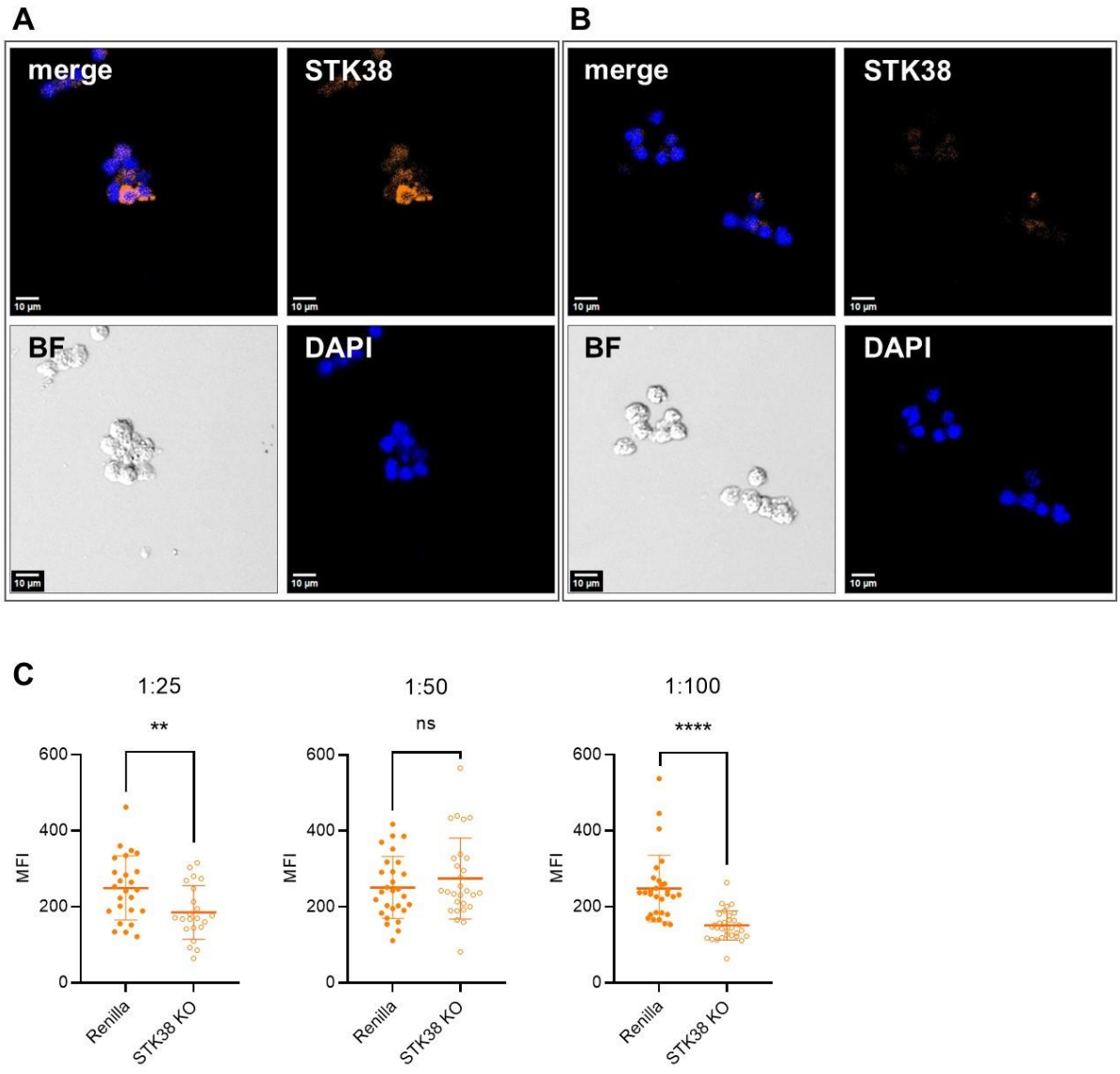

Figure 14. A 1:100 dilution of the anti-STK38 antibody (Santa Cruz, sc-100404) showed the highest specificity in immunofluorescence staining of NK-92 cells. *Staining of (A) Renilla KO NK-92 and (B) STK38 KO NK-92 cells for STK38 (orange) and DAPI (blue). Confocal immunofluorescence and bright field images were collected on an AX / AX R with NSPARC confocal microscope system (Nikon). Shown here is one representative picture for each genotype of the 1:100 antibody dilution. (C) The mean fluorescence intensity (MFI) of each individual cell was assessed via the Fiji ImageJ program. The scattered dot plots show the MFI of individual cells plotted as mean with SD. An unpaired t-test was performed for each dilution, resulting in the following p values: for 1:25: 0.0077 (Renilla: n = 25, STK38 KO: n = 22), for 1:50: 0.3485 (Renilla & STK38 KO: n = 28), and for 1:100: <0.0001 (Renilla: n = 29, STK38 KO: n = 31). BF: bright field, DAPI: 4',6-diamidino-2-phenylindole, MFI: mean fluorescence intensity*

with an AX / AX R with NSPARC confocal microscope system (Nikon). The highlighted pictures show one representative image per genotype of the 1:100 dilution. Interestingly, we observed a high variability in the STK38 staining intensity of control NK-92 cells, which was however markedly reduced in STK38 KO NK-92 cells. The mean fluorescence intensity was assessed for each individual cell for all tested dilutions *via* Fiji ImageJ program, and was plotted for Renilla KO NK-92 *versus* STK38 KO NK-92 cells (**Figure 14.C**). The 1:100 antibody dilution obtained the best results, showing the biggest MFI difference between the two genotypes and demonstrating the lowest MFI for STK38 KO cells. For these reasons, the 1:100 dilution of the anti-STK38 antibody was used in further PLA experiments.

9.4.2 PLA assay to study the physical interaction of STAT1 and STK38 in hNK cells

Here, we aimed to investigate the potential physical interaction between STAT1 and STK38 at the immunological synapse of human NK cells. To this end, human NK cells were either left untreated, co-cultured with CTFR-stained STAT1 KO K562 tumor cells, or stimulated with PMA/ionomycin or rhIFNβ (data not shown). Cells were stained with DAPI to visualize nuclei and with phalloidin to highlight the cytoskeleton. STAT1 and STK38 were probed using antibodies from two different species, followed by PLA PLUS and MINUS secondary antibodies. These secondary antibodies are conjugated to single stranded oligonucleotides. When the PLUS and MINUS probes are in close proximity, connector oligonucleotides and a ligase enable the formation of circular DNA, which is then amplified by a polymerase. The amplified DNA encodes for a fluorescent dye (in this case Texas Red), allowing visualization of protein-protein interactions.

PLA signals were visualized *via* immunofluorescence using a Leica SP8 confocal microscope. In hNK cells stimulated with STAT1 KO tumor cells, distinct PLA signals appeared as discrete fluorescent dots, suggesting close proximity between STAT1 and STK38 proteins (**Figure 15.A**). Interestingly the majority of PLA signals were located within the STAT1 KO tumor cells. Since these cells lack STAT1 by definition, the signal was considered non-specific. **Figure 15.B** shows the negative control, unstimulated STAT1 KO NK-92 cells. Despite the absence of STAT1, a positive PLA signal was still detected, indicating potential cross-reactivity of the STAT1 protein. To address this issue, the STAT1 antibody (Cell Signaling #14994) was further tested for specificity in subsequent immunofluorescence experiments.

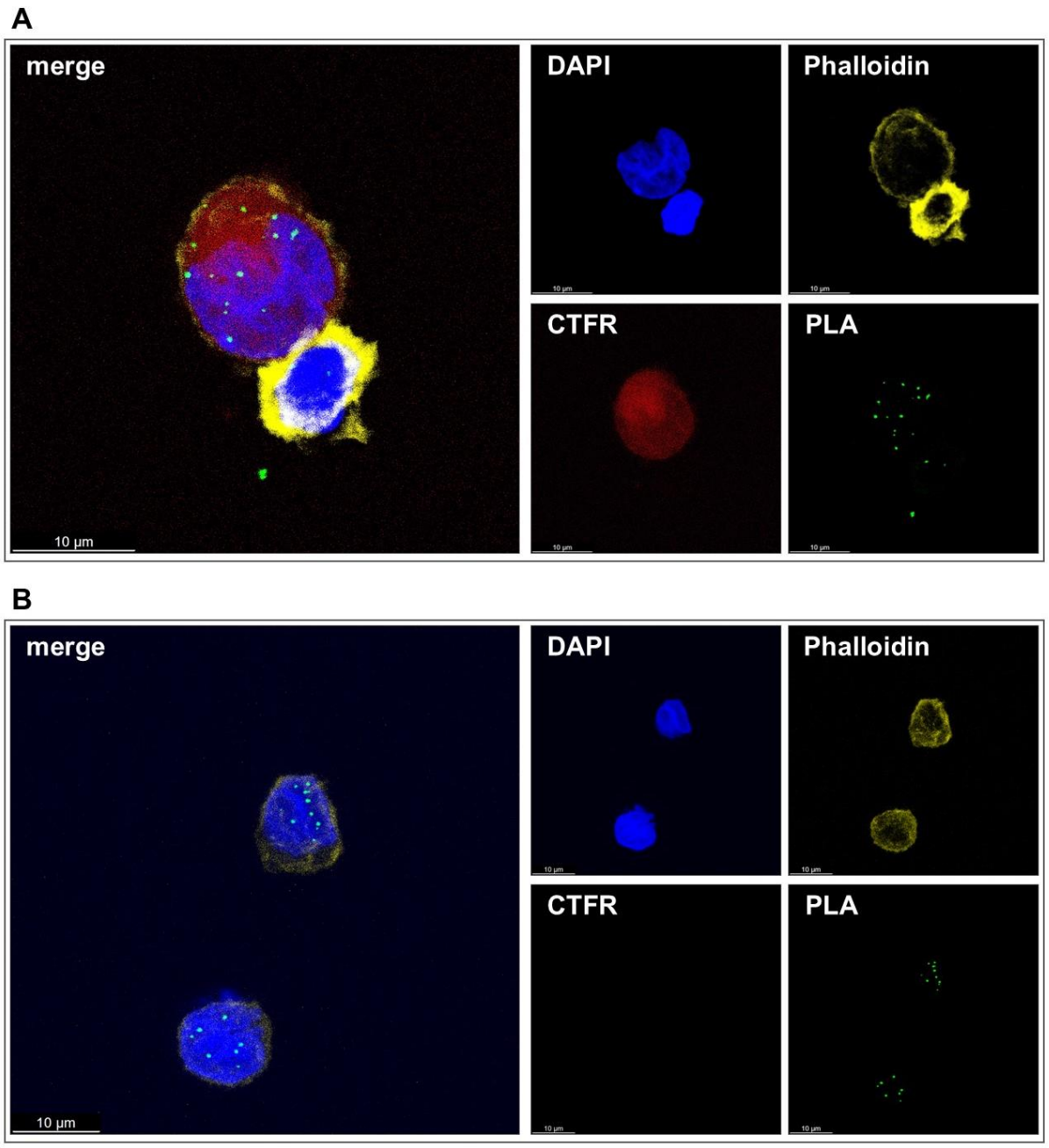

Figure 15. Proximity ligation assay shows non-specific signals. *A proximity ligation assay was performed as described in detail in the Methods section. Discrete fluorescent dots indicative of close proximity of two proteins of interest were visualized via confocal microscopy. Cells were stained with DAPI (nuclei, shown in blue) and phalloidin (F-actin, shown in yellow). The PLA was probed for the two proteins of interest STK38 and STAT1 (in the images referred to as PLA, shown in green). The merged image shows an overlay of all stainings. (A) Human NK cells were co-cultured for 5 minutes with CTFR-stained STAT1 KO K562 cells before fixation and staining. PLA signals were detected in both, hNK and STAT1-deficient tumor cells indicating non-specific binding of the STAT1 antibody. (B) As a negative control, unstimulated STAT1 KO NK-92 cells were assayed and stained for DAPI, phalloidin, and PLA (STK38 and STAT1). The PLA signal (in green) in these negative control cells seems to be non-specific. CTFR: cell trace far red, DAPI: 4',6-diamidino-2-phenylindole, PLA: proximity ligation assay*

9.4.3 STAT1 antibody (Cell Signaling, #14994) exhibits non-specific binding

To assess the specificity of the anti-STAT1 antibody from Cell Signaling (#14994), WT and STAT1 KO K562 tumor cells were stained for STAT1. DAPI was used to portrait nuclei and cells were imaged using the Nikon NSPARC confocal microscope system. Immunofluorescence images of K562 WT cells stained for STAT1 (1:200) are shown in **Figure 16.A** and compared to STAT1 KO K562 cells in **Figure 16.B**. Despite the absence of STAT1 protein in the KO cells, a pronounced STAT1 signal was still observed. A higher antibody dilution (1:400) was also tested, yielding similar results with generally lower staining intensity (data not shown). These findings led us to conclude that the previously performed PLA experiments could not be interpreted reliably, as the fluorescent signals could not be clearly attributed to specific *versus* non-specific binding.

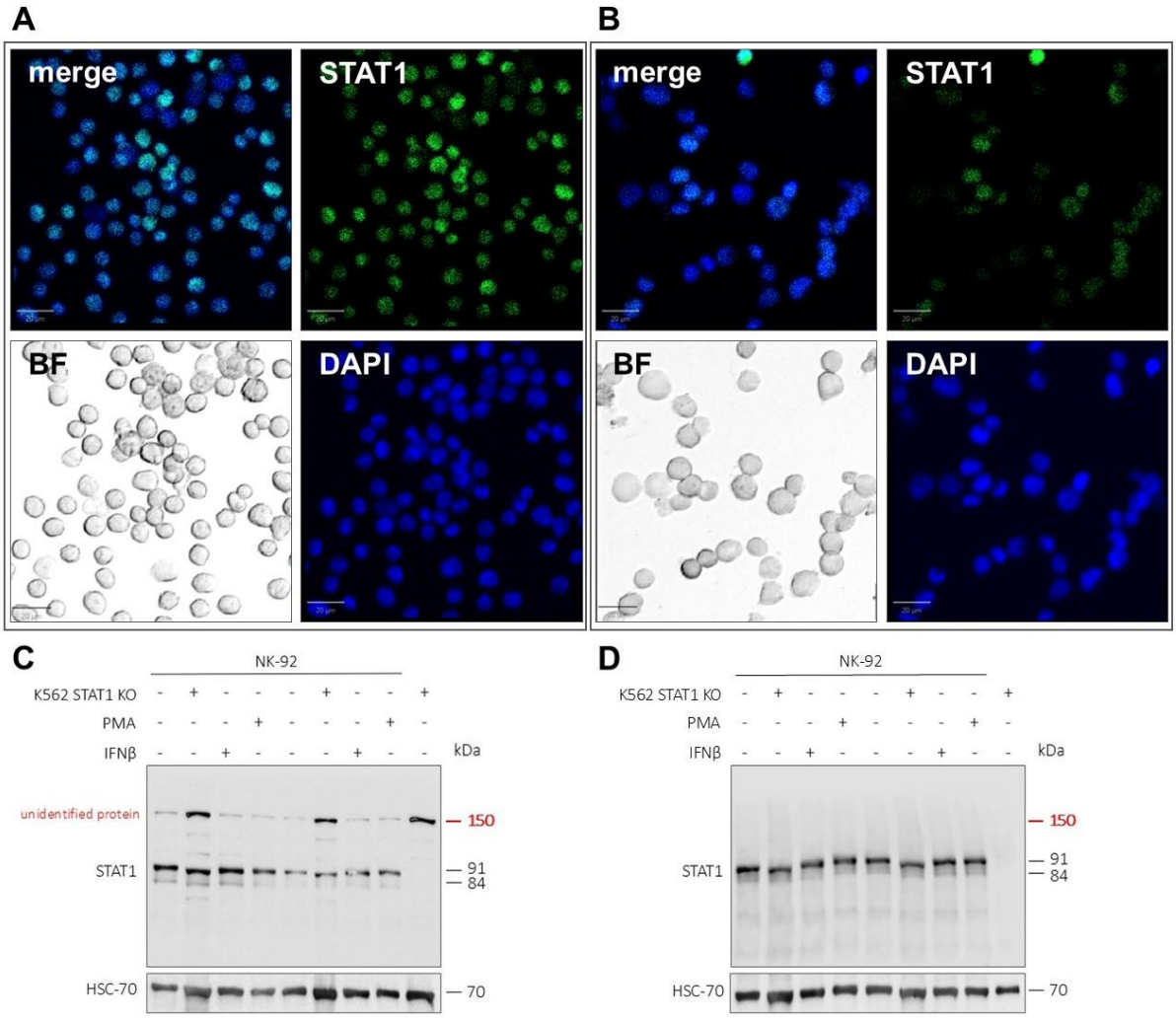

Figure 16. STAT1 antibody from Cell Signaling, #14994, shows non-specific binding in immunofluorescence stainings in K562 WT and STAT1 KO cells, as well as non-specific bands in Western Blot, whereas STAT1 antibody from Proteintech, 82016-1-RR, shows no cross reaction. *(A-B) Immunofluorescent staining of (A) WT K562 and (B) STAT1 KO K562 cells using an anti-STAT1 antibody (shown in green) and DAPI (shown in blue) to visualize nuclei. Bright-field (BF) images were included as visual controls. (C-D) Western blot analysis of lysates from Renilla KO and STK38 KO NK-92 cells co-cultured, among others, with STAT1 KO K562 cells. Membranes were probed with anti-STAT1 antibodies from (C) Cell Signaling (#14994) or (D) Proteintech (82016-RR). The Cell Signaling antibody revealed a prominent non-specific band at approximately 150 kDa, which was absent when membranes were probed with the Proteintech antibody.*

To further assess this issue, Western blotting was used to investigate the specificity of the STAT1 antibody in NK-92 cells co-cultured with STAT1 KO K562 cells (**Figure 16.C**). While the absence of STAT1 in the KO cells was confirmed, a pronounced band was detected at approximately 150 kDa, indicating that the antibody cross-reacts with a larger, unrelated protein. We concluded that this signal likely contributed to the false-positive PLA signals. As this cross-reactive band could not be identified or eliminated, we tested an alternative STAT1 antibody from Proteintech (82016-RR). As shown in **Figure 16.D**, this antibody did not exhibit any non-specific binding or cross-reactivity to other proteins.

Moving forward, it is planned to stain WT and STAT1 KO K562 cells using the 82016-RR antibody. If no substantial cross-reactivity or non-specific signal is observed in STAT1 KO cells, the PLA assay will be repeated in the hope of attaining more reliable results and drawing definitive conclusions.

10 DISCUSSION

This thesis aimed to elucidate the novel non-canonical phosphorylation of STAT1-S727 in NK cells, which was shown to reduce NK cell cytotoxicity against tumor cells[65]. Based on previously obtained data, we hypothesized that upon interaction with tumor cells, NK cells are phosphorylated on STAT1-S727 by STK38(L) within the immunological synapse. To test this hypothesis, we assessed the ability of STK38(L) to interact with the STAT1 protein, and further investigated the subcellular localization and proximity of STAT1 and STK38(L) during NK cell-mediated killing. In this study, following co-culture of primary hNK cells, NK-92 cells, primary mNK cells, as well as murine $CD8^+$ T cells with tumor cells, a pronounced STAT1-S727 phosphorylation was observed. Interestingly, no phosphorylation of STAT1-Y701 was detected under these conditions. Upon loss of STK38, NK-92 cells showed reduced levels of STAT1-pS727 compared to the Renilla KO control. Additionally, a general decrease in total STAT1 protein levels was detected in cells ablated of STK38. An *in vitro* kinase activity assay showed the ability of recombinant STK38 and STK38L proteins to phosphorylate STAT1 at S727. Finally, immunofluorescent staining and a proximity ligation assay were performed to elucidate the location of STAT1 and STK38 in NK cells upon tumor cell contact. However, due to non-specific antibody binding, which was identified during the course of this thesis, these data could not be used.

Possible inhibitory role of STAT1-pS727 in NK Cell cytotoxicity

While phosphorylation at STAT1-Y701 is necessary for STAT1 dimer formation and downstream signaling[62], a plethora of studies[74,81,115–117] mention the importance of STAT1-S727 phosphorylation to reach full transcriptional activation of STAT1. Our previous findings however show increased NK cell cytotoxicity upon inhibition of S727 phosphorylation or S727A point mutation[65]. It is thus necessary to first introduce potential mechanisms by which STAT1-pS727 could lead to reduced NK cell cytotoxicity. Putz et al.[65] could demonstrate, that in primary mouse S727A NK cells perforin, and especially granzyme B expression was significantly enhanced, compared to wild type control. Correlating with the increased amounts of granzyme B and perforin upon S727A mutation, miRNA-378 and -30e levels were shown to be reduced. Overexpression of miRNA-378 was shown to post-transcriptionally inhibit granzyme B mRNA and hence impede protein expression. Additionally, miRNA-30e is responsible for negatively regulating perforin levels[118]. Consequently, lower levels of these miRNAs could be one reason for enhanced NK cell cytotoxicity upon ablation of S727 phosphorylation.

Further, Cheon et al.[119] showed that IRF9 cannot bind to the unphosphorylated STAT1-STAT2 dimer, hence the lack of ISGF3 complex formation would lead to downregulation of core ISGs. This finding is in agreement with another study by Varinou et al., reporting a significant decrease in the expression of pro-inflammatory ISGs in macrophages harboring a STAT1-S727A mutation[115]. In general, the S727A mutation leads to a reduced amount of promotor-bound CDK8, which overall modified transcription of ISGs[81]. Even though the altered transcription pattern and its effect is not elucidated yet, this may be one contributing factor to the suppressive effect of STAT1-S727 phosphorylation on NK cell cytotoxicity.

Another possibility lies in the S727 phosphorylation-induced conformational change of STAT1. Phosphorylation at Y701 triggers the formation of parallel STAT1 homo- or heterodimers through Src-homology 2 (SH2) domain phospho-tyrosine interactions, which leads to nuclear translocation of the dimer and strong transcription factor binding to DNA[120]. Unlike activated STAT1, the SH2 domains of unphosphorylated STAT1 monomers do not contribute to dimer formation and are instead positioned at opposite ends of the dimer in an antiparallel arrangement[119]. Wenta et al.[120] demonstrated that this antiparallel STAT1 dimer conformation strongly impairs DNA binding. Although no data are available on STAT1 conformation when phosphorylated only at S727 but not on Y701, studies confirm low levels of nuclear translocation of unphosphorylated STAT1. STAT1 might enter through the nuclear pore complex by direct interaction with nucleoporins or interact with a heterologous protein containing a nuclear localization signal, like IRF1[121]. Hence it is possible that such a modification could promote the formation of an antiparallel dimer, thereby leading to reduced transcriptional activity.

Mechanisms underlying STAT1-S727 phosphorylation: The potential role of STK38(L)

Our results show a strong NK cell-intrinsic STAT1-S727 phosphorylation after tumor cell contact. To our knowledge, this phenomenon has not yet been described for any immune cell in the literature. The absence of STAT1-Y701 phosphorylation suggests that stimulation *via* cytokines released from the tumor cells can be excluded. Hence this mechanism likely is not part of the classical JAK/STAT pathway, but rather belongs to a novel non-canonical and potentially receptor-mediated STAT1 activation pathway.

In literature, various non-canonical STAT1 activation mechanisms, as well as crosstalk between JAK/STAT signaling and other pathways have been described[74,76,122]. However, only little data exists specialized on NK cell signaling. As similar JAK/STAT signaling patterns were discovered in macrophages and T cells[123], it is plausible that analogous pathways occur in NK cells. This hypothesis is supported by our own data, showing a comparable upregulation of STAT1-S727 phosphorylation in $CD8^+$ cells after tumor cell co-culture.

Studies in macrophages have reported phosphorylation on STAT1-S727, but not Y701, after stimulation with various toll-like-receptor (TLR) ligands such as lipopolysaccharide[124]. Kovarik et al. concluded that such JAK independent phosphorylation represents a non-canonical STAT1 pathway[125]. NK cells express different TLRs, which have been shown to engage in cross-talk with STAT signaling pathways[124,126]. Tumor cells, including K562 cells, are known to release extracellular vesicles[127] containing damage-associated molecular patterns (DAMPs), which can bind to TLRs on immune cells[128]. This mechanism may explain the strong activation of STAT1-pS727 in NK cells following tumor cell co-culture.

Wen et al. demonstrated that STK38 is a negative regulator of TLR9-mediated immune responses in macrophages[104]. However, further data are needed to determine whether STK38(L) plays a role in TLR signaling in NK cells. Another potential mechanism for STAT1-S727 phosphorylation involves stress signaling. Generally, CDK8 is responsible for STAT1-S727 phosphorylation upon type I and type II IFN stimulation, which was shown in NK cells and macrophages[65,81]. Additionally, in stress-induced macrophages, STAT1-S727 was found to be a target of p38 mitogen-activated protein kinase (p38MAPK). Kovarik et al.[129] suggested that phosphorylation of STAT1-S727 is induced through p38MAPK or another yet unidentified downstream kinase activated by stress signals. Even though the S727 phosphorylation promotes activation in macrophages, a similar non-canonical STAT1 pathway may exist in NK cells, with STK38(L) as a potential candidate for the unidentified kinase involved.

STAT1-pS727 as a negative feedback mechanism

When examining the temporal distribution of STAT1-S727 phosphorylation, it becomes evident that maximum activation is reached within 30 minutes to one hour after introducing NK cells to tumor cells. According to the literature, primary hNK cells are typically capable of inducing target cell death within less than 20 minutes after NK cell conjugate formation[130]. This introduces the possibility that S727 phosphorylation functions as a negative feedback mechanism to regulate NK cell cytotoxicity. Three different types of proteins are known to be involved in the negative regulation of NK cell signaling, namely the protein inhibitor of activated STAT (PIAS), suppressors of cytokine signaling (SOCS), and protein tyrosine phosphatases (PTPs). These proteins employ different mechanisms to inhibit JAK/STAT signaling, such as interfering with STAT dimer binding to DNA, hindering STAT recruitment, inhibiting Y701 phosphorylation, promoting proteasomal degradation of JAK/STAT components, and dephosphorylating Y701 to trigger dimer dissociation[122]. These mechanisms show the grand variety of cellular regulations in the JAK/STAT

pathway, presenting numerous points of cross-talk. The induction of STAT1-S727 phosphorylation may represent an additional, possibly NK cell-specific, negative feedback regulation, whose potential mechanisms have been outlined above.

Potential crosstalk between STAT1 and STK38(L) signaling pathways

Upon ablation of STK38 we observed reduced phosphorylation of STAT1-S727 in both the NK-92 cell line and primary mNK cells, leading to enhanced NK cell cytotoxicity. In preliminary data, we proposed a potential interaction between STAT1 and STK38(L) upon tumor cell contact, and observed their co-localization in the IS during NK cell-mediated killing. Thus, we hypothesize, that STK38(L) is an upstream kinase of STAT1, responsible for S727 phosphorylation. In the literature, no direct interaction between STAT1 and STK38(L) has been described. However, a protein known as exportin-1 (CRM1 aka XPO1) could serve as a link between the two distinct pathways. Both STK38 and (un)phosphorylated STAT1 have been found shuttling between the nucleus and the cytoplasm[97,131]. Nuclear trafficking of STAT1 homodimers depends on tyrosine phosphorylation, which leads to rapid translocation of STAT1 dimers to the nucleus *via* a nuclear import carrier protein, importin-α5[119]. In the nucleus, STAT1 binds to specific DNA sites after dissociation from its carrier, to act as a transcription factor. For STAT1 to be released from DNA, a tyrosine phosphatase needs to dephosphorylate STAT1-Y701, resulting in dissociation into monomers. This enables CRM1 to mediate STAT1 nuclear export, transporting the transcription factor back to the cytoplasm[132,133]. STK38, on the other hand, has been shown to activate CRM1 by phosphorylating it at S1055, thereby regulating its cargo export activity, which in turn may influence STAT1 recycling[97].

Interestingly, our data revealed that both NK-92 cells and primary mNK cells deficient in STK38 exhibited reduced total STAT1 protein levels and STAT1 mRNA abundance, compared to controls. This is in accordance with another study, which showed that nuclear STK38 promotes STAT1 translation, and that STK38 KO inhibits STAT1 expression. This effect is mediated by the direct binding of STK38 to the intergenic region of micro-RNA 146a (miR146a), a known translational inhibitor of STAT1 and a negative feedback regulator in TLR signaling[105]. Binding of STK38 to the miR146a locus inhibits its nuclear factor κB (NF-κB)-mediated transcription, and thereby promotes STAT1 protein translation. Additionally, in human NK cells, miR146a mediates IFNγ production by targeting upstream signaling components of the NF-κB pathway[134]. Taken together, these data - along with our findings - provide new insights into non-canonical STAT1 signaling and introduce STK38 as a potential target to enhance NK cell cytotoxicity.

To date and to the best of our knowledge, there are no specific inhibitors of STK38 available. In tumors, STK38 has been shown to exert both tumor-promoting and tumor-suppressing functions, which makes it difficult to predict the effects of potential STK38 inhibitors on tumor cells. STK38 is associated with enhanced cellular proliferation, the promotion of metastasis, and the downregulation of TLRs, resulting in decreased production of inflammatory cytokines. On the other hand, STK38 has also been shown to promote apoptosis in certain cancers and is known to positively influence immune cell infiltration into the tumor microenvironment[92]. This highlights the versatile, sometimes tumor specific functions of STK38, which complicate the use of systemic inhibitors. Therefore, NK cell specific inhibition of STK38 may offer a more targeted and effective approach.

The final aim of this study was to assess the subcellular location of STAT1 and STK38 during NK cell-mediated killing, and to determine the spatial proximity of the two proteins of interest. Unfortunately, due to cross-reactivity of antibodies, no conclusions could be drawn from the immunofluorescence images or proximity ligation assays, which will need to be repeated using more specific antibodies. Currently, limited data exist on STAT1 localization in NK cells and on the receptor-based signaling events that may lead to the recruitment of STAT1 to the cell membrane. We could demonstrate that STK38(L) is able to significantly phosphorylate STAT1 on S727 using *in vitro* kinase activity assays, albeit this does not prove their spatial proximity. As described above, many potential mechanisms of cross-talk between STAT1 and STK38 exist, but the specific signaling pathway remains yet to be determined. Besides, little is known about the closely related paralog STK38L. Further research is needed to elucidate a potential connection between these kinases and STAT1 signaling pathways.

As for now, many open questions remain: Are STK38 and STK38L both involved in the phosphorylation of STAT1-S727, and thereby in the attenuation of NK cell cytotoxicity? Is STAT1-S727 phosphorylation a negative feedback mechanism to regulate NK cell killing? Which upstream receptors are responsible for inducing non-canonical STAT1-S727 phosphorylation in NK cells upon tumor cell contact?

Future experiments will include performing interactome studies of STAT1 and STK38(L) at the IS in hNK and/or NK-92 cells during target cell killing to identify potential interaction partners. Furthermore, by employing CDK8 inhibitors in NK-tumor cell co-culture assays, it may be possible to demonstrate that the STAT1-S727 phosphorylation occurs independently of CDK8 and is mediated exclusively by STK38(L).

Limitations and outlook

This work provides a strong foundation for future studies, because STAT1-pS727 activation was consistently observed across different human NK cell lines, as well as in mNK cells and mCD8$^+$ T cells. The reproducibility of this phosphorylation in diverse cell types demonstrates the robustness of this finding. Yet, additional experiments need to be performed in CD8$^+$ T cells to confirm that the observed elevated pS727 levels occur through the same signaling pathway.

One limitation of this thesis is the frequent reliance on Western blotting as a quantification method, which can be prone to variability. In general, the methods are very focused on Western blots, which are less precise for detecting phosphorylation events. In the future, it is recommended to incorporate alternative techniques, such as proteomics, which offer greater detail and accuracy. To ensure reproducibility, multiple Western blots were performed on the same lysates, consistently yielding results that support the reliability of our findings.

Furthermore, during the course of this work, certain antibodies (anti-STAT1, anti-STK38) exhibited non-specific binding, which compromised the reliability of Western blot analyses, IF staining and the PLA. This was especially challenging for PLA, as cross-reactivity can easily lead to false-positive results. As described in the results section, a more specific antibody for STAT1 was found; however, the available STK38 antibody remained the best option despite its limitations. Additionally, IF analysis suffers from signal variability, background noise, and subjective image interpretation. Model system restrictions present certain limitations in this work. The co-culture presents a reasonable model to study the interactions between NK and tumor cells. However, it does not fully replicate the complexity of the tumor microenvironment, potentially leading to discrepancies between *in vitro* cell culture experiments and subsequent *in vivo* studies with mice. Furthermore, variability in protein yield can occur despite normalization with loading controls such as HSC-70, because cells may remain attached to the well prior to lysis. For the kinase assay, the primary limitation was the lack of a positive control, making it difficult to determine whether the observed phosphorylation resulted from specific kinase activity or nonspecific phosphorylation. To mitigate this, rigorous negative controls and statistical analyses were applied. Moreover, despite using specialized kinase assay buffers, the *in vitro* system lacked the physiological context, including the relevant protein-protein interactions that occur in cells. To partially address this, an *in vitro* kinase activity assay was performed using HEK293T cells. However, due to differences in the regulation of STAT1-S727 phosphorylation between HEK293T and NK cells, the expected results were not observed.

In conclusion, this work demonstrates a novel, non-canonical STAT1-S727 phosphorylation occurring in hNK cells, NK-92 cells, mNK cells, and mCD8$^+$ T cells upon tumor cell contact, independently of STAT1-pY701. The temporal kinetics of this phosphorylation event peaked after 30 minutes to one hour, while STAT1-pY701 levels remained low throughout the experiment, indicating JAK/STAT-independent signaling. Ablation of STK38 resulted in reduced S727 phosphorylation in NK-92 cell lines and was associated with increased NK cell cytotoxicity. Furthermore, STK38 and STK38L recombinant proteins were shown to phosphorylate STAT1 at S727 *in vitro*. Overall, these results strongly support a role for STK38(L) in non-canonical STAT1 signaling, potentially acting as part of a negative feedback mechanism that dampens NK cell cytotoxicity. The observed reduction in STAT1 protein and mRNA levels in STK38-deficient cells further indicate potential cross-talk between STK38 and STAT1 signaling pathways. Although the spatial localization of these proteins remains to be elucidated, the data generated in this thesis provide new insights into a novel non-canonical STAT1 signaling pathway and offer a promising opportunity to enhance NK cell cytotoxicity.

11 REFERENCES

1. Morton, L. T. *et al.* T cell receptor engineering of primary NK cells to therapeutically target tumors and tumor immune evasion. *J. Immunother. Cancer* **10**, e003715 (2022).
2. Stucci, S. *et al.* Immune-related adverse events during anticancer immunotherapy: Pathogenesis and management. *Oncol. Lett.* **14**, 5671–5680 (2017).
3. Vivier, E. *et al.* Natural killer cell therapies. *Nature* **626**, 727–736 (2024).
4. Kiessling, R., Klein, E. & Wigzell, H. „Natural" killer cells in the mouse. I. Cytotoxic cells with specificity for mouse Moloney leukemia cells. Specificity and distribution according to genotype. *Eur. J. Immunol.* **5**, 112–117 (1975).
5. Kiessling, R., Klein, E., Pross, H. & Wigzell, H. „Natural" killer cells in the mouse. II. Cytotoxic cells with specificity for mouse Moloney leukemia cells. Characteristics of the killer cell. *Eur. J. Immunol.* **5**, 117–121 (1975).
6. Herberman, R. B., Nunn, M. E., Holden, H. T. & Lavrin, D. H. Natural cytotoxic reactivity of mouse lymphoid cells against syngeneic and allogeneic tumors. II. Characterization of effector cells. *Int. J. Cancer* **16**, 230–239 (1975).
7. Blum, K. S. & Pabst, R. Lymphocyte numbers and subsets in the human blood: Do they mirror the situation in all organs? *Immunol. Lett.* **108**, 45–51 (2007).
8. Mace, E. M. Human natural killer cells: Form, function, and development. *J. Allergy Clin. Immunol.* **151**, 371–385 (2023).
9. Lodoen, M. B. & Lanier, L. L. Natural killer cells as an initial defense against pathogens. *Curr. Opin. Immunol.* **18**, 391–398 (2006).
10. Coënon, L., Geindreau, M., Ghiringhelli, F., Villalba, M. & Bruchard, M. Natural Killer cells at the frontline in the fight against cancer. *Cell Death Dis.* **15**, 1–14 (2024).
11. Kucuksezer, U. C. *et al.* The Role of Natural Killer Cells in Autoimmune Diseases. *Front. Immunol.* **12**, (2021).
12. Wu, S.-Y., Fu, T., Jiang, Y.-Z. & Shao, Z.-M. Natural killer cells in cancer biology and therapy. *Mol. Cancer* **19**, 120 (2020).

13. Ackermann, M., Liebhaber, S., Klusmann, J. & Lachmann, N. Lost in translation: pluripotent stem cell-derived hematopoiesis. *EMBO Mol. Med.* **7**, 1388–1402 (2015).
14. Sun, J. C. & Lanier, L. L. NK cell development, homeostasis and function: parallels with CD8+ T cells. *Nat. Rev. Immunol.* **11**, 645–657 (2011).
15. Rieger, M. A. & Schroeder, T. Hematopoiesis. *Cold Spring Harb. Perspect. Biol.* **4**, a008250 (2012).
16. Abel, A. M., Yang, C., Thakar, M. S. & Malarkannan, S. Natural Killer Cells: Development, Maturation, and Clinical Utilization. *Front. Immunol.* **9**, (2018).
17. Scoville, S. D., Freud, A. G. & Caligiuri, M. A. Modeling Human Natural Killer Cell Development in the Era of Innate Lymphoid Cells. *Front. Immunol.* **8**, (2017).
18. Freud, A. G., Mundy-Bosse, B. L., Yu, J. & Caligiuri, M. A. The Broad Spectrum of Human Natural Killer Cell Diversity. *Immunity* **47**, 820–833 (2017).
19. Rosmaraki, E. E. *et al.* Identification of committed NK cell progenitors in adult murine bone marrow. *Eur. J. Immunol.* **31**, 1900–1909 (2001).
20. Luetke-Eversloh, M., Killig, M. & Romagnani, C. Signatures of Human NK Cell Development and Terminal Differentiation. *Front. Immunol.* **4**, (2013).
21. Geiger, T. L. & Sun, J. C. Development and maturation of natural killer cells. *Curr. Opin. Immunol.* **39**, 82–89 (2016).
22. Stokic-Trtica, V., Diefenbach, A. & Klose, C. S. N. NK Cell Development in Times of Innate Lymphoid Cell Diversity. *Front. Immunol.* **11**, (2020).
23. Eckelhart, E. *et al.* A novel Ncr1-Cre mouse reveals the essential role of STAT5 for NK-cell survival and development. *Blood* **117**, 1565–1573 (2011).
24. Angelo, L. S. *et al.* Practical NK cell phenotyping and variability in healthy adults. *Immunol. Res.* **62**, 341–356 (2015).
25. Cooper, M. A. *et al.* Human natural killer cells: a unique innate immunoregulatory role for the CD56bright subset. *Blood* **97**, 3146–3151 (2001).
26. Jacobs, R. *et al.* CD56bright cells differ in their KIR repertoire and cytotoxic features from CD56dim NK cells. *Eur. J. Immunol.* **31**, 3121–3126 (2001).

27. Mandelboim, O. *et al.* Human CD16 as a lysis receptor mediating direct natural killer cell cytotoxicity. *Proc. Natl. Acad. Sci.* **96**, 5640–5644 (1999).
28. Poli, A. *et al.* CD56bright natural killer (NK) cells: an important NK cell subset. *Immunology* **126**, 458–465 (2009).
29. Rodriguez-Mogeda, C. *et al.* The role of CD56bright NK cells in neurodegenerative disorders. *J. Neuroinflammation* **21**, 48 (2024).
30. Ljunggren, H.-G. & Kärre, K. In search of the 'missing self': MHC molecules and NK cell recognition. *Immunol. Today* **11**, 237–244 (1990).
31. Chen, S., Zhu, H. & Jounaidi, Y. Comprehensive snapshots of natural killer cells functions, signaling, molecular mechanisms and clinical utilization. *Signal Transduct. Target. Ther.* **9**, 1–39 (2024).
32. Yu, Y. Y. L., Kumar, V. & Bennett, M. Murine Natural Killer Cells and Marrow Graft Rejection. *Annu. Rev. Immunol.* **10**, 189–213 (1992).
33. Zamora, A. E. *et al.* Licensing delineates helper and effector NK cell subsets during viral infection. *JCI Insight* **2**, (2017).
34. Wu, Z. *et al.* Dynamic variability in SHP-1 abundance determines natural killer cell responsiveness. *Sci. Signal.* **14**, eabe5380 (2021).
35. Delconte, R. B. *et al.* NK Cell Priming From Endogenous Homeostatic Signals Is Modulated by CIS. *Front. Immunol.* **11**, (2020).
36. Pegram, H. J., Andrews, D. M., Smyth, M. J., Darcy, P. K. & Kershaw, M. H. Activating and inhibitory receptors of natural killer cells. *Immunol. Cell Biol.* **89**, 216–224 (2011).
37. Romee, R., Leong, J. W. & Fehniger, T. A. Utilizing Cytokines to Function-Enable Human NK Cells for the Immunotherapy of Cancer. *Scientifica* **2014**, 205796 (2014).
38. Islam, R. *et al.* Enhancing a Natural Killer: Modification of NK Cells for Cancer Immunotherapy. *Cells* **10**, 1058 (2021).
39. Fehniger, T. A. *et al.* Differential cytokine and chemokine gene expression by human NK cells following activation with IL-18 or IL-15 in combination with IL-12: implications for the innate immune response. *J. Immunol. Baltim. Md 1950* **162**, 4511–4520 (1999).

40. Yang, L., Pang, Y. & Moses, H. L. TGF-β and immune cells: an important regulatory axis in the tumor microenvironment and progression. *Trends Immunol.* **31**, 220–227 (2010).
41. Fehniger, T. A., Cooper, M. A. & Caligiuri, M. A. Interleukin-2 and interleukin-15: immunotherapy for cancer. *Cytokine Growth Factor Rev.* **13**, 169–183 (2002).
42. Kalina, U. *et al.* IL-18 activates STAT3 in the natural killer cell line 92, augments cytotoxic activity, and mediates IFN-gamma production by the stress kinase p38 and by the extracellular regulated kinases p44erk-1 and p42erk-21. *J. Immunol. Baltim. Md 1950* **165**, 1307–1313 (2000).
43. Zeng, R. *et al.* The molecular basis of IL-21-mediated proliferation. *Blood* **109**, 4135–4142 (2007).
44. Shin, E. *et al.* Understanding NK cell biology for harnessing NK cell therapies: targeting cancer and beyond. *Front. Immunol.* **14**, 1192907 (2023).
45. Prager, I. & Watzl, C. Mechanisms of natural killer cell-mediated cellular cytotoxicity. *J. Leukoc. Biol.* **105**, 1319–1329 (2019).
46. Paul, S. & Lal, G. The Molecular Mechanism of Natural Killer Cells Function and Its Importance in Cancer Immunotherapy. *Front. Immunol.* **8**, (2017).
47. Topham, N. J. & Hewitt, E. W. Natural killer cell cytotoxicity: how do they pull the trigger? *Immunology* **128**, 7–15 (2009).
48. Orange, J. S. The Lytic NK Cell Immunological Synapse and Sequential Steps in Its Formation. in *Immune-Mediated Diseases* (eds. Shurin, M. R. & Smolkin, Y. S.) 225–233 (Springer, New York, NY, 2007). doi:10.1007/978-0-387-72005-0_23.
49. Stinchcombe, J. C. & Griffiths, G. M. Secretory Mechanisms in Cell-Mediated Cytotoxicity. *Annu. Rev. Cell Dev. Biol.* **23**, 495–517 (2007).
50. Peter, M. E. & Krammer, P. H. The CD95(APO-1/Fas) DISC and beyond. *Cell Death Differ.* **10**, 26–35 (2003).
51. Smyth, M. J. *et al.* Tumor necrosis factor-related apoptosis-inducing ligand (TRAIL) contributes to interferon gamma-dependent natural killer cell protection from tumor metastasis. *J. Exp. Med.* **193**, 661–670 (2001).

52. Li, J. *et al.* Real-time detection of CTL function reveals distinct patterns of caspase activation mediated by Fas versus granzyme B. *J. Immunol. Baltim. Md 1950* **193**, 519–528 (2014).
53. Gwalani, L. A. & Orange, J. S. Single Degranulations in NK Cells Can Mediate Target Cell Killing. *J. Immunol. Baltim. Md 1950* **200**, 3231–3243 (2018).
54. Lo Nigro, C. *et al.* NK-mediated antibody-dependent cell-mediated cytotoxicity in solid tumors: biological evidence and clinical perspectives. *Ann. Transl. Med.* **7**, 105 (2019).
55. Li, F. & Liu, S. Focusing on NK cells and ADCC: A promising immunotherapy approach in targeted therapy for HER2-positive breast cancer. *Front. Immunol.* **13**, 1083462 (2022).
56. Wang, S.-Y., Racila, E., Taylor, R. P. & Weiner, G. J. NK-cell activation and antibody-dependent cellular cytotoxicity induced by rituximab-coated target cells is inhibited by the C3b component of complement. *Blood* **111**, 1456–1463 (2008).
57. Lim, C. M. *et al.* Phase I study of expanded natural killer cells in combination with cetuximab for recurrent/metastatic nasopharyngeal carcinoma. *Cancer Immunol. Immunother. CII* **71**, 2277–2286 (2022).
58. Kaplan, D. H. *et al.* Demonstration of an interferon γ-dependent tumor surveillance system in immunocompetent mice. *Proc. Natl. Acad. Sci.* **95**, 7556–7561 (1998).
59. Brown, A. C. N., Dobbie, I. M., Alakoskela, J.-M., Davis, I. & Davis, D. M. Super-resolution imaging of remodeled synaptic actin reveals different synergies between NK cell receptors and integrins. *Blood* **120**, 3729–3740 (2012).
60. Fauriat, C., Long, E. O., Ljunggren, H.-G. & Bryceson, Y. T. Regulation of human NK-cell cytokine and chemokine production by target cell recognition. *Blood* **115**, 2167–2176 (2010).
61. Meissl, K., Macho-Maschler, S., Müller, M. & Strobl, B. The good and the bad faces of STAT1 in solid tumours. *Cytokine* **89**, 12–20 (2017).
62. Putz, E. M. *et al.* Novel non-canonical role of STAT1 in Natural Killer cell cytotoxicity. *Oncoimmunology* **5**, e1186314 (2016).
63. Gotthardt, D. & Sexl, V. STATs in NK-Cells: The Good, the Bad, and the Ugly. *Front. Immunol.* **7**, 694 (2017).

64. Kovacic, B. *et al.* STAT1 acts as a tumor promoter for leukemia development. *Cancer Cell* **10**, 77–87 (2006).
65. Putz, E. M. *et al.* CDK8-Mediated STAT1-S727 Phosphorylation Restrains NK Cell Cytotoxicity and Tumor Surveillance. *Cell Rep.* **4**, 437–444 (2013).
66. Lee, C. K. *et al.* Distinct requirements for IFNs and STAT1 in NK cell function. *J. Immunol. Baltim. Md 1950* **165**, 3571–3577 (2000).
67. Lucas, M., Schachterle, W., Oberle, K., Aichele, P. & Diefenbach, A. Dendritic cells prime natural killer cells by trans-presenting interleukin 15. *Immunity* **26**, 503–517 (2007).
68. Zimmerman, O. *et al.* STAT1 Gain-of-Function Mutations Cause High Total STAT1 Levels With Normal Dephosphorylation. *Front. Immunol.* **10**, 1433 (2019).
69. Tabellini, G. *et al.* Impaired natural killer cell functions in patients with signal transducer and activator of transcription 1 (STAT1) gain-of-function mutations. *J. Allergy Clin. Immunol.* **140**, 553-564.e4 (2017).
70. Lv, K. *et al.* A novel loss-of-function variant in STAT1 causes Mendelian susceptibility to mycobacterial disease. *Front. Cell. Infect. Microbiol.* **15**, (2025).
71. Wu, C. *et al.* STAT1 is phosphorylated and downregulated by the oncogenic tyrosine kinase NPM-ALK in ALK-positive anaplastic large-cell lymphoma. *Blood* **126**, 336–345 (2015).
72. Zhang, W. *et al.* Clinical Relevance of Gain- and Loss-of-Function Germline Mutations in STAT1: A Systematic Review. *Front. Immunol.* **12**, 654406 (2021).
73. Ott, N., Faletti, L., Heeg, M., Andreani, V. & Grimbacher, B. JAKs and STATs from a Clinical Perspective: Loss-of-Function Mutations, Gain-of-Function Mutations, and Their Multidimensional Consequences. *J. Clin. Immunol.* **43**, 1326–1359 (2023).
74. Majoros, A. *et al.* Canonical and Non-Canonical Aspects of JAK–STAT Signaling: Lessons from Interferons for Cytokine Responses. *Front. Immunol.* **8**, (2017).
75. Ivashkiv, L. B. & Donlin, L. T. Regulation of type I interferon responses. *Nat. Rev. Immunol.* **14**, 36–49 (2014).

76. Mazewski, C., Perez, R. E., Fish, E. N. & Platanias, L. C. Type I Interferon (IFN)-Regulated Activation of Canonical and Non-Canonical Signaling Pathways. *Front. Immunol.* **11**, 606456 (2020).
77. Kim, Y.-M. & Shin, E.-C. Type I and III interferon responses in SARS-CoV-2 infection. *Exp. Mol. Med.* **53**, 750–760 (2021).
78. Owen, K. L., Brockwell, N. K. & Parker, B. S. JAK-STAT Signaling: A Double-Edged Sword of Immune Regulation and Cancer Progression. *Cancers* **11**, 2002 (2019).
79. Levy, D. E. & Darnell, J. E. STATs: transcriptional control and biological impact. *Nat. Rev. Mol. Cell Biol.* **3**, 651–662 (2002).
80. Steen, H. C. & Gamero, A. M. STAT2 phosphorylation and signaling. *JAK-STAT* **2**, e25790 (2013).
81. Bancerek, J. *et al.* CDK8 Kinase Phosphorylates Transcription Factor STAT1 to Selectively Regulate the Interferon Response. *Immunity* **38**, 250–262 (2013).
82. Stenger, T. D. & Miller, J. S. Therapeutic approaches to enhance natural killer cell cytotoxicity. *Front. Immunol.* **15**, 1356666 (2024).
83. Bourel, C., Souza-Fonseca-Guimaraes, F. & Lesage, S. Highlights of 2024: unleashing the power of NK cells—cancer's worst nightmare. *Immunol. Cell Biol.* **n/a**, (2025).
84. Witalisz-Siepracka, A. *et al.* NK Cell–Specific CDK8 Deletion Enhances Antitumor Responses. *Cancer Immunol. Res.* **6**, 458–466 (2018).
85. Hofmann, M. H. *et al.* Selective and Potent CDK8/19 Inhibitors Enhance NK-Cell Activity and Promote Tumor Surveillance. *Mol. Cancer Ther.* **19**, 1018–1030 (2020).
86. Clarke, P. A. *et al.* Assessing the mechanism and therapeutic potential of modulators of the human Mediator complex-associated protein kinases. *eLife* **5**, e20722 (2016).
87. Chen, M. *et al.* Systemic Toxicity Reported for CDK8/19 Inhibitors CCT251921 and MSC2530818 Is Not Due to Target Inhibition. *Cells* **8**, 1413 (2019).
88. Ma, C. *et al.* NDR1 protein kinase promotes IL-17- and TNF-α-mediated inflammation by competitively binding TRAF3. *EMBO Rep.* **18**, 586–602 (2017).
89. Hergovich, A., Stegert, M. R., Schmitz, D. & Hemmings, B. A. NDR kinases regulate essential cell processes from yeast to humans. *Nat. Rev. Mol. Cell Biol.* **7**, 253–264 (2006).

90. Pearce, L. R., Komander, D. & Alessi, D. R. The nuts and bolts of AGC protein kinases. *Nat. Rev. Mol. Cell Biol.* **11**, 9–22 (2010).

91. Lu, J. *et al.* A review of nuclear Dbf2-related kinase 1 (NDR1) protein interaction as promising new target for cancer therapy. *Int. J. Biol. Macromol.* **259**, 129188 (2024).

92. Liu, Y. *et al.* Prognostic and Immunological Role of STK38 across Cancers: Friend or Foe? *Int. J. Mol. Sci.* **23**, 11590 (2022).

93. Hergovich, A. The Roles of NDR Protein Kinases in Hippo Signalling. *Genes* **7**, 21 (2016).

94. Sharif, A. A. D. & Hergovich, A. The NDR/LATS protein kinases in immunology and cancer biology. *Semin. Cancer Biol.* **48**, 104–114 (2018).

95. Bichsel, S. J., Tamaskovic, R., Stegert, M. R. & Hemmings, B. A. Mechanism of Activation of NDR (Nuclear Dbf2-related) Protein Kinase by the hMOB1 Protein*. *J. Biol. Chem.* **279**, 35228–35235 (2004).

96. Stegert, M. R., Tamaskovic, R., Bichsel, S. J., Hergovich, A. & Hemmings, B. A. Regulation of NDR2 Protein Kinase by Multi-site Phosphorylation and the S100B Calcium-binding Protein*. *J. Biol. Chem.* **279**, 23806–23812 (2004).

97. Martin, A. PJ., Aushev, V. N., Zalcman, G. & Camonis, J. H. The STK38–XPO1 axis, a new actor in physiology and cancer. *Cell. Mol. Life Sci. CMLS* **78**, 1943–1955 (2020).

98. Wang, S. *et al.* The Crosstalk Between Hippo-YAP Pathway and Innate Immunity. *Front. Immunol.* **11**, (2020).

99. Ma, S., Meng, Z., Chen, R. & Guan, K.-L. The Hippo Pathway: Biology and Pathophysiology. *Annu. Rev. Biochem.* **88**, 577–604 (2019).

100. Hong, W. & Guan, K.-L. The YAP and TAZ transcription co-activators: Key downstream effectors of the mammalian Hippo pathway. *Semin. Cell Dev. Biol.* **23**, 785–793 (2012).

101. Meng, Z., Moroishi, T. & Guan, K.-L. Mechanisms of Hippo pathway regulation. *Genes Dev.* **30**, 1–17 (2016).

102. Hergovich, A., Cornils, H. & Hemmings, B. A. Mammalian NDR protein kinases: From regulation to a role in centrosome duplication. *Biochim. Biophys. Acta BBA - Proteins Proteomics* **1784**, 3–15 (2008).

103. Bisikirska, B. C. *et al.* STK38 is a critical upstream regulator of MYC's oncogenic activity in human B-cell lymphoma. *Oncogene* **32**, 5283–5291 (2013).

104. Wen, M. *et al.* Stk38 protein kinase preferentially inhibits TLR9-activated inflammatory responses by promoting MEKK2 ubiquitination in macrophages. *Nat. Commun.* **6**, 7167 (2015).

105. Liu, Z. *et al.* Downregulated NDR1 protein kinase inhibits innate immune response by initiating an miR146a-STAT1 feedback loop. *Nat. Commun.* **9**, 2789 (2018).

106. Fukasawa, T. *et al.* The Role of Mammalian STK38 in DNA Damage Response and Targeting for Radio-Sensitization. *Cancers* **15**, 2054 (2023).

107. Martin, A. P. & Camonis, J. H. The hippo kinase STK38 ensures functionality of XPO1. *Cell Cycle* **19**, 2982–2995.

108. Hogquist, K. A. *et al.* T cell receptor antagonist peptides induce positive selection. *Cell* **76**, 17–27 (1994).

109. Buri, M. C. *et al.* Natural killer cell–mediated cytotoxicity shapes the clonal evolution of B cell leukaemia. *Cancer Immunol. Res.* **13**, 430–446 (2025).

110. Romera-Cárdenas, G. *et al.* Ionomycin Treatment Renders NK Cells Hyporesponsive. *PLoS ONE* **11**, e0150998 (2016).

111. Chatila, T., Silverman, L., Miller, R. & Geha, R. Mechanisms of T cell activation by the calcium ionophore ionomycin. *J. Immunol. Baltim. Md 1950* **143**, 1283–1289 (1989).

112. Zhang, Y. *et al.* STAT1β enhances STAT1 function by protecting STAT1α from degradation in esophageal squamous cell carcinoma. *Cell Death Dis.* **8**, e3077–e3077 (2017).

113. Klingemann, H. The NK-92 cell line—30 years later: its impact on natural killer cell research and treatment of cancer. *Cytotherapy* **25**, 451–457 (2023).

114. Putz, E. M. *et al.* Targeting cytokine signaling checkpoint CIS activates NK cells to protect from tumor initiation and metastasis. *OncoImmunology* **6**, e1267892 (2017).

115. Varinou, L. *et al.* Phosphorylation of the Stat1 Transactivation Domain Is Required for Full-Fledged IFN-γ-Dependent Innate Immunity. *Immunity* **19**, 793–802 (2003).

116. Sadzak, I. *et al.* Recruitment of Stat1 to chromatin is required for interferon-induced serine phosphorylation of Stat1 transactivation domain. *Proc. Natl. Acad. Sci. U. S. A.* **105**, 8944–8949 (2008).

117. Tehrani, S. S. *et al.* STAT1 is required to establish but not maintain interferon-γ-induced transcriptional memory. *EMBO J.* **42**, e112259 (2023).

118. Wang, P. *et al.* Identification of Resting and Type I IFN-Activated Human NK Cell miRNomes Reveals MicroRNA-378 and MicroRNA-30e as Negative Regulators of NK Cell Cytotoxicity. *J. Immunol.* **189**, 211–221 (2012).

119. Philips, R. L. *et al.* The JAK-STAT pathway at 30: Much learned, much more to do. *Cell* **185**, 3857–3876 (2022).

120. Wenta, N., Strauss, H., Meyer, S. & Vinkemeier, U. Tyrosine phosphorylation regulates the partitioning of STAT1 between different dimer conformations. *Proc. Natl. Acad. Sci.* **105**, 9238–9243 (2008).

121. Reich, N. C. & Liu, L. Tracking STAT nuclear traffic. *Nat. Rev. Immunol.* **6**, 602–612 (2006).

122. Hu, X., Li, J., Fu, M., Zhao, X. & Wang, W. The JAK/STAT signaling pathway: from bench to clinic. *Signal Transduct. Target. Ther.* **6**, 1–33 (2021).

123. Fortelny, N. *et al.* JAK-STAT signaling maintains homeostasis in T cells and macrophages. *Nat. Immunol.* **25**, 847–859 (2024).

124. Luu, K. *et al.* STAT1 plays a role in TLR signal transduction and inflammatory responses. *Immunol. Cell Biol.* **92**, 761–769 (2014).

125. Kovarik, P., Stoiber, D., Novy, M. & Decker, T. Stat1 combines signals derived from IFN-γ and LPS receptors during macrophage activation. *EMBO J.* **17**, 3660–3668 (1998).

126. Fernández-Figueroa, E. A. *et al.* Down-Regulation of TLR and JAK/STAT Pathway Genes Is Associated with Diffuse Cutaneous Leishmaniasis: A Gene Expression Analysis in NK Cells from Patients Infected with Leishmania mexicana. *PLoS Negl. Trop. Dis.* **10**, e0004570 (2016).

127. Savina, A., Vidal, M. & Colombo, M. I. The exosome pathway in K562 cells is regulated by Rab11. *J. Cell Sci.* **115**, 2505–2515 (2002).

128. Abu, N., Rus Bakarurraini, N. A. A. & Nasir, S. N. Extracellular Vesicles and DAMPs in Cancer: A Mini-Review. *Front. Immunol.* **12**, 740548 (2021).

129. Kovarik, P. *et al.* Stress-induced phosphorylation of STAT1 at Ser727 requires p38 mitogen-activated protein kinase whereas IFN-γ uses a different signaling pathway. *Proc. Natl. Acad. Sci.* **96**, 13956–13961 (1999).

130. Vanherberghen, B. *et al.* Classification of human natural killer cells based on migration behavior and cytotoxic response. *Blood* **121**, 1326–1334 (2013).

131. Gambin, A., Charzyńska, A., Ellert-Miklaszewska, A. & Rybiński, M. Computational models of the JAK1/2-STAT1 signaling. *JAK-STAT* **2**, e24672 (2013).

132. McBride, K. M. & Reich, N. C. The Ins and Outs of STAT1 Nuclear Transport. *Sci. STKE* **2003**, (2003).

133. Tur, J. *et al.* Induction of CIITA by IFN-γ in macrophages involves STAT1 activation by JAK and JNK. *Immunobiology* **226**, 152114 (2021).

134. Wang, H. *et al.* Regulation of Human Natural Killer Cell IFN-γ Production by MicroRNA-146a via Targeting the NF-κB Signaling Pathway. *Front. Immunol.* **9**, 293 (2018).